An Empirical and Simulation-Based Assessment of Tree Growth in Temperate Alley-Cropping Systems

Von der Fakultät für Umwelt und Naturwissenschaften

der Brandenburgischen Technischen Universität Cottbus-Senftenberg

zur Erlangung des akademischen Grades eines

Doktor der Ingenieurwissenschaften (Dr.-Ing.)

genehmigte Dissertation

vorgelegt von

Master of Science (M. Sc.)

Diana-Maria Seserman

aus Iași (Jassy), Rumänien

Gutachter: Apl. Prof. Dr. agr. habil. Dirk Freese

Brandenburgischen Technischen Universität (BTU) Cottbus–Senftenberg

Fachgebiet Bodenschutz und Rekultivierung, Cottbus, Deutschland

Gutachter: Prof. Dr. Jörg Michael Greef

Bundesforschungsinstitut für Kulturpflanzen

Julius Kühn-Institut (JKI), Braunschweig, Deutschland

Datum und Ort der mündlichen Prüfung: 13. Dezember 2019, Cottbus

Preface

The SIGNAL-Project (Sustainable Intensification of Agriculture through Agroforestry) was initiated and planed in relation to the proposal call “Soil as a Sustainable Resource for the Bioeconomy – BonaRes” (www.signal.uni-goettingen.de).

The present dissertation was carried out under the BonaRes - SIGNAL project (FKZ 031A562E, 2015-2018) and funded by the German Federal Ministry of Education and Research (BMBF – Bundesministerium für Bildung und Forschung).

In the following, a compilation of three peer-reviewed journal papers, together with several conference papers, are presented as central components of the dissertation. For an adequate readability of the printed version, some of the illustrations were realigned or altered. These studies were written and published during four years of scientific work at the Brandenburg University of Technology Cottbus–Senftenberg, Institute of Environmental Sciences, Chair of Soil Protection and Recultivation.

Seserman, D.M.; Pohle, I.; Veste, M.; Freese, D. Simulating Climate Change Impacts on Hybrid-Poplar and Black Locust Short Rotation Coppices. *Forests* **2018**, *9(7)*, 419.

Seserman, D.M.; Freese, D.; Swieter, A.; Langhof, M.; Veste, M. Trade-Off between Energy Wood and Grain Production in Temperate Alley-Cropping Systems: An Empirical and Simulation-Based Derivation of Land Equivalent Ratio. *Agriculture* **2019**, *9(7)*, 147.

Seserman, D.M.; Freese, D. Handling Data Gaps in Reported Field Measurements of Short Rotation Forestry. *Data* **2019**, *4(4)*, 132.

Table of Contents

List of Abbreviations

ACS	alley-cropping system
AP	alley-cropping-plot
BHD	breast height diameter
CCC	concordance correlation coefficient
CV	coefficient of variation
DM	dry matter
LER	land equivalent ratio
H	height
MAR	missing at random
MCAR	missing completely at random
MP	monoculture-plot
RHD	root height diameter
SB	simulation bias from observations
SRC	short rotation coppice
SRF	short rotation forestry

List of Figures

List of Tables

Summary

The potential of raw materials for bio-based sectors progressively grows recognition stemming from the current efforts to reduce dependence on fossil fuels and greenhouse gas emissions, altogether with mitigating climate change. Biomass generated from dedicated energy crops, used in short-rotation forestry (SRF) and short-rotation coppices (SRC), is regarded as a flexible primary source for the generation of energy, heat, fuel, and bio-based materials and chemicals.

Agroforestry systems, which integrate trees into agriculturally managed fields, are often regarded as an adaptable multi-crop land-use strategy that can provide ecological and economic benefits. A variation of agroforestry is represented by the so-called alley-cropping systems (ACSs) for the production of woody biomass for energy purposes, in which several hedgerows of fast-growing trees are established in parallel strips at varying distances on an agricultural field. The tree strips can be managed as SRC, while the alleys between them are managed as conventional agricultural areas with annual crops.

Understanding whether ACSs with SRC are productive and environmentally sustainable requires long-term assessments of tree and crop yield production in relation to changes in site-specific conditions. Empirical data on such systems are scarce and establishing ACSs under a gradient of management options, climatic and edaphic conditions would be cumbersome, time-consuming, and would demand a notable large amount of funding. Therefore, an alternative method was crucial for achieving yield predictions in ACSs under wide-ranging scenarios.

The research aim of the present dissertation has focused on investigating the prospective implications of different site-specific conditions and scenarios on tree growth in ACSs with SRC, thus incorporating several experimental and simulation-based studies. Through a considerable amount of simulations, the main target was to investigate the ability of a process-oriented, eco-physiological tree growth model to (**i**) impute missing empirical data, thus securing a reliable repository of tree growth characteristics, (**ii**) simulate the tree growth in terms of woody biomass production with satisfactory accuracy, (**iii**) predict and evaluate the tree growth sensitivity to prospective climate changes, thus performing risk assessments for the near and distant future, (**iv**) simulate the tree growth in strong relation to the interactions with adjacent crops and their respective resource capture, (**v**) project the yield of both trees and crops in ACSs under different

climatic, soil, and management conditions, and (**vi**) derive and assess the land equivalent ratio (LER) and gross energy yield for different climatic, soil, and management scenarios.

Establishing a reliable repository of tree growth characteristics is essential for the analysis of primary data, forests statistics, land-use strategies, as well as for the calibration/validation of tree growth models. However, forest research frequently confronts with missing data in field measurements due to sampling infeasibilities, sampling irregularities across years, or failure of measurement equipment, to name a few. In order to handle such cases of missing data, several models belonging to (**i**) regression analysis, (**ii**) statistical imputation, (**iii**) forest growth functions, and (**iv**) a process-oriented tree growth model have been applied and investigated in Chapter 2. Based on the findings of this study, several tools were identified for researchers and practitioners dealing with incomplete data sets. Moreover, the role of a process-oriented eco-physiological tree growth model to bridge the data gaps on several temporal scales has been confirmed and discussed.

Chapter 3 has investigated and evaluated the prospective growth sensitivity of two tree species managed as SRC to a considerable spectrum of weather conditions and long-term climate change, from 2015 to 2054. Through a combined experimental and simulation study, the analysis has employed (**i**) a process-oriented, eco-physiological model to simulate the daily tree growth and (**ii**) 100 realisations of the statistical regional climate model STAR 2K. The findings have corroborated the potential tree growth vulnerability to prospective climatic changes, particularly to changes in water availability, and have underlined the importance of coping management strategies in SRC for forthcoming risk assessments and adaptation scenarios.

Chapter 4 has focused on the ability of a process-oriented eco-physiological model to adequately simulate the growth of both trees and crops in two ACSs with SRC. Consequently, projections of tree and crop yield production have been generated under different climatic and edaphic conditions and implementation design scenarios. Furthermore, the yield performance and land-use efficiency of two ACSs have been assessed by deriving the land equivalent ratio (LER) and gross energy yield for different site-specific conditions and implementation design scenarios. Both LER and gross energy yields had resulted in a convex curve where the maximum values were achieved when either the tree or crop component was dominant (>75% of the land area) and minimum when these components shared similar proportions of land area.

Collectively, the implications of different site-specific conditions and scenarios on tree growth in ACSs with SRC have been investigated in order to improve the decision-making, optimization, and adaptation of such systems. Last but not least, this dissertation has emphasized the considerable potential of modelling approaches in ACSs, as they can impute missing data from scarce available data and simulate tree and crop yields for specific site-conditions in a non-intrusive, inexpensive, and prompt way while supporting early site-setup planning.

Zusammenfassung

Das Potenzial von nachwachsenden Rohstoffen gewinnt aufgrund der derzeitigen Bestrebungen, die Abhängigkeit von fossilen Brennstoffen und die Emission von Treibhausgasen zu verringern und gleichzeitig den Einfluss des Klimawandels zu mildern, zunehmend an Bedeutung. Die aus speziellen Energiepflanzen, wie sie in der Kurzumtriebsforstwirtschaft und in Kurzumtriebsplantagen (KUP) verwendet werden, gewonnenen Biomasse, gilt als flexible Primärquelle für biobasierte Materialien und Chemikalien, sowie für die Erzeugung von Energie, Wärme, und Kraftstoff.

Agroforstwirtschaftliche Systeme, die Bäume in landwirtschaftlich genutzte Flächen integrieren, werden oft als anpassungsfähige Multi-Crop-Flächennutzungsstrategie angesehen, welche ökologische und wirtschaftliche Vorteile bringen kann. Eine Variante der Agroforstwirtschaft stellen die sogenannten Alley-Cropping-Systeme (ACSs) zur Herstellung von holzartiger Biomasse für Energiezwecke dar. In ACSs werden mehrere Hecken von schnell wachsenden Bäumen, in parallelen Streifen und in unterschiedlichen Abständen auf einer Agrarfläche angelegt, wobei die Baumstreifen zum Beispiel als KUP bewirtschaftet werden können, während die Alleen zwischen ihnen als konventionelle landwirtschaftliche Flächen mit einjährigen Kulturen genutzt werden.

Um zu verstehen, ob ACSs mit KUPs produktiv und ökologisch nachhaltig sind, müssen langfristige Bewertungen der Baum- und Ernteerträge in Bezug auf mögliche Veränderungen der standortspezifischen Bedingungen vorgenommen werden. Jedoch sind empirische Daten über solche Systeme rar. Des Weiteren ist die Einrichtung von ACSs für eine Reihe von Managementoptionen, und für verschiedene klimatische und edaphische Bedingungen umständlich, zeitaufwendig und teuer. Daher war es notwendig, eine alternative Methode zu finden, welche die Prognose von Erträgen in ACSs unter verschiedensten Szenarien ermöglicht.

Die vorliegende Dissertation hat sich auf die Untersuchung der prospektiven Auswirkungen verschiedener standortspezifischer Bedingungen und Szenarien auf das Baumwachstum in ACSs mit KUP konzentriert. Für diesen Zweck wurden mehrere experimentelle und simulationsbasierte Studien angefertigt.

Das Hauptziel dieser Dissertation war es, die Anwendbarkeit eines prozessorientierten, ökophysiologischen Baumwachstumsmodells auf die folgenden Problemstellungen hin zu untersuchen:

i. Ermittlung fehlender empirischer Daten für die Schaffung eines zuverlässigen Datenbestandes von Baumwachstumsmerkmalen.
ii. Simulation des Baumwachstums in Bezug auf die Produktion von holzartiger Biomasse mit angemessener Genauigkeit.
iii. Vorhersage und Bewertung der Empfindlichkeit des Baumwachstums gegenüber zukünftigen Klimaänderungen, und die Durchführung von Risikobewertungen für die nahe und ferne Zukunft.
iv. Simulation des Baumwachstums in Zusammenhang mit den Wechselwirkungen zwischen benachbarten Ackerkulturen und deren jeweiliger Ressourcennutzung.
v. Projektion des Ertrages von Bäumen und Ackerkulturen in ACSs unter unterschiedlichen Klima-, Boden- und Managementbedingungen.
vi. Ableitung und Bewertung des Flächenäquivalenzverhältnises (Land Equivalent Ratio; LER) und des Bruttoenergieertrages von ACSs für verschiedene Klima-, Boden- und Managementszenarien.

Der Aufbau eines zuverlässigen Datenbestandes von Baumwachstumsmerkmalen ist unerlässlich für die Analyse von Primärdaten, Forststatistiken, Landnutzungsstrategien sowie für die Kalibrierung/Validierung von Baumwachstumsmodellen. Die Forstwissenschaft ist jedoch häufig mit fehlenden Daten bei Feldmessungen konfrontiert. Die Gründe für fehlende Daten sind vielfältig und reichen von der Undurchführbarkeit der Probenahme, über Unregelmäßigkeiten bei der Probenahme über mehrere Jahre, bis hin zum Ausfall von Messgeräten, um nur einige zu nennen. Um mit solchen Fällen von fehlenden Daten umzugehen, wurden mehrere Modelle aus den Bereichen (**i**) Regressionsanalyse, (**ii**) statistische Imputation, (**iii**) Waldwachstumsfunktionen und (**iv**) ein prozessorientiertes Baumwachstumsmodell angewendet und in Kapitel 2 untersucht. Basierend auf den Erkenntnissen dieser Studie wurden mehrere Werkzeuge für Forscher und Praktiker, die sich mit unvollständigen Datensätzen befassen, identifiziert. Darüber hinaus wurde die Notwendigkeit eines prozessorientierten ökophysiologischen Baumwachstumsmodells zur Überbrückung von Datenlücken für verschiedene zeitliche Auflösungen diskutiert und bestätigt.

In Kapitel 3 wurde die prospektive Wachstumsempfindlichkeit zweier als KUP bewirtschafteter Baumarten für ein breites Spektrum von Wetterbedingungen und für den langfristigen Klimawandel von 2015 bis 2054 untersucht und bewertet. In einer kombinierten Experimental- und Simulationsstudie wurden (**i**) ein prozessorientiertes ökophysiologisches Modell zur Simulation des täglichen Baumwachstums und (**ii**) 100 Realisierungen des statistischen regionalen Klimamodells STAR 2K für die Analyse verwendet. Die Ergebnisse der Studie haben die potenzielle Anfälligkeit des Baumwachstums für künftige klimatische Veränderungen, insbesondere hinsichtlich der Entwicklung der Wasserverfügbarkeit, bestätigt. Desweiteren wurde die Bedeutung von Bewältigungsstrategien in KUP für bevorstehende Risikobewertungen und Anpassungsszenarien durch die Studie hervorgehoben.

Das vierte Kapitel konzentrierte sich auf die Fähigkeit eines prozessorientierten ökophysiologischen Modells, das Wachstum von Bäumen zusammen mit Ackerkulturen in zwei ACSs mit KUP angemessen zu simulieren. Dafür wurden Prognosen der Baum- und Ernteerträge, unter verschiedenen klimatischen und edaphischen Bedingungen, sowie unter unterschiedlichen Implementierungsdesigns, erstellt. Darüber hinaus wurden die Ertragsleistung und die Landnutzungseffizienz von zwei ACSs, mithilfe des Flächenäquivalenzverhältnis und des Brutto-Energieertrages, für verschiedene standortspezifische Bedingungen und Implementierungsszenarien untersucht. Sowohl das Flächenäquivalenzverhältnis als auch die Brutto-Energieerträge führten zu einer konvexen Kurve, bei der die Maximalwerte erreicht wurden, wenn entweder die Baum- oder die Pflanzenkomponente dominant war (>75% der Landfläche). Die Minimalwerte wurden erreicht, wenn beide Komponenten ähnliche Anteile der Landfläche hatten.

Zusammenfassend wurden die Auswirkungen verschiedener standortspezifischer Bedingungen und Szenarien auf das Baumwachstum in ACSs mit KUP untersucht, um die Entscheidungsfindung zu erleichtern, sowie die Optimierung und Adaptierung solcher Systeme zu verbessern. Abschließend, unterstrich diese Dissertation das erhebliche Potenzial von Modellierungsansätzen in ACSs, da sie fehlende Informationen aus wenigen verfügbaren Daten implizieren, und Baum- und Ernteerträge für bestimmte Standortbedingungen auf eine nicht intrusive, kostengünstige und schnelle Art und Weise simulieren können, und gleichzeitig eine frühzeitige Planung des Standortaufbaus unterstützen.

1. General Introduction

1.1. Domain Analysis

As outlined by the European Commission in the Energy Roadmap 2050 (European Commission, 2011), the share of renewable energy sources must increase in gross final energy consumption to at least 55% and in electricity consumption to at least 64%, while simultaneously striving for a low-carbon goal. Stemming from these efforts to reduce dependence on fossil fuels and greenhouse gas emissions, while mitigating climate change, the potential of raw materials for bio-based sectors progressively grows recognition (European Commission, 2011).

Dedicated energy crops

Since biomass is regarded as flexible primary energy for the generation of energy, heat, fuel, bio-based materials, and chemicals, it can play an essential role in achieving the renewable energy goal set by 2050 (Strelher, 2000; BWE, 2015). Biomass generated from dedicated energy crops such as short-rotation forestry (SRF) and short-rotation coppices (SRC) is accompanied by many advantages such as efficient nutrient utilization, low erosion potential (Abbasi *et al.*, 2010), and low to no requirement for pesticide and fertilizer (Evans *et al.*, 2010). Furthermore, SRCs have shown high biomass yields (Ceulemans *et al.*, 1999), adequate fuel properties (Hauck *et al.*, 2014), and low emissions from alternative fuels and flexibility to consumer demand (Evans *et al.*, 2010).

In Europe, the high demand for woody biomass for energy purposes has increased the planting popularity of fast-growing tree species belonging to the genera *Populus*, *Eucalyptus*, *Pinus*, *Acacia*, and *Salix*, (Ceulemans *et al.*, 1996; Aravanopoulos *et al.*, 1999; Sims *et al.*, 2001; Walle *et al.*, 2007; Sochacki *et al.*, 2007; Zewdie *et al.*, 2009; Carl *et al.*, 2017), but has also heightened the pressure on arable lands. In this context, a need to redesign the agricultural landscapes towards a multifunctional land-use has been identified in order to ensure a sustainable and resilient forest and agricultural production in the 21st century (Landis, 2017; Birkhofer *et al.*, 2018).

Alley-cropping systems

Agroforestry systems, which integrate trees into agriculturally managed fields, are often regarded as a flexible multi-crop land-use strategy to provide ecological and economic benefits (Morhart *et al.*, 2014; Veste & Böhm, 2018). Agroforestry systems have been

shown to preserve high levels of agricultural yields while delivering ecosystem services, hence increasing land-use efficiency (Fagerholm *et al.*, 2016; Paul *et al.*, 2017), and concurrently providing effective adaptation measures (Verchot *et al.*, 2007; Schoeneberger *et al.*, 2012) and climate change mitigation, such as reducing the atmospheric carbon dioxide, and adaptation measures (De Stefano & Jacobson, 2018).

A variation of agroforestry is represented by the so-called alley-cropping systems (ACSs) for the production of woody biomass for energy purposes, in which several hedgerows of fast-growing trees are established in parallel strips at varying distances on an agricultural field (Morhart *et al.*, 2014). The tree strips can be managed as SRF or SRC, while the alleys between them are managed as conventional agricultural areas with annual crops (Tsonkova *et al.*, 2012). As an example, Figure 1 depicts the SIGNAL Plot no. 3, under a conventional setting (**a**), as well as under an alley-cropping setting (**b**), as established at Neu Sacro (Brandenburg).

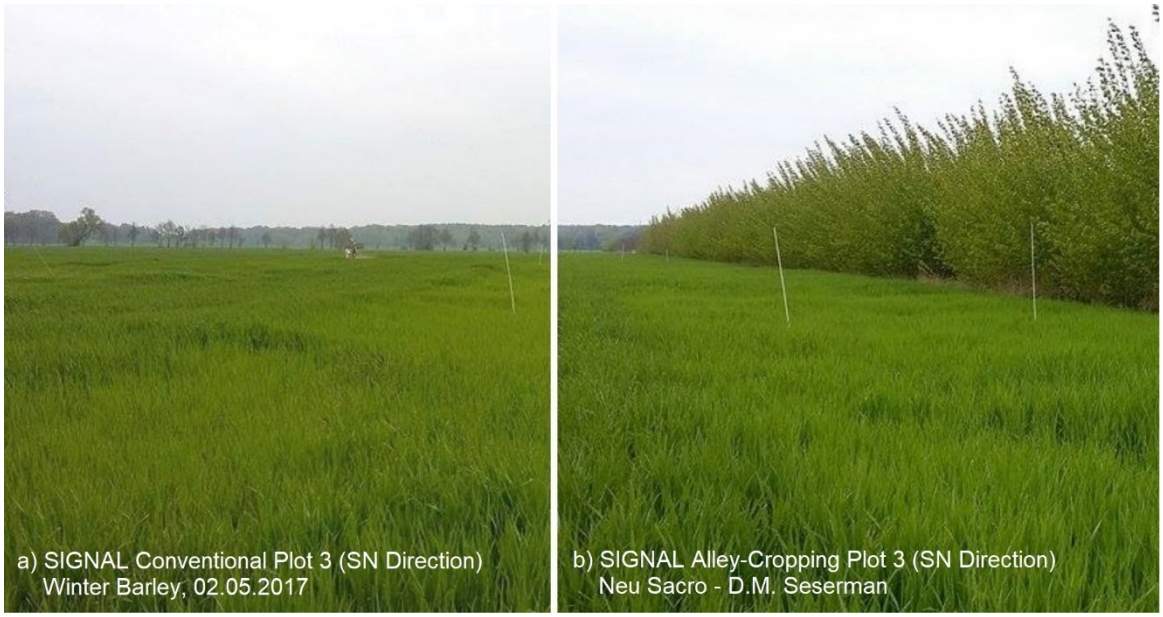

Figure 1. Comparison between a conventional (**a**) and alley-cropping setting (**b**) at Neu Sacro (Brandenburg) with winter barley and hybrid-poplar trees. The white poles mark some of the measurement points.

1.2. Problem Statement

In order to quantify the production of woody biomass, accurate estimates of tree height, root height diameter (RHD), and breast height diameter (BHD) are paramount for the forest management and research (Diamantopolou *et al.*, 2016). However, this data is oftentimes unavailable due to sampling infeasibilities (bad weather, lack of equipment, lack of technical expertise), sampling irregularities across years, inaccurate estimations (allometric

functions and the vast amount of methods to be used for calculating one parameter), or failure of equipment (dendrometers, lysimeters, station maintenance) (Wang *et al.*, 2012). Missing data not only represents a loss of information and a source of uncertainty in data analysis but a severe drawback from present investigations, as well as for future decision-making, coping management strategies, risk assessments, and adaptation scenarios.

Optimizing and adapting the ACSs for energy purposes demands for a considerable amount of experimental sites established under different climatic and edaphic conditions, with ACSs implemented under different designs, i.e.,, tree arrangement (scattered or lined, leeward or windward), the distance between trees, and proportion of land covered by either trees or crops. Establishing such experimental sites, however, would be a cumbersome, time-consuming process and would demand a notable large amount of funding.

Understanding whether ACSs with SRF or SRC are economically profitable and environmentally sustainable, given their long-time planning horizon, demands for systematic assessments of tree and crop biomass production in strong relation to site-specific climatic and edaphic conditions, as well as to prospective changes in environmental conditions like the ongoing climate change (Evans *et al.*, 2010; van Vooren *et al.*, 2016; Gerstengarbe *et al.*, 2003). In Central Europe, projections of future climate warn about increasing climate variability and number of extreme weather events (Jacob *et al.*, 2014; Christensen *et al.*, 2007).

Moreover, regarding the productivity of ACSs, practitioners have expressed concern due to the reduced area covered by agricultural crops (Tsonkova *et al.*, 2018). Through negative attributes reported by practitioners, the existence of trees has been perceived to decline the crop yield (Graves *et al.*, 2009), to impede farm machinery, and to attract diseases (Rois-Díaz *et al.*, 2018).

1.3. Research Aim and Objectives

Against this background, the research aim of the present dissertation has focused on evaluating the prospective implications of different site-specific conditions and scenarios on tree growth in ACSs, thus incorporating several experimental and simulation-based studies. Achieving the overall aim has built on a considerable amount of simulations investigating the ability of a process-oriented, eco-physiological tree and crop growth model, as well as the implications of the resulted output:

a) To impute missing empirical data, thus achieving a reliable repository of tree growth characteristics for the analysis of primary data, forests statistics, land-use strategies, as well as for the calibration and validation of tree growth models.

b) To simulate tree growth in terms of woody biomass production with satisfactory accuracy.

c) To predict and evaluate the tree growth sensitivity to a variety of weather conditions and prospective long-term climate change, from 2015 to 2054, thus performing risk assessments for the near and distant future.

d) To simulate the tree growth in strong relation to the interactions with adjacent crops and their respective resource capture.

e) To project the yield of both trees and crops in ACSs under different climatic and edaphic conditions, as well as under several implementation design scenarios.

f) To derive and assess the land equivalent ratio and gross energy yield for existing ACSs schemes and under several implementation design scenarios, thus assessing the implications of integrating trees on arable lands, as compared to forestry and conventional monocultures with annual arable crops (Figure 2).

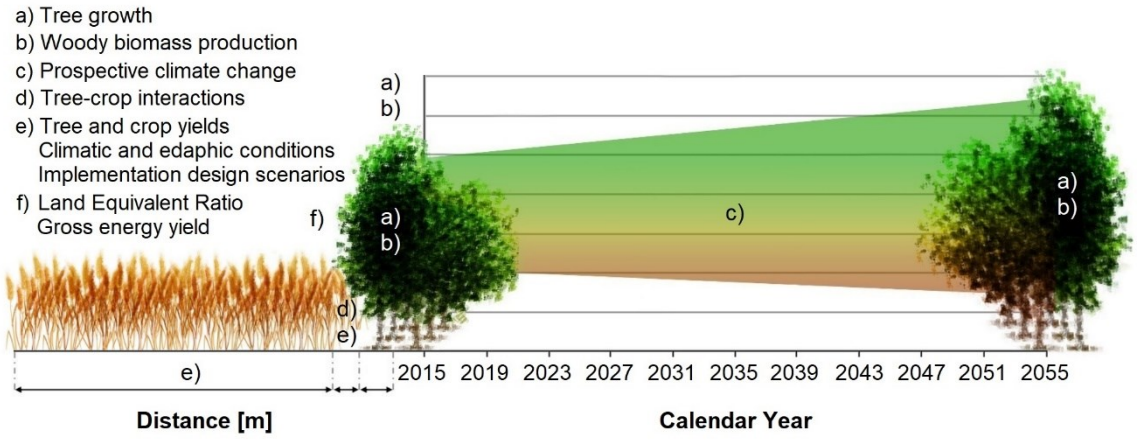

Figure 2. Scheme of main investigations emerging as a consequence of the overall research aim.

1.4. Methodological Approach

Experimental Sites

Initially, a database of main parameters, such as trees (species, planting density, management, yield, $DOY_{planting}$, $DOY_{harvest}$), crops (species, management, yield, DOY_{sowing}, $DOY_{harvest}$), soil physical characteristics (texture, structure, porosity, bulk density, organic matter), and weather conditions (precipitation, temperature, solar radiation) was created for

three existing long-term alley-cropping systems at Dornburg (Thuringia), Wendhausen (Lower Saxony), and Neu Sacro (Brandenburg). All sites consisted of fast-growing tree strips of hybrid-poplar clone "Max I" (*Populus nigra* L. x *P. maximowiczii* Henry) with alleys of different annual arable crops and cover a gradient of climatic and edaphic conditions (Table 1). While the tree planting density varied between the sites (i.e.,, 2,200 trees ha^{-1}, 10,000 trees ha^{-1}, and 9,800 trees ha^{-1} at Dornburg, Wendhausen, and Neu Sacro, respectively), the tree strips were around 10m wide (without the so-called buffer zone, a distance of about 1.5m allocated between the tree strip and crop alleys for the agricultural machinery) and the crop alleys in between the tree strips were 48m wide at all sites.

Table 1: Climatic and edaphic comparison between the investigated experimental sites.

Experimental Site	**Dornburg**	**Wendhausen**	**Neu Sacro**
Latitude; Longitude	51˚00' N; 11˚38' E	52˚20' N; 10˚38' E	51˚47' N; 14˚37' E
Altitude	280m a.s.l	85m a.s.l.	67m a.s.l.
Year of planting	Winter season 2006/2007 [1]	Winter season 2007/2008 [2]	Winter season 2010/2011 [3]
Year of first harvest	Winter season 2014/2015 [1]	Winter season 2013/2014 [2]	Winter season 2014/2015 [3]
Year of second harvest	-	Winter season 2017/2018	Winter season 2017/2018
Soil characteristics			
Soil type	Luvisol [1], Pseudogley-Pararendzina [4]	Pelosol [2,4]	Pseudogleysol, Gley-Vega [3,4]
Soil texture	Clayey silt [1]	Silty clay [2]	Loamy sand [3]
Clay [%]	26 [4]	49 [4]	9 [4]
Silt [%]	70 [4]	36 [4]	27 [4]
Sand [%]	4 [4]	15 [4]	64 [4]
Meteorological conditions			
Mean annual temperature [°C]	8.9 [a]	9.8 [b]	9.6 [c]
Average annual precipitation [mm]	612 [a]	616 [b]	568 [c]

[1] Bärwolf *et al.* (2016); [2] Lamerre *et al.* (2015); [3] Kanzler & Böhm (2016); [4] Beuschel *et al.* (2018); [a] Weather station Weimar of the German Weather Service (DWD); [b] Weather station Braunschweig of the German Weather Service (DWD); [c] Weather station Cottbus of the German Weather Service (DWD).

Tree Growth Characteristics

Establishing a reliable repository of tree growth characteristics is essential for the analysis of primary data, forests statistics, land-use strategies, as well as for the

calibration/validation of forest growth models. Paramount for forest research and management are accurate estimates of tree heights, root height diameter (RHD), and breast height diameter (BHD) for the determination of timber volume (Diamantopolou *et al.*, 2016). Data cleansing (i.e., the process of detecting and imputing incomplete or inaccurate records from the dataset) was, therefore, an intrinsic part of this section. Several models belonging to regression analysis, statistical imputation, and forest growth functions were applied and investigated in order to retrieve information about the trees from existing annual measurements. For this, the analysis employed:

- The "Curve Fitting Toolbox" from Matlab (version R2017a, Mathworks);
- The "Amelia II" R-Package (Honaker *et al.*, 2011);
- The R software (version 3.4.2, R Core Team 2017).

The Yield-SAFE Model

Additionally, a parameter-sparse, ecophysiological, process-oriented model was employed, and namely the Yield-SAFE model (Yield Estimator for Long-term Design of Silvoarable AgroForestry in Europe). Developed for growth processes in forestry, agriculture, and agroforestry systems (van der Werf *et al.*, 2007; Graves *et al.*, 2010; Keesman *et al.*, 2011), Yield-SAFE has been confirmed to render robust and plausible results under a scarcity of data (Graves *et al.*, 2010).

The concept and algorithm of the Yield-SAFE model were made as simple as possible, which allowed the fast identification of parameters and the analysis of uncertainties in model predictions (van der Werf *et al.*, 2007). An organigram of the Yield-SAFE model is presented in Figure 3.

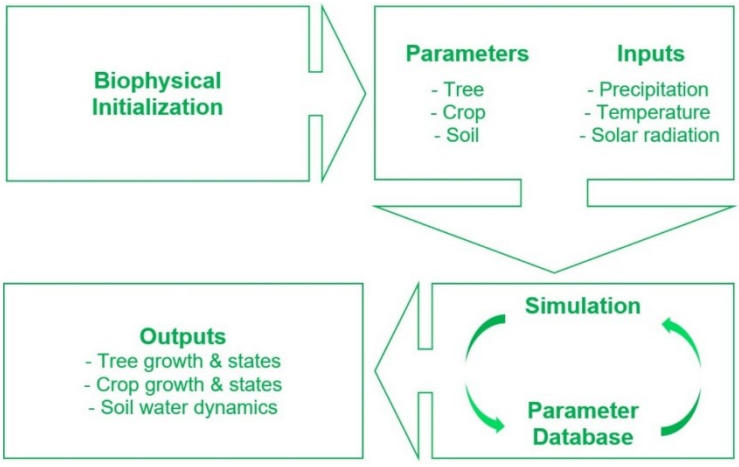

Figure 3. Organigram of the Yield-SAFE model.

The biophysical initialization refers to the setting up of initial tree and crop states (e.g. initial biomass, initial leaf area), soil states (e.g. initial soil water content), implementation design (e.g. planting density), and management practices (e.g. tree and crop species and rotation, day of the year for tree pruning and thinning and for crop planting and harvest). Having set this foundation, more specific tree and crop parameters, as well as soil physical properties and climatic inputs are required by the model. The simulation is based on algorithms and differential equations regarding the tree, crop, and soil rates and the static relations and states of the system as a whole. A loop depending on the number of days follows, where parameter outputs are determined and stored, on a daily temporal scale.

Accordingly, the Yield-SAFE model was calibrated with the initial biophysical parameters, as well as with tree and crop parameters, soil physical properties, and climatic inputs either collected on-site or available from literature and reports, together with ecophysiological parameters based on bibliography and expert knowledge, as instructed in Graves *et al.* (2010), Keesman *et al.* (2011), Burgess *et al.* (2005), and Wösten *et al.* (1999). Once calibrated, the model output was validated against measured values in order to generate projections of energy wood and grain production under several implementation designs, climatic, and edaphic scenarios in ACSs. Regarding the adaptations and improvements implemented in the Yield-SAFE model, the approach aimed to represent a set of realistic situations without expanding the set of variables or equations, and by adjusting parameters to site-specific conditions of the experimental sites of our consortium.

The performance of the Yield-SAFE model was evaluated using the R software (version 3.4.2, R Core Team 2017) independently for determining the coefficient of determination (R^2), sum of squared errors (SSE), root-mean-square error (RMSE), mean average error (MAE), and the simulation bias (SB) from the observations, as well a by using the package "epiR" (Stevenson *et al.*, 2019) for calculating the concordance correlation coefficient (CCC).

Under reduced sample size, the Yield-SAFE model was used both for imputing missing data and generating projections of tree and crop yields under different scenarios, while accounting for the competition for resources, interactions, and possible impacts in ACSs.

Proccesses and Possible Impacts in ACSs

In order to evaluate the empirical and Yield-SAFE simulations of tree and crop yields in ACSs, the processes and possible impacts in such systems were compiled and adapted after Young (1989) and Spitters & Schapendonk (1990) (Figure 4).

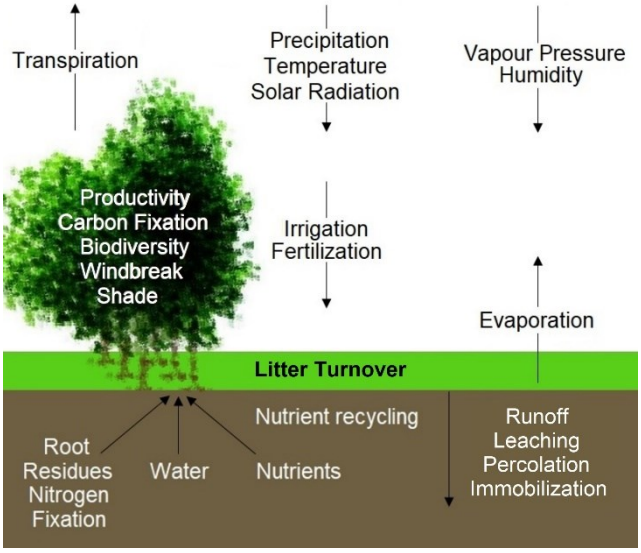

Figure 4. Processes and possible impacts in alley-cropping systems, adapted after Young (1989) and Spitters & Schapendonk (1990).

1.5. Dissertation Structure and Outline

The present dissertation is a compilation of three peer-reviewed journal papers, together with several conference papers, inserted in Chapters 2 to 4 and should be regarded as such. For adequate readability of the printed version, some of the illustrations were realigned or altered where suitable. The general structure of the dissertation follows the investigations emerging as a consequence of the overall research aim defined in Section 1.3. with the help of the methodological approach described in Section 1.4. (Figure 5).

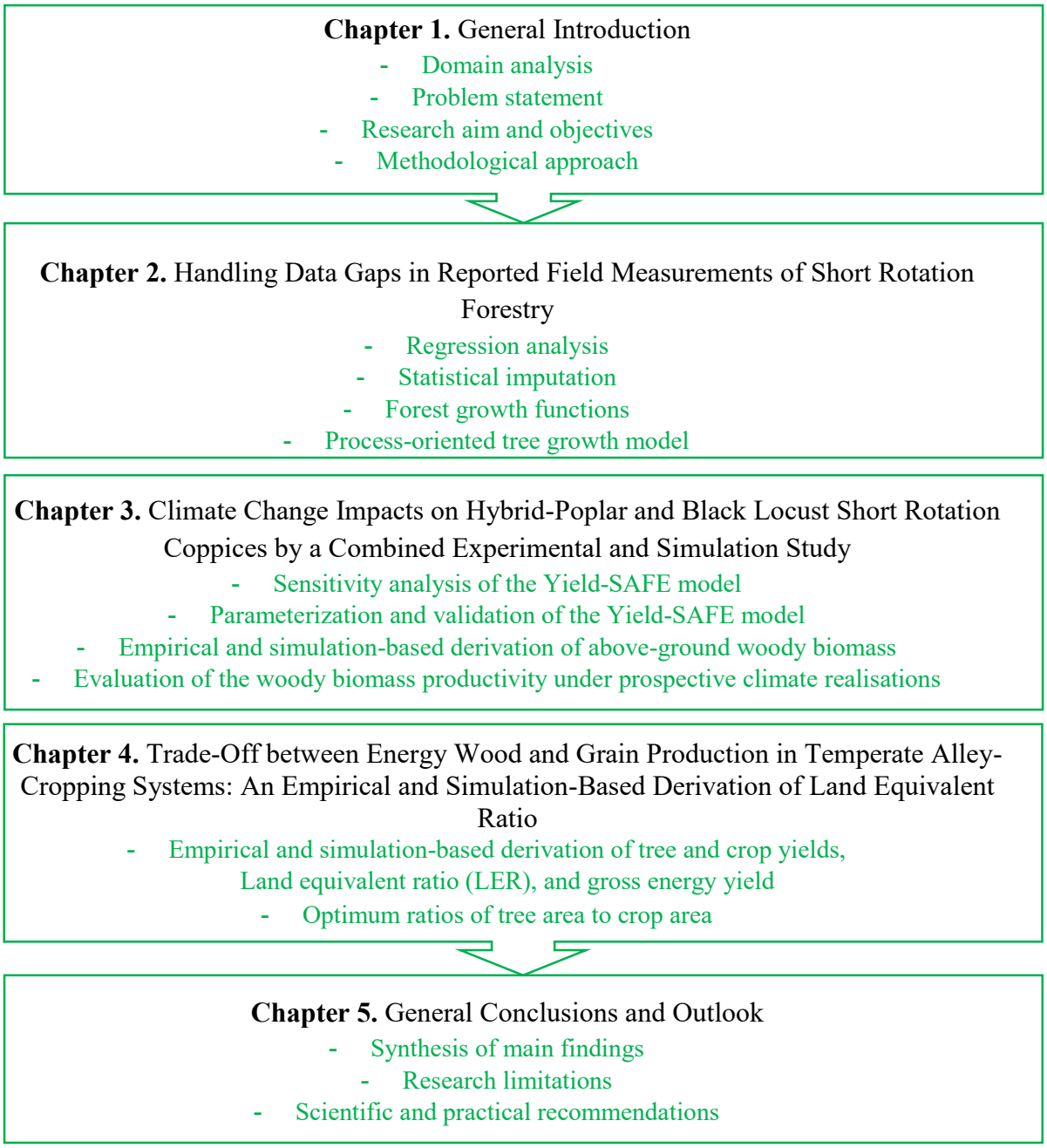

Figure 5. Structure and overview of present dissertation

2. Handling Data Gaps in Reported Field Measurements of Short Rotation Forestry

Diana-Maria Seserman [1,*], Dirk Freese [1]

[1] Brandenburg University of Technology Cottbus–Senftenberg, Institute of Environmental Sciences, Chair of Soil Protection and Recultivation, Konrad-Wachsmann-Allee 6, 03046 Cottbus, Germany; seserman@b-tu.de; freese@b-tu.de

* Correspondence: seserman@b-tu.de;

MDPI Publisher of Open Access Journals: Data Journal, Special Issue: Forest Monitoring Systems and Assessments at Multiple Scales

Received: 30th June 2019 / Revised: 4th August 2019 / Accepted: 23rd September 2019 / Published: 25th September 2019

Abstract: Filling missing data in forest research is paramount for the analysis of primary data, forests statistics, land use strategies, as well as for the calibration/validation of forest growth models. Consequently, our main objective was to investigate several methods of filling missing data under a reduced sample size. From a complete dataset containing yearly first-rotation tree growth measurements over a period of eight years we have gradually retrieved two and then four years of measurements, hence operating on 100%, 72%, and 43% of the original data. Secondly, 15 statistical models, five forest growth functions, and one biophysical, process-oriented, tree growth model were employed for filling these data gap representations accounting for 72%, and 43% of the available data. Several models belonging to (**i**) regression analysis, (**ii**) statistical imputation, (**iii**) forest growth functions, and (**iv**) tree growth models were tested in order to retrieve information about the trees from existing yearly measurements. Subsequently, the findings of this study can lead to finding a handy tool for both researchers and practitioners dealing with incomplete data sets. Moreover, we underlined the paramount demand for far-sighted, long-term research projects for the expansion and maintenance of a SRF repository.

Keywords: Missingness, Data gap, Statistics, Amelia, Yield-SAFE

2.1. Background and Summary

Biomass generated from dedicated energy crops such as short rotation forestry (SRF) is growing recognition as a flexible source of energy, heat, fuel, bio-based materials, and chemicals (Strelher, 2000; BWE, 2015). SRF refers to growing fast-growing tree species, planted at a high-density (Christersson & Verma, 2006), and harvesting the trees in rotations of 2-6 years in order to produce woody biomass (Tsonkova *et al.*, 2012). Hence, the planting popularity of fast fast-growing tree species belonging to the genera *Populus*, *Eucalyptus*, *Pinus*, *Acacia*, and *Salix* increased as a result from the progressively higher demand for woody biomass for energy purposes (Carl *et al.*, 2017; Ceulemans *et al.*, 1996; Walle *et al.*, 2007; Sims *et al.*, 2001; Aravanopoulos *et al.*, 1999; Zewdie *et al.*, 2009; Sochacki *et al.*, 2007).

In order to support such demands, management decisions in the practice of SRF require systematic measurements of trees for repository and monitoring databases. Paramount for forest managers are accurate estimates of tree heights, root height diameter (RHD), and breast height diameter (BHD) for the determination of timber volume (Diamantopolou *et al.*, 2016).

However, forest research oftentimes confronts with missing data in field measurements (Diamantopolou *et al.*, 2016) due to sampling infeasibilities (bad weather, lack of equipment, lack of technical expertise), sampling irregularities across years, inaccurate estimations (allometric functions and the vast amount of methods to be used for calculating one parameter), or failure of equipment (dendrometers, lysimeters, station maintenance) (Wang *et al.*, 2012). Moreover, the available studies performed on SRF describe annual data values, collected over a few years from tens or hundreds of tree measurements, occasionally together with the standard deviation and number of samples, which nevertheless, leads to condensed annual information about the actual growth characteristics.

Missing data not only represents a loss of information and a source of uncertainty on data analysis, but a severe drawback from present investigations, as well as for future decision-making, coping management strategies, risk assessments, and adaptation scenarios. Therefore, filling missing data in forest research is paramount for the analysis of primary data, forests statistics, land use strategies, as well as for the calibration/validation of forest growth models.

Heretofore, little to no investigation was carried for handling missing forestry data. In a study performed by Diamantopolou *et al.* (2016), tree diameters were inferred with the help of a database containing more than 440 measurement points and under several artificial neural network models. However, studies on handling missing forestry data under a reduced sample size (e.g., yearly values over a five to ten years of growth) and for management practices such as SRF are rare.

Consequently, our main objective was to investigate several methods of filling missing data under a reduced sample size. Firstly, we have employed the complete dataset containing yearly first-rotation tree growth measurements in an SRF over a period of eight years, as reported by Bärwolf *et al.* (2016). From this complete dataset, we have gradually retrieved two and then four years of measurements, hence operating on 100%, 72%, and 43% of the original data. Secondly, 15 statistical models, five forest growth functions, and one biophysical, process-oriented, tree growth model were employed for filling these data gap representations accounting for 72%, and 43% of the available data.

Differences between the investigated models were addressed in order to retrieve information about the trees from existing yearly measurements, which could subsequently lead to finding a handy tool for both researchers and practitioners dealing with incomplete data sets. Moreover, we underlined the paramount demand for far-sighted, long-term research projects for the expansion and maintenance of a SRF repository.

2.2. Data Description

As a case study, we have employed the reported measurements of first-rotation hybrid-poplar trees (*Populus nigra* L. x *P. maximowicii* A. Henry, clone Max I) established near Dornburg, Germany (N51˚01'N, E11˚39'; 260m a.s.l.), on around 2 ha of a total area of 51.3 ha, and managed as short rotation forestry (SRF), over a time period of eight years (Bärwolf *et al.*, 2016). The poplar trees were planted in March 2007, at a planting density of 2,200 trees per hectare (i.e., at a tree spacing of 1.5 m x 3 m). With the exception of 2007, yearly measurements of height (H), root height diameter (RHD, measured at the height of 0.1 m above the ground), and breast height diameters (BHD, measured at the height of 1.3 m above the ground) were collected by the Thuringian Center for Renewable Resources, Thuringian State Institute for Agriculture between end of vegetation period 2008 and 2014.

Therefore, the initially reported data consisted of seven points collected from the end of vegetation period 2008 (winter season 2009) to end of vegetation period 2014 (winter season 2015). From this original data (100%), we randomly retrieved data accounting for two years (28%) and four years (57%) in order to create representations that simulate data gaps. The available range of observed data (i.e., n = 869, 975, 1350, and 1357 measurement values collected at the beginning of 2009, 2010, 2011, and 2012, respectively) is represented by the standard deviation (Figure 6).

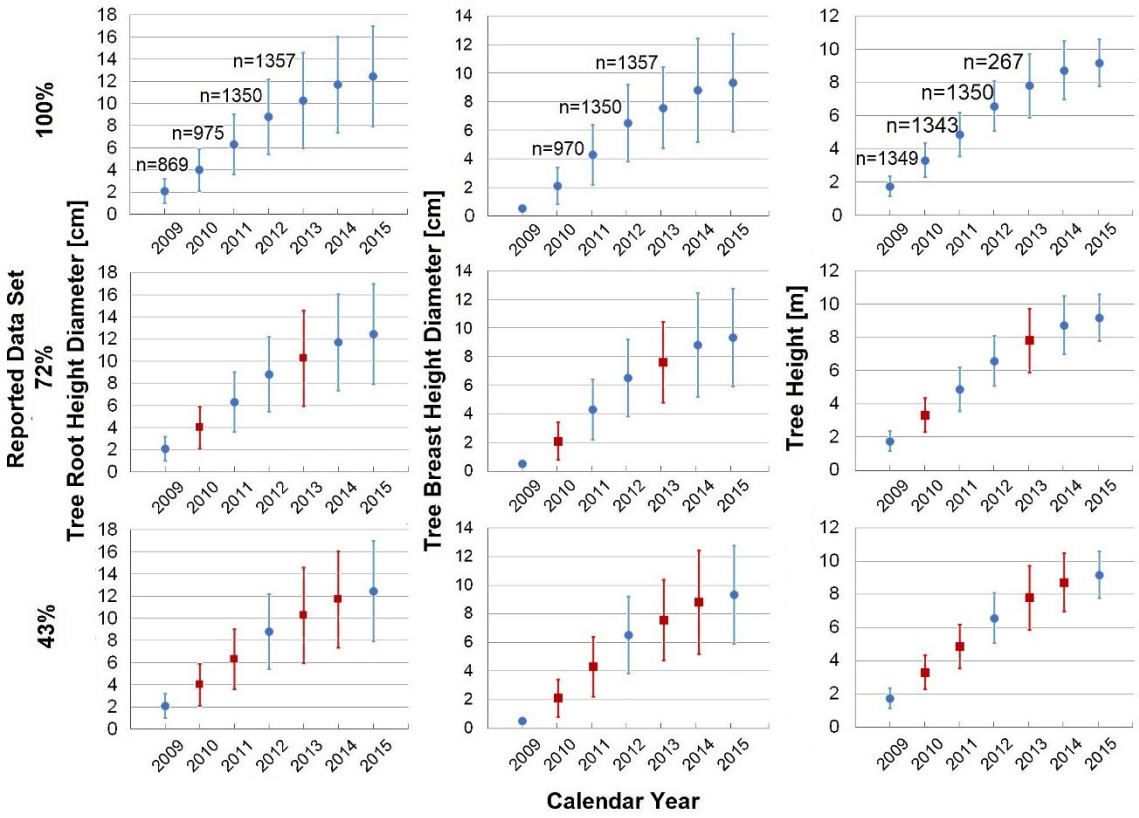

Figure 6. Originally reported data set (100%), as well as two data gap representations containing 72% and 43% of the original data for the tree root height diameter, breast height diameter, and tree height. The data is represented by the average value (blue circles and red squares for the existing and missing data, respectively), together with the standard deviation (blue and red error bars for the existing and missing data, respectively) and the sample size (n), when available.

In addition to separating the original data into two data gap representations containing 72% and 43% of the available data, we have also separated the analysis between the progression of an individual parameter in time and the progression of an individual parameter depending on another parameter. This way, the analysis has discerned between data missing completely at random (MCAR, i.e., values that are randomly missing from an original dataset do not relate to each other, and there is no pattern to the actual values of the missing

data) and data missing at random (MAR, i.e., values that are randomly missing from an original dataset and relate to other variables two by two). Due to physical and physiological factors that exist between tree dimensions in forest stands (Pretzsch, 2009), the relationship between variables was considered nonlinear throughout the study and numerical.

2.3. Methods and Materials

For the objective of this study, we have neglected the listwise deletion, an approach where missing observations are removed, and focused on imputing those missing values from the existing part of the data. In statistics, imputation is an approach where missing data is substituted, thus making this a standard method of handling missing data (Takanaschi, 2017). Nevertheless, we will not use zero or constant imputation, that replace the missing value with either zero or a constant value, respectively.

However, when filling missing data only through statistical imputations, the temporal resolution remains dependent on the existing data. Therefore, we also investigated the possibility of retrieving information on a finer temporal resolution (monthly, daily) from existing yearly measurements, with the help of a biophysical, process-oriented, tree growth model. Collectively, our analysis employed (**i**) regression analysis, (**ii**) statistical imputation, (**iii**) forest growth functions, and (**iv**) a tree growth model, which also takes into consideration the competition for resources between trees.

2.3.1. Regression Analysis

Regression analysis is a part of inference statistics where relationships between parameters are examined. Here, a "best fit" function (curve) with minimum residuals is assigned to the existing data points. For conciseness purposes, we recommend some standard textbooks for inference biostatistics methods from Linder (1951), Mudra (1958), and Rasch (1987).

Accordingly, ten regression models (Table 2) were applied to the established data gap representations by using the "Curve Fitting Toolbox" from Matlab (version R2017a, Mathworks).

Table 2. Investigated regression analysis models.

Model Name	General Model
Exponential	a*exp(b*x)
Fourier	a0 + a1*cos(x*w) + b1*sin(x*w)
Gaussian	a1*exp(-((x-b1)/c1)^2)
Power: 1 term	a*x^b
Power: 2 terms	a*x^b+c
Rational	(p1) / (x + q1)
Sum of Sine	a1*sin(b1*x+c1)
Linear Fit	a*(sin(x-pi)) + b*((x-10)^2) + c
Polynomial: 1st degree	p1*x + p2
Polynomial: 2nd degree	p1*x^2 + p2*x + p3

In this section, only MCAR data was taken into consideration because the data size of the response variable had to be the same as for the predictor variable. Accordingly, the progression of an individual parameter was investigated in time, together with the progression of an individual parameter depending on another parameter.

2.3.2. Interpolation

Interpolation is a part of inference statistics where an exact fit to the existing data points is identified. Accordingly, four regression models (Table 3) were applied to the established data gap representations by using the "Curve Fitting Toolbox" from Matlab (version R2017a, Mathworks).

Table 3. Investigated interpolation models.

Model Name	General Model
Interpolant: Nearest Neighbor	piecewise polynomial computed from p
Interpolant: Linear	
Interpolant: Cubic	
Interpolant: PCHIP ((Piecewise Cubic Hermite Interpolation)	

2.3.3. Multiple Imputation

Substituting missing data by multiple imputations has been a general-purpose approach of handling such data. Just as the name suggests, this approach creates multiple substitutes for a missing data point from all the information present in an existing dataset (Honaker *et al.*, 2011).

One of the most robust and accessible multiple imputation programs is represented by the Amelia II R-Package (Honaker *et al.*, 2011). Here, both MCAR data and MAR data were taken into consideration for analyzing the progression of an individual parameter in time and the progression of an individual parameter depending on another parameter. For this section, we have used the R software (version 3.4.2, R Core Team 2017).

2.3.4. Forest Growth Functions

Some of the investigated forest growth functions (Pretzsch, 2009) are presented in Table 4. Other functions were not added to this list because they resemble a general model presented previously, in Section 2.3.1. For example, the diameter-height relationship proposed by Assmann (1943) (H=a0+a1*d+a2*d^2) resembles the 2nd-degree Polynomial, and the allometric function (Pretzsch, 2009) (a*x^b) resembles a Power function with one term, as presented in Section 2.3.1. For this section, we have used Matlab (version R2017a, Mathworks).

Table 4. Investigated forest growth functions.

Model Name	General Model
Assmann (1943)	H=a+b*lnD
Korsun (1935)	H=exp(a0+a1 ×ln(D)+a2*ln^2(D))
Michailoff (1943)	H=a0*exp(−a1/D)+1.3
Petterson (1955)	H= (D/(a0 +a1 ×D))^3+1.3
Prodan (1951)	H=D^2/(a0+a1 *D+a2*D^2)+1.3

H: Height; D: diameter

In this case, only MAR data was used and only for analyzing the progression of tree height with respect to tree diameter.

2.3.5. Process-Oriented Growth Model

By a thorough review, Pretzsch *et al.*, (2015) compared 54 forest growth models in terms of characteristics and interactions that occur in forests both at an individual tree level and stand level. Accordingly, several models were identified as able to simulate the growth of poplar trees with respect to the specific tree phenology, light, and water availability. However, since our study focuses on retrieving information about the tree growth from limited availability of data, the Yield-SAFE model was employed.

The Yield-SAFE model (Yield Estimator for Long-term Design of Silvoarable AgroForestry in Europe) is a parameter-sparse, ecophysiological, process-oriented model, developed for growth processes in forestry, agriculture, and agroforestry systems (van der Werf *et al.*, 2007; Graves *et al.*, 2010; Keesman *et al.*, 2011). Heretofore, the Yield-SAFE model was calibrated and validated for poplar, walnut, cherry, holm oak, and stone pine trees in the Atlantic and Mediterranean regions of Europe (Burgess *et al.*, 2004; Burgess *et al.*, 2005; Palma *et al.*, 2007; Keesman *et al.*, 2011).

The main reasoning behind choosing the Yield-SAFE model, as implemented in Matlab, stood in its ability to render robust results under a scarcity of data (Graves *et al.*, 2010). In order to calibrate the model, a set of parameters and inputs was required, namely daily weather data (average daily temperature, precipitation, and radiation) over the investigated growth period, and site-specific soil and tree parameters.

The weather data was gathered from the DWD (Deutscher Wetterdienst) station Weimar (station ID: 05419). The tree parameters were set according to annual reports (Bärwolf *et al.*, 2016) and adapted from literature (Graves *et al.*, 2010; Keesman *et al.*, 2011). The clay and sand contents were 28, and 8%, respectively (Bärwolf *et al.*, 2016), which classified the soil texture as “medium-fine” and hence, the Mualem-van Genuchten soil parameters were set accordingly from existing estimations (Wösten *et al.*, 1999). Collectively, the tree and soil parameters used in the Yield-SAFE model are shown in appendixed Table A.1. In this case, only the progression of the BHD in time was substituted as part of MAR data.

2.3.6. Statistical Analysis

The performance of the investigated models was evaluated by the coefficient of determination (R^2), the sum of squared errors (SSE), root-mean-square error (RMSE), mean absolute error (MAE), as well a by the concordance correlation coefficient (CCC)

and the simulation bias (SB) from the observations. A fit is generally considered useful for prediction when R^2 values are closer to 1.0 and when SSE, RMSE, and MAE values are closer to 0.

In order to account for the variability of observations, the best fit of the investigated models was chosen with respect to the closeness to the average, as a representative for the location of the majority of measurements. Regarding the CCC and SB, a study performed by Ojeda *et al.*, (2017) proposed the following labels for the model validation: "very good" for CCC > 0.90 and SB < 20%, "satisfactory" for 0.75 < CCC < 0.90 and 20% < SB < 30%, "acceptable" for 0.60 < CCC < 0.75 and 30% < SB < 40% and "poor" for the rest of the cases. Together with these recommendations, we have categorized the performance of the models in terms of the CCC and SB, as well as in terms of the R^2, SSE, RMSE, and MAE, while striving for a normal distribution of the residuals.

2.4. Results and Discussion

Regarding the original available data set, the data points for a single year were spread out over a wide range of values, especially for the diameter measurements (Figure 6), amounting to around ±25% for the tree heights and around ±40% for the tree diameters, as compared to their respective average values. This is, however, the case for many fast-growing tree species such as black locust (*Robinia Pseudoacacia* L.) (Kanzler & Böhm, 2016) and poplar (*Populus* spp.) (Kanzler & Böhm, 2016; Lamerre *et al.*, 2016) that show great growth variability, even when planted at the same time and on the same land area. By comparison, first-rotation poplar trees established at the experimental site Neißetal reported a standard deviation of about ±30% for the tree heights and about ±40% for the root height diameter (RHD) over three years of growth (Kanzler & Böhm, 2016). At Wendhausen, the measurement variability of breast height diameter (BHD) amounted to around 39%, as compared to the average of all values and over six growing years at Wendhausen (Lamerre *et al.*, 2016).

2.4.1. Regression Analysis

Most of the investigated ten regression models were able to fit a curve to the existing data within the limits set by the standard deviation, except for the Exponential and the one-term Power model, due to an inability to fit the progression of tree dimensions in time and the Fourier model, due to an inability to fit when subjected to the 43% data gap

representation. For the conciseness of the paper, appendixed Table A.2. presents the goodness of validation of all applied regression models.

Generally, the Gaussian model performed the best, being tightly followed by the Power model with two terms, Sum of Sine, and the Polynomial of 1st Degree, then the Polynomial of 2nd Degree. The lower end was represented by the Rational, Fourier, Exponential, and one term Power model in descending order, ending with the Linear Fitting.

As an example of the capability of the models to infer missing data from the available 43% data gap representation of RHD, three regression models labelled as "very good" (Gaussian), "satisfactory" (Sum of Sine), and "poor" (Linear Fitting), were selected and presented in Figure 7.

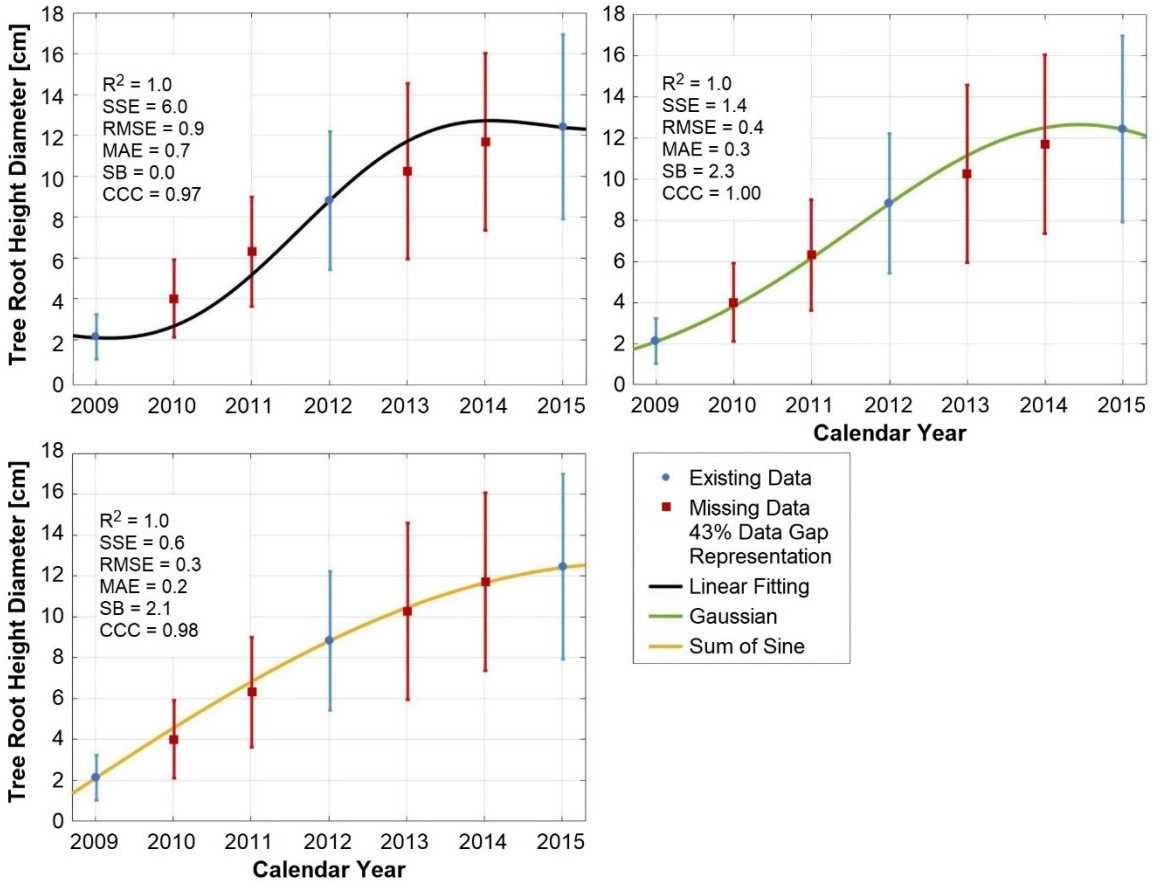

Figure 7. Linear fitting (black line), Gaussian (green line), and Sum of Sine (orange line) applied on the tree root height diameter data gap representation accounting for 43% of the original data set in terms of the coefficient of determination (R^2), sum of squared errors (SSE), root-mean-square error (RMSE), mean absolute error (MAE), as well as the concordance correlation coefficient (CCC) and the simulation bias (SB) from the observations. The error bars (blue and red for the existing and missing data, respectively) represent the standard deviation of the tree root height diameter over the investigated period.

Visible differences exist between the three regression models presented in Figure 7 and show that even slight differences in SSE, RMSE, and MAE should not be neglected. Even if the deviations from the fitted curve to the observations seem small, significant biases can later arise from further calculations.

2.4.2. Interpolation

All of the investigated interpolation models were capable of finding a fit encompassed in the range of observations. However, when striving for the average value, as a central tendency for most of the observations, the interpolation models generally performed the best to worse in the following sequence: Linear > Cubic > PCHIP > Nearest Neighbor. For the conciseness of the paper, appendixed Table A.3. presents the goodness of validation of all applied interpolation models.

However, since the SSE, RMSE, and MAE values were rather high when fitting the tree height in time, the 72% data gap representation of tree height is furtherly examined (Figure 8).

Since interpolation techniques find an exact fit to the existing data, they assume no measurement errors, suggesting that their applicability to real-life scenarios is limited. However, Figure 8 shows rather accurate estimations of tree height in time and under limited data availability. Nevertheless, while interpolation is easy and fast, it does not factor the correlations between features, and it does not account for the uncertainty in the imputations.

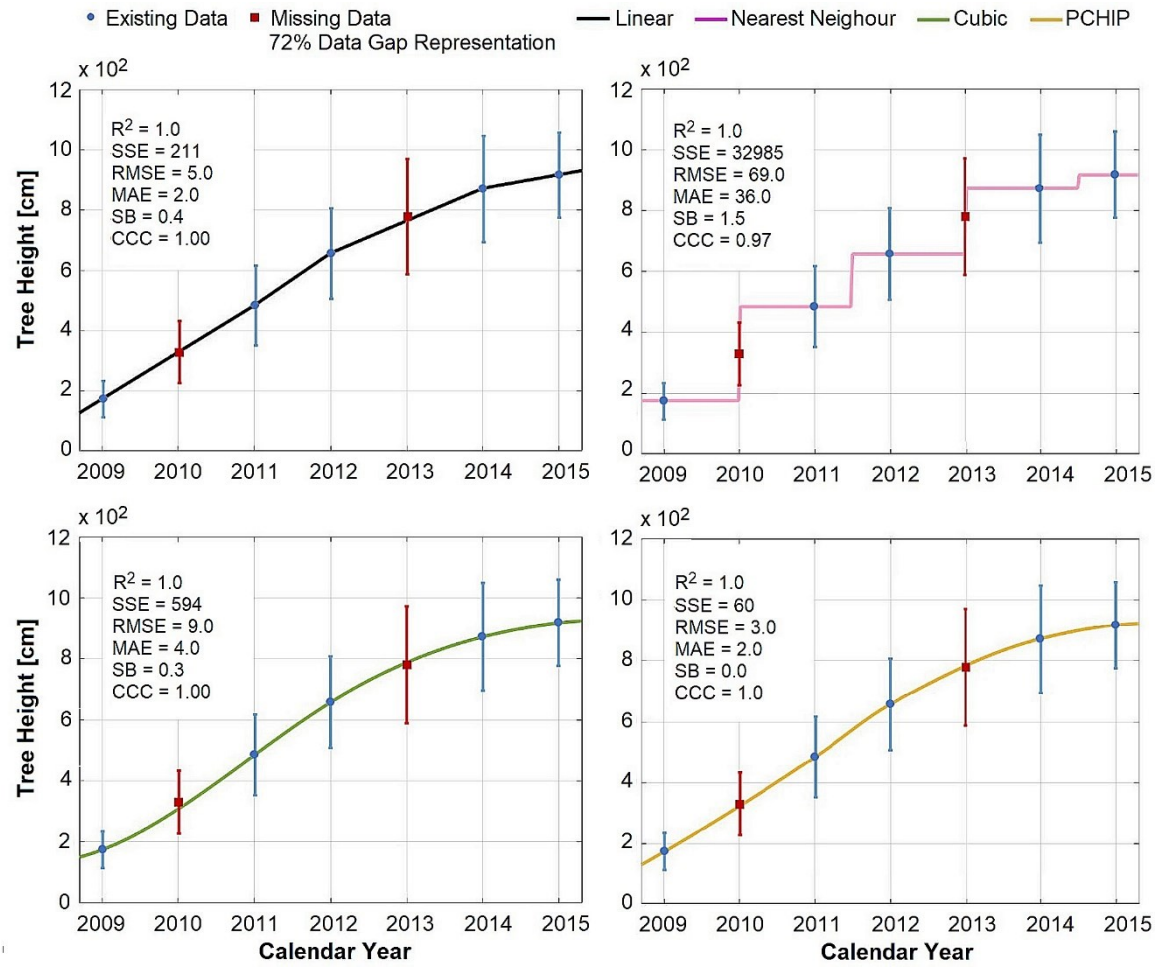

Figure 8. Interpolation models Linear (black line), Nearest Neighbor (pink line), Cubic (green line), and PCHIP (orange line) applied on the tree height data gap representation accounting for 72% of the original data set together with the coefficient of determination (R^2), sum of squared errors (SSE), root-mean-square error (RMSE), mean absolute error (MAE), as well as the concordance correlation coefficient (CCC) and the simulation bias (SB) from the observations. The error bars (blue and red for the existing and missing data, respectively) represent the standard deviation of the tree height over the investigated period.

2.4.3. Multiple Imputation

Most of the investigated imputations rendered by Amelia II represented values within the whole range of measurements. However, when considering the majority of values, only a few results of Amelia II were labeled as delivering more than an "acceptable" performance (Table 5).

Table 5. Goodness of validation of Amelia II in terms of the coefficient of determination (R^2), sum of squared errors (SSE), root-mean-square error (RMSE), mean absolute error (MAE), as well as the concordance correlation coefficient (CCC) and the simulation bias (SB) from the observations.

Model	Variable	Data Gap Representation	R^2	SSE	RMSE	MAE	SB [%]	CCC	Label
Amelia	RHD	72	1.00	0.2	0.3	0.3	6.4	1.00	Satisfactory
		43	1.00	4.1	1.0	0.8	14.9	0.00	Poor
	BHD	72	0.99	0.7	0.6	0.6	11.5	0.97	Poor
		43	0.99	0.4	0.3	0.3	5.5	0.99	Acceptable
	Height	72	0.99	10110.2	71.1	57.3	14.1	0.94	Poor
		43	0.99	24478.6	78.2	70.4	4.3	0.92	Satisfactory
	BHD &	72	1.00	0.9	0.7	0.6	15.1	0.97	Poor
	RHD	43	0.99	5.0	1.1	1.0	3.6	0.44	Poor
	Height &	72	1.00	1627.5	20.5	20.4	10.1	0.98	Poor
	BHD	43	0.98	2986.8	19.6	16.7	7.6	0.98	Poor
	Height &	72	1.00	1214.8	17.7	17.3	3.6	0.99	Poor
	RHD	43	0.99	3065.4	19.8	17.9	4.7	0.49	Poor

RHD: root height diameter; BHD: breast height diameter

2.4.4. Forest Growth Functions

Most of the investigated forest growth functions were labeled as delivering a “very good” performance (Table 6). Accounting for all statistical coefficients, the Korsun (1935) model fit the best, followed by Michailoff (1943) and Petterson (1955), Prodan (1951), and then Assmann (1943).

Table 6. Goodness of validation of forest growth functions in terms of the coefficient of determination (R^2), sum of squared errors (SSE), root-mean-square error (RMSE), mean absolute error (MAE), as well as the concordance correlation coefficient (CCC) and the simulation bias (SB) from the observations.

Model	Variable	Data Gap Representation	R^2	SSE	RMSE	MAE	SB [%]	CCC	Label
Assmann (1943)	Height	72	0.99	3.68	0.73	0.64	3.8	0.97	Poor
	BHD	43	0.98	4.77	0.83	0.66	7.5	0.96	Poor
	Height	72	0.99	5.49	0.89	0.79	1.8	0.75	Poor
	RHD	43	0.99	7.10	1.01	0.84	6.1	0.70	Poor
Prodan (1951)	Height	72	0.98	1.51	0.46	0.34	4.3	0.99	Satisfactory
	BHD	43	0.98	91.19	3.61	2.22	25.1	0.68	Poor
	Height	72	1.00	0.10	0.12	0.10	-0.3	1.00	Very good
	RHD	43	1.00	0.13	0.14	0.10	0.2	1.00	Very good
Petterson (1955)	Height	72	0.97	1.70	0.49	0.33	4.2	0.99	Acceptable
	BHD	43	0.97	1.65	0.49	0.34	4	0.99	Acceptable
	Height	72	1.00	0.10	0.12	0.08	-0.5	1.00	Very good
	RHD	43	1.00	0.10	0.12	0.09	0.3	1.00	Very good
Korsun (1935)	Height	72	1.00	0.11	0.13	0.08	1.1	1.00	Very good
	BHD	43	1.00	0.11	0.13	0.07	1	1.00	Very good
	Height	72	1.00	0.12	0.13	0.11	-0.2	1.00	Very good
	RHD	43	1.00	0.11	0.13	0.09	1.1	1.00	Very good
Michailoff (1943)	Height	72	0.99	0.92	0.36	0.23	3.5	0.99	Satisfactory
	BHD	43	0.98	0.90	0.36	0.25	3.2	0.99	Satisfactory
	Height	72	0.99	0.62	0.30	0.25	-1.7	1.00	Very good
	RHD	43	0.99	0.76	0.33	0.27	-1.2	1.00	Satisfactory

RHD: root height diameter; BHD: breast height diameter

2.4.5. Process-Oriented Growth Model

If not for a high simulation bias from observations in the first years (Figure 9), the performance of the Yield-SAFE model would have been generally labelled as "very good" for this experimental site (Table 7).

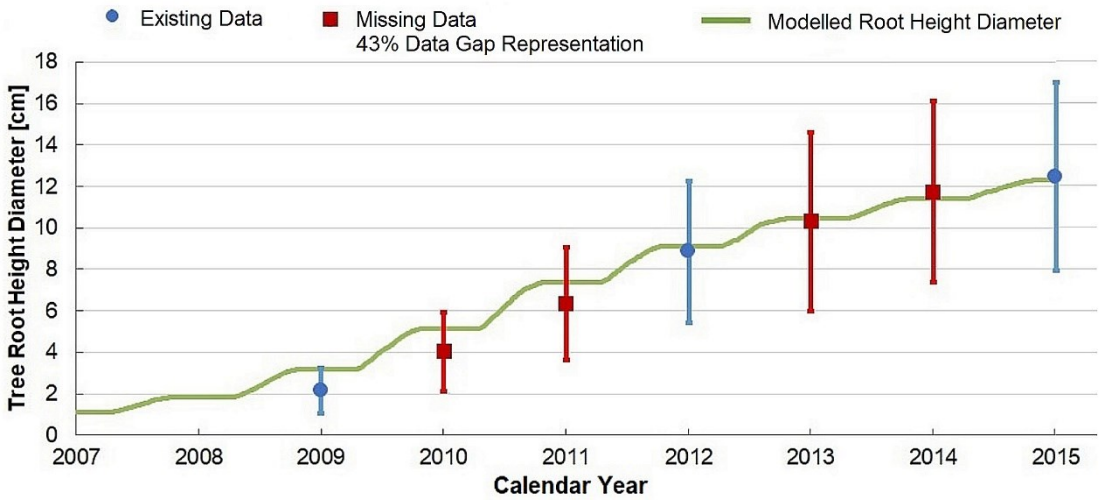

Figure 9. The tree root height diameter, as simulated with the Yield-SAFE model (green line) given the existing data (blue circles) and the missing data (red squares). The error bars (blue and red for the existing and missing data, respectively) represent the standard deviation of the root height diameter over the investigated period.

Table 7. Goodness of validation of Yield-SAFE in terms of the coefficient of determination (R^2), sum of squared errors (SSE), root-mean-square error (RMSE), mean absolute error (MAE), as well as the concordance correlation coefficient (CCC) and the simulation bias (SB) from the observations.

Model	Variable	Data Gap Representation	R^2	SSE	RMSE	MAE	SB [%]	CCC	Label
Yield-SAFE	RHD	72	1.00	3.7	1.0	0.9	12.4	0.99	Satisfactory
		43	1.00	4.0	1.1	1.1	15.1	0.99	Satisfactory

RHD: root height diameter

Nevertheless, the Yield-SAFE model rendered "satisfactory" correspondences with the measured tree root height diameter under 43% availability of data, with deviations between 17% and 51% in the first three years and between 1% and 4% in the later years.

Notable to this section is that, by using a biophysical, process-oriented model, there is the possibility of retrieving information on a finer temporal resolution (monthly, daily)

from existing yearly measurements and even information about other parameters, such as woody biomass and soil water content (Figure 10).

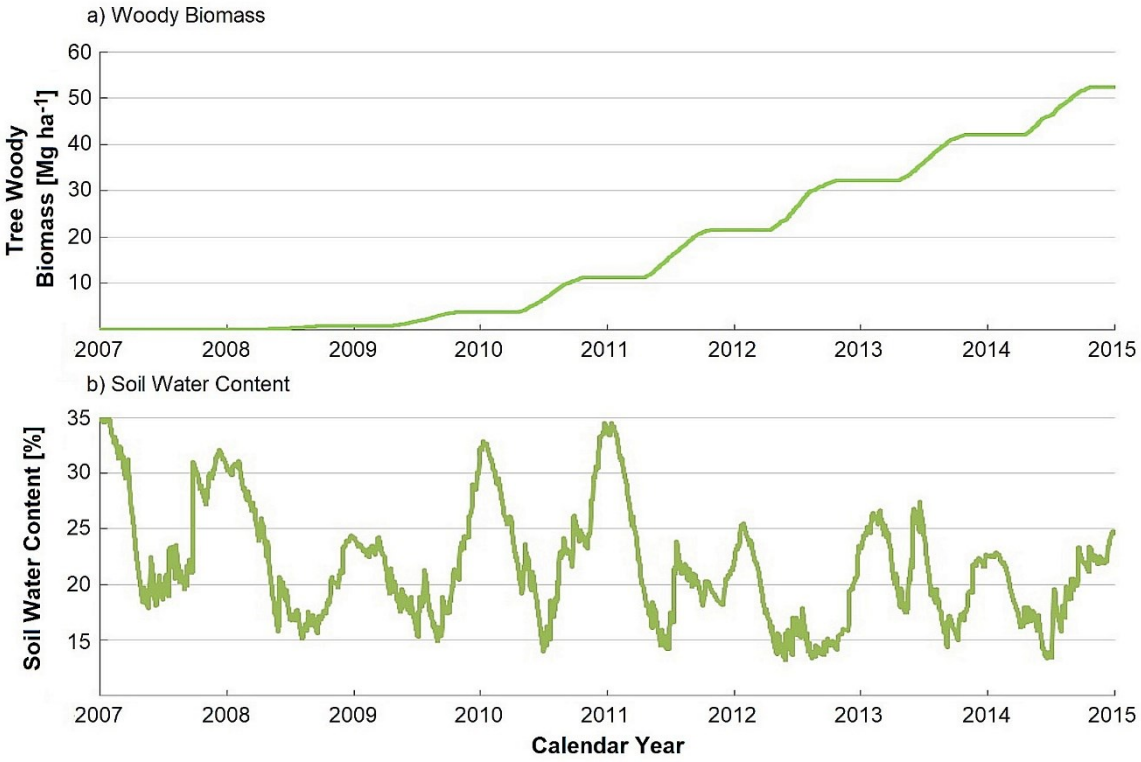

Figure 10. The tree woody biomass (**a**) and soil water content (**b**), as simulated with the Yield-SAFE model (green lines) from the day of planting (2007) to the day of harvest (2015).

The tree woody biomass and the soil water content, as simulated by the Yield-SAFE model were broadly corroborated by on-site assessments. According to reported values, an average tree woody biomass of around 52 Mg ha^{-1} was harvested from the poplar SRF at the end of vegetation period 2014 (winter season 2015) (Bärwolf *et al.*, 2016). Regarding the soil water content, between 13% and 24% water was reported at the tree strips at the beginning of June 2012, and between 15% and 35% at the end of November 2012.

Notable would be that, while tree growth models are widely used for prediction purposes, either for future risk assessments, or under different climatic, edaphic, and management scenarios, this study emphasizes another role of such models and namely for imputing the gaps in knowledge.

2.5. Conclusions

This paper presented and analyzed the performance of several models belonging to (**i**) regression analysis, (**ii**) statistical imputation, (**iii**) forest growth functions, and (**iv**) tree

growth models to retrieve information about the trees from existing yearly measurements. Taking into consideration the entire range of measured data deemed the performance of all investigated models as “very good”. However, focusing on the area comprising most of the observations, or central tendency of the data, as shown by the average, arose significant differences between the models.

From the curve-fitting models, the Gaussian model performed the best, being tightly followed by the Power model with two terms, Sum of Sine, and the Polynomial of 1st Degree, then the Polynomial of 2nd Degree. Nearing this performance, the interpolation models Linear, Cubic, and PCHIP have also shown good correspondences with the measurements, both under 72% and 43% data gap representations. The forest growth functions rendered good results, following the sequence: Korsun (1935) > Michailoff (1943) and Petterson (1955) > Prodan (1951) > Assmann (1943). Unsurprisingly, most of these models performed better under higher data availability, i.e., under 72% of existing data, as compared to 43% of existing data.

The Yield-SAFE model simulated the daily growth of hybrid-poplar clone “Max I” in terms of root height diameter with satisfactory accuracy, responding sensitively to changes in the edaphic and climatic conditions. Additionally, the performance of the model is sustained by other parameters, such as the tree woody biomass and soil water content, which matched reported values. Last but not least, this study showed that a process-oriented model such as Yield-SAFE could provide with descriptions of tree growth and soil water content on a finer, daily temporal scale from scarce availability of data.

Therefore, the findings of this study could subsequently lead to finding a handy tool for both researchers and practitioners dealing with incomplete data sets. In the future, for a better understanding and reproducibility of studies, box plots should be increasingly used, showing minimums, maximums, medians, means, outliers, and the interquartile range. Moreover, we underlined the paramount demand for far-sighted, long-term research projects for the expansion and maintenance of a SRF repository.

Author Contributions

The SIGNAL project was initiated and planed in relation to the proposal call “Soil as a Sustainable Resource for the Bioeconomy – BonaRes” (http://www.signal.uni-goettingen.de). Diana Seserman analysed the data and wrote the manuscript. Dirk Freese contributed by revising the manuscript.

Funding

This research was carried out under the BonaRes - SIGNAL project (FKZ 031A562E, 2015-2018) and funded by BMBF - German Federal Ministry of Education and Research (Bundesministerium für Bildung und Forschung).

Acknowledgments

We are grateful to the editor and reviewers for their time, assistance, and suggestions that helped improve this paper.

Conflicts of Interest

The authors declare no conflict of interest. The founding sponsors had no role in the design of the study; in the collection, analyses, or interpretation of data, in the writing of the manuscript, and in the decision to publish the results.

3. Climate Change Impacts on Hybrid-Poplar and Black Locust Short Rotation Coppices by a Combined Experimental and Simulation Study

Diana-Maria Seserman [1,*], Ina Pohle [2,3], Maik Veste [4,5], Dirk Freese [1]

[1] Brandenburg University of Technology Cottbus–Senftenberg, Institute of Environmental Sciences, Soil Protection and Recultivation, Konrad-Wachsmann-Allee 8, 03046 Cottbus, Germany; seserman@b-tu.de; dirk.freese@b-tu.de

[2] The James Hutton Institute, Environmental and Biochemical Sciences, Craigiebuckler, Aberdeen AB15 8QH, Scotland, United Kingdom; ina.pohle@hutton.ac.uk

[3] Brandenburg University of Technology Cottbus–Senftenberg, Institute of Environmental Sciences, Hydrology and Water Resources Management, Siemens-Halske-Ring 8, 03046 Cottbus, Germany; ina.pohle@b-tu.de

[4] University of Hohenheim, Institute of Botany, Garbenstrasse 30, 70599 Stuttgart-Hohenheim, Germany; maik.veste@uni-hohenheim.de

[5] CEBra – Centrum for Energy Technology Brandenburg e.V., Friedlieb-Runge-Strasse 3, 03046 Cottbus, Germany;

* Correspondence: seserman@b-tu.de; Tel.: +49-355-69-4329

MDPI Publisher of Open Access Journals: Forests Journal, Section Forest Ecophysiology and Biology

Received: 20th June 2018 / Revised: 8 th July 2018 / Accepted: 9 th July 2018 / Published: 12 th July 2018

Abstract: In Brandenburg, north-eastern Germany, climate change is associated with increasing annual temperatures and decreasing summer precipitation. Appraising short rotation coppices (SRCs) given their long-time planning horizon demands for systematic assessments of woody biomass production under a considerable spectrum of climate change prospects. This paper investigates the prospective growth sensitivity of poplar and black locust SRCs, established in Brandenburg to a variety of weather conditions and long-term climate change, from 2015 to 2054, by a combined experimental and simulation study. The analysis employed (**i**) a biophysical, process-based model to simulate the daily tree growth and (**ii**) 100 realisations of the statistical regional climate model STAR 2K. In the last growing rotation, the simulations showed that the assumed climate change could lead to a decrease in the woody biomass of about 5 Mg ha^{-1} (18%) for poplar and a decrease of about 1.7 Mg ha^{-1} (11%) for black locust trees with respect to the median observed in the reference period. The findings corroborate the potential tree growth vulnerability to prospective climatic changes, particularly to changes in water availability and underline the importance of coping management strategies in SRCs for forthcoming risk assessments and adaptation scenarios.

Keywords: Climate scenario; Tree growth; Tree biomass; Yield-SAFE;

3.1. Introduction

As outlined by the European Commission in the Energy Roadmap 2050 (European Commission, 2011), the share of renewable energy sources must increase in gross final energy consumption to at least 55% and in electricity consumption to at least 64%, while simultaneously striving for a low-carbon goal. Stemming from these efforts to reduce energy wastage, fossil fuels, and greenhouse gas emissions, to mitigate climate change and the availability of natural resources, the potential of raw materials for bio-based sectors progressively grows recognition (European Commission, 2011).

Since biomass is regarded as a flexible primary energy for the generation of energy, heat, fuel, bio-based materials, and chemicals, it can play an important role in achieving the renewable energy goal set by 2050 (Strelher, 2000; BWE, 2015). Biomass generated from dedicated energy crops such as short rotation coppices (SRCs) is accompanied by many advantages such as efficient nutrient utilization, low erosion potential (Abbasi *et al.*, 2010), and low to no requirement for pesticide and fertilizer (Evans *et al.*, 2010). Furthermore, SRCs have shown high biomass yields (Ceulemans *et al.*, 1999), adequate fuel properties (Hauck *et al.*, 2014), and low emissions from alternative fuels and flexibility to consumer demand (Evans *et al.*, 2010). In Europe, the high demand for woody biomass for energy purposes increased the planting popularity of fast-growing tree species belonging to the genera *Populus*, *Eucalyptus*, *Pinus*, *Acacia*, and *Salix* (Carl *et al.*, 2017; Ceulemans *et al.*, 1996; Walle *et al.*, 2007; Sims *et al.*, 2001; Aravanopoulos *et al.*, 1999; Zewdie *et al.*, 2009; Sochacki *et al.*, 2007).

Understanding whether SRCs are economically profitable and environmentally sustainable requires long-term assessments of woody biomass production in strong relation to changes in environmental conditions like the ongoing climate change (Evans *et al.*, 2010; van Vooren *et al.*, 2016; Gerstengarbe *et al.*, 2003). During the past decade, increasing annual temperature and tendencies towards decreasing summer and increasing winter precipitation were reported in north-eastern Germany (Gädeke *et al.*, 2017; Rauthe *et al.*, 2013). In Central Europe, projections of future climate assume increasing climate variability and number of extreme weather events (Jacob *et al.*, 2014; Christensen *et al.*, 2007).

However, evaluating the climate change impacts on the tree woody biomass from observational and experimental studies has been subject to various limitations in what

regards the influence of interacting factors. Moreover, potential future climate changes have been reported to go beyond historical observations (Ruane *et al.*, 2016).

Therefore, simulation studies have been widely applied to model the tree growth in relation to environmental factors (Horeman *et al.*, 2017; de Vries *et al.*, 2017), assessing climate change impacts on the growth performance of aspen (*Populus tremula* L.), Norway spruce (*Picea abies* L. Karst.), Scots pine (*Pinus sylvestris* L.), European beech (*Fagus sylvatica* L.), oak (*Quercus robur* L. x *Quercus petraea* Liebl.), and Douglas fir (*Pseudotsuga menziesii* (Mirb.) Franco) (Lasch *et al.*, 2010; Lasch-Born *et al.*, 2015; Reyer *et al.*, 2014; Wang *et al.*, 2017). Field experiments for short rotation forestry were carried for *Populus* and *Salix* and for breeding of clones (Monclus *et al.*, 2005; Calfapietra *et al.*, 2010). However, long-term studies on the variability of woody biomass production under different climatic conditions for certain tree species such as black locust (*Robinia pseudoacacia* L.) and for management practices such as short-term forestry are rare (Carl *et al.*, 2017).

The objective of this paper was to evaluate the potential growth vulnerability of two fast-growing tree species established in Brandenburg, Germany and managed as short rotation coppices (SRCs), to a considerable spectrum of weather conditions and long-term climate change. By a combined experimental and simulation study, we investigated the prospective growth of hybrid-poplar clone "Max I" (*Populus nigra* L. x *P. maximowiczii* Henry) and black locust (*Robinia pseudoacacia* L.) trees in terms of above-ground woody biomass production, from 2015 to 2054.

Based on the implications of this study, it will be possible to develop and optimize the designs of SRCs and to provide with a reliable estimation of achievable woody biomass yields according to tree species, management, and climate change effects.

3.2. Materials and Methods

In order to handle uncertainties in assessing the climate change impacts on tree growth due to interrelations between various factors, Medlyn *et al.* (2011) suggested an integration of experimental and simulation studies. Thus, our methodology to investigate the impacts of weather conditions and long-term climate change on the above-ground woody biomass of hybrid-poplar and black locust trees employed (**i**) an experimental site with SRCs in Brandenburg, Germany, (**ii**) a biophysical, process-based model to simulate the daily tree growth on the basis of tree parameters, soil physical characteristics, and weather data (van

der Werf *et al.*, 2007), and (**iii**) 100 realisations of a scenario of the statistical regional climate model STAR, which assumed an increase in annual temperature of 2K, as well as a decreasing annual precipitation by 30–40 mm, between 2000 and 2055 (Gerstengarbe *et al.*, 2003; Werner & Gerstengarbe, 1997; Orlowsky *et al.*, 2008).

3.2.1. Site Description

The study site at Neu Sacro (N 51˚46'54'', E 14˚37'18'', 67 m a.s.l.) is situated in Lower Lusatia, in the south of the German Federal State of Brandenburg. The SRC is established 500 m away from the Lusatian Neisse river, comprising around 5 ha, out of which black locust trees (planted in spring 2010) spread over 2 ha and poplar trees (re-planted in spring 2011) spread over 2.5 ha. These two tree species were planted in double rows, resulting in a planting density of about 8700 trees per hectare (0.75 m x 0.90 m spacing with a 1.80 m tree strip along the tree row) (Kanzler & Böhm, 2016).

The climate in the area has an average temperature of about 8.9°C and an average annual precipitation of 563 mm a^{-1} (standard reference period: 1960–1990; weather station Cottbus of the German Weather Service, about 25 km west of the site) and an average temperature of about 9.9°C and an average annual precipitation of 577 mm a^{-1} (current period: 1990–2015).

The site is characterized by a Gley-Vega and Pseudogley-Vega soil with a sandy loam texture. The ploughing horizon (0–30 cm depth) is characterized by a mean particle size distribution of 65% sand, 29% silt, and 6% clay, a content of soil total organic carbon of 10.44%, a content of total nitrogen of 0.95%, and a pH ($CaCl_2$) value of 5.75. The groundwater level varies between 0.8 m and 2.0 m below the surface (Kanzler & Böhm, 2016).

3.2.2. Yearly Measurements of Above-Ground Woody Biomass

The rotations were five years (2010-2014) for black locust and four years (2011-2014) for poplar. These growing periods correspond to the length of a medium rotation cycle (Bielefeldt *et al.*, 2008). Tree shoot basal diameters were measured at the end of every year. At the end of the vegetation period, in 2014, fifty poplar and fifty black locust trees were harvested about 10 cm above the ground for the measurement of fresh weight. The stem and branches of these trees were shredded into wood chips, and sub-samples of every

shredded tree were taken to the laboratory for the determination of above-ground tree dry woody biomass by drying at 105˚C until constant weight (Verwijst & Telenius, 1999).

Subsequently, the above-ground woody biomass was estimated for the earlier years by using an allometric equation, as given in Equation (1) (Zianis & Mencuccini, 2003; Böhm *et al.*, 2011):

$$B = a \cdot D^b, \qquad \text{Eq.(1)}$$

where B is the above-ground tree dry woody biomass [kg], D is the shoot basal diameter [cm], and a and b are constants. By applying a least-square linear regression of natural-logarithmic-transformed data for the diameter and tree biomass measured in 2014, a and b were determined as the intercept and slope of the regression, respectively. Thus, the obtained values were a = 0.0551, b = 2.2963 for poplar (R^2 = 0.98) and a = 0.0396, b = 2.5594 for black locust (R^2 = 0.96).

For comparison purposes, this study focused on the above-ground woody biomass over the growing period of four years from 2010 to 2013 for black locust and from 2011 to 2014 for poplar.

3.2.3. Modelling the Above-Ground Woody Biomass

3.2.3.1. Description of the Yield-SAFE model

For the simulations of site-specific, long-term tree yields under competitive conditions, we used the Yield-SAFE model (Yield Estimator for Long-term Design of Silvoarable AgroForestry in Europe), a parameter-sparse, eco-physiologically based model (Stappers *et al.*, 2003; van der Werf *et al.*, 2007; Keesman *et al.*, 2011), as implemented in Matlab (Graves *et al.*, 2010).

Heretofore, the performance of the Yield-SAFE model was evaluated with respect to long-term tree yields measured across 19 landscape test sites in Spain, France, and the Netherlands (Burgess *et al.*, 2005). Yield-SAFE was parameterized and validated for cherry, poplar, walnut, and oak trees given data from the Atlantic and Mediterranean regions of Europe (Stappers *et al.*, 2003; Burgess *et al.*, 2005; van der Werf *et al.*, 2007; Keesman *et al.*, 2011; Palma *et al.*, 2007; Palma *et al.*, 2014).

The model requires information about the trees (species, dimensions, planting density, day of bud-burst, day of leaf-fall), soil physical characteristics (soil texture, bulk density),

and daily weather data (global radiation [W m^{-2}], air temperature [°C], and precipitation [mm]). The potential tree growth is modelled in terms of resource use efficiency of primarily air temperature (due to the developmental and phenological processes), global radiation (as the main driver for photosynthesis), and, to a lesser extent, water (van der Werf *et al.*, 2007). Under this potential growth assumption, nutrient availability is not considered to be a yield-limiting factor (van der Werf *et al.*, 2007).

Consequently, the Yield-SAFE simulations require four state equations regarding: (1) the tree biomass, used to derive temporally-integrated timber volumes by means of tree harvest index, dry wood density, and a factor accounting for the proportion of biomass that produces timber; (2) the tree leaf area, for the regulation of the radiation capture, thus of the dry matter production and the water losses through transpiration; (3) the number of shoots per tree, for the annual potential leaf area, and (4) the soil water content, with respect to the water holding properties of the given soil and the degree of water limitation (such as precipitation, soil depth).

In the Yield-SAFE model, the water uptake is implemented by means of a root inter-zone between trees. The model assumes one soil layer, homogeneous in its physical characteristics, whose volumetric water content is calculated in terms of precipitation, drainage of soil water below the potential tree rooting zone, and the actual soil evaporation. The evaporation is calculated in terms of heat of vaporization, radiation incident on the soil, and a factor that accounts for the reduction in soil evaporation. Altogether, the water used by the trees per unit area per day is implemented so that it accounts for the biomass reductions due to respiration losses or senescence and is calculated by multiplying the water-limited growth rate per tree with the tree density and the transpiration coefficient (van der Werf *et al.*, 2007; Keesman *et al.*, 2011).

A detailed description of the assumptions, equations, and parameters embodied in the Yield-SAFE model can be found in van der Werf *et al.* (2007) and Keesman *et al.* (2011), together with default parameter values for a substantial range of tree species, as determined by Burgess *et al.* (2005).

3.2.3.2. Sensitivity analysis of the Yield-SAFE model

In order to minimize uncertainties and gain insight into which parameters influence the model output the most, a one-at-a-time sensitivity analysis was conducted (Equation (2)). This meant that the nominal value of each previously calibrated parameter was changed by

± 10% while fixing the other parameters at their default values (Keesman *et al.*, 2011). The sensitivity, *S* was calculated by:

$$S = \frac{B_{t(+10)} - B_{t(-10)}}{X_{(+10)} - X_{(-10)}}, \quad \text{Eq.(2)}$$

where B_t is the modelled tree biomass (g tree^{-1}) obtained through Yield-SAFE simulations with a ±10% change in parameter *X*. In order to compare the parameter sensitivity independently of scale, a relative, normalized sensitivity was computed (Equation (3)):

$$S_{norm.} = S \cdot \frac{X}{B_t}, \quad \text{Eq.(3)}$$

Accordingly, all parameters with an absolute normalized sensitivity higher than 0.1 were labelled as dominant, as they exhibited a comparative high influence on the model output.

3.2.3.3. Parameterization and validation of the Yield-SAFE model

The Yield-SAFE model was parametrized separately for poplar and black locust trees, given their distinct growth behaviour and the site-specific conditions, such as weather and edaphic conditions. Initial estimates of tree and soil parameters were adapted from field measurements and studies performed by Keesman *et al.* (2011), Graves *et al.* (2010), and Wösten *et al.* (1999) (appendixed Table B.1.).

The start and end of vegetation period were given as static inputs (poplar: $DOY_{bud\text{-}burst}$ = 105, $DOY_{leaf\text{-}fall}$ = 280; black locust: $DOY_{bud\text{-}burst}$ = 125; $DOY_{leaf\text{-}fall}$ = 310 (Küppers *et al.*, 2017). Therefore, the weather data have been analysed for the distinctive vegetation periods of the tree species.

The historical weather data were taken from the weather station Cottbus. As global radiation was not measured at this weather station, it was estimated for the years 2010 – 2015, according to the Ångström regression equation modified by Page (1964) (Equation (4)):

$$\overline{H} = \overline{H_0}\left(a + b \cdot \frac{\overline{n}}{\overline{N}}\right), \quad \text{Eq.(4)}$$

where $\overline{H}$ is the monthly average daily radiation on the horizontal surface, $\overline{H_0}$ is the monthly average daily extra-terrestrial solar radiation, $\overline{n}$ is the monthly mean daily sunshine duration, and $\overline{N}$ is the monthly mean maximum possible sunshine duration. The empirical

coefficients *a* and *b* were derived from the German Weather Service station Lindenberg (52°20'85''N, 14°11'80''E; 98m a.s.l., about 90 km north-west of the experimental site) and transferred to the weather station Cottbus. Accordingly, a = 0.14 and b = 0.47 for the months between November and February, a = 0.24 and b = 0.40 for June, July, and August, and a = 0.36 and b = 0.23 for the rest of the months.

The resulted values for the modelled tree woody biomass were validated against the measured values in order to test the applicability of the Yield-SAFE model to simulate and subsequently project the tree woody biomass production under various prospective weather conditions. The performance of the model was evaluated visually by comparing the measured and modelled tree woody biomass, as well as by the normalized root-mean-square error (NRMSE) and the coefficient of determination (R^2).

3.2.4. Prospective Climate Change

Once validated, the Yield-SAFE model simulated the tree woody biomass production under prospective weather conditions from the statistical regional climate model Statistical Analogue Resampling scheme (STAR, scenario STAR 2K) (Werner & Gerstengarbe, 1997, Orlowsky *et al.*, 2008).

STAR generates daily time series of meteorological variables by stochastically resampling segments of daily observations at climate stations. The resampling is conditioned by a predefined air temperature increase. The scenario STAR 2K assumes a linear increase of the mean annual temperature of 2 K from 2000 to 2055 (Gerstengarbe *et al.*, 2003; Orlowsky *et al.*, 2008). Under the assumption that the relationships between meteorological variables will persist in the future, the scenario is associated with decreases of the mean annual precipitation in the wider region of the experimental site of interest for this study. In a comparison study on the Lusatian river catchments of Spree, Schwarze Elster, and Weißer Schöps in North-Eastern Germany (Gädeke *et al.*, 2014), the outcomes of STAR have been evaluated as warm and dry, compared to results of dynamical regional climate models, such as REMO or CCLM. STAR has been widely applied as climate input to simulate potential climate change impacts on hydrology and plant growth (Lasch *et al.*, 2010; Pohle *et al.*, 2015).

We performed model simulations driven by air temperature, global radiation, and precipitation of 100 realisations of STAR 2K for the time period from 2015 to end of 2054, with respect to the vegetation period of both tree species, and taking into consideration a

rotation of four years. As a reference basis, a growing period from 2010 to end of 2013 for black locust and from 2011 to end of 2014 for poplar was simulated. Additionally, ten hypothetical four-year growing periods from 2015 to end of 2054 were created and simulated under the assumption that shoots and seedlings were replanted at the beginning of each growing period in the same system and under the same management and soil conditions.

Consequently, the 100 realisations were adjusted given the specific vegetation period of each tree species and arrayed according to their intent as follows: identifying realisations with minimum, mean, and maximum (1) average precipitation sum and (2) mean temperature values for the timeframe 2015-2054 compared to 1974-2014, as a base period, and analyzing the correspondences with the tree woody biomass; identifying realisations with minimum and maximum (3) average precipitation sum and (4) mean temperature values with respect to the ten hypothetical four-year growing periods, and analyzing the correspondences with the tree biomass; (5) identifying the main realisations that rendered minimum and maximum woody biomass after each of the ten growing periods, and (6) identifying realisations that rendered minimum and maximum woody biomass increments over the 2015-2054 timeframe.

3.3. Results

3.3.1. Observed Woody Biomass Productivity of Poplar and Black Locust Trees

The woody biomass observations showed considerable differences between the tree species over the investigated four years of growth (Table 8). The number of measured trees was also taken into consideration for the determination of the standard deviation.

Table 8. Mean (± standard deviation) woody biomass for poplar and black locust trees with respect to the planting density and number of samples (n).

Species	**Biomass after 1 Year** [Mg ha^{-1}]	**Biomass after 2 Years** [Mg ha^{-1}]	**Biomass after 3 Years** [Mg ha^{-1}]	**Biomass after 4 Years** [Mg ha^{-1}]
Poplar	0.4 ± 0.1 (n=333)	2.0 ± 0.5 (n=150)	12.9 ± 0.1 (n=242)	28.2 ± 2.7 (n=50)
Black Locust	0.1 ± 0.1 (n=360)	3.6 ± 0.5 (n=306)	9.1 ± 1.4 (n=152)	15.3 ± 3.4 (n=219)

The growth difference between the two tree species in terms of woody biomass varied inter-annually, but after four years, poplar trees grew almost twice as much as black locust trees

in terms of woody biomass. The standard deviations obtained for each year and with respect to the number of samples showed large differences, underlying the variability of observations.

3.3.2. Sensitivity Analysis of the Yield-SAFE Model

Parameters with an absolute value of the normalized sensitivity in the model output higher than 0.1 were considered as main influencing parameters and are presented in Figure 11. Reversely, all parameters with a normalized sensitivity < 0.1 were considered as minor important due to a comparably small influence on the model output and thus were not included in a deeper evaluation.

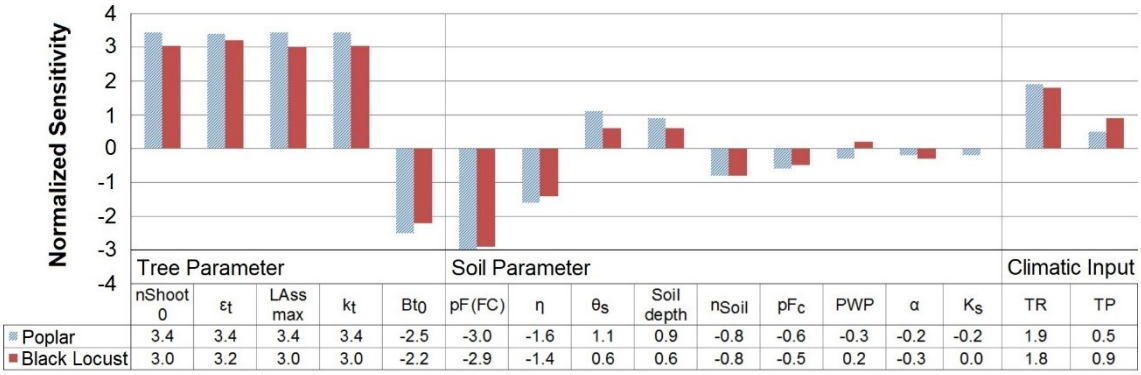

	nShoot 0	εt	LAss max	kt	Bt0	pF(FC)	η	θs	Soil depth	nSoil	pFc	PWP	α	Ks	TR	TP
Poplar	3.4	3.4	3.4	3.4	-2.5	-3.0	-1.6	1.1	0.9	-0.8	-0.6	-0.3	-0.2	-0.2	1.9	0.5
Black Locust	3.0	3.2	3.0	3.0	-2.2	-2.9	-1.4	0.6	0.6	-0.8	-0.5	0.2	-0.3	0.0	1.8	0.9

Figure 11. The normalized sensitivity of the model's output to tree and soil parameters, as well as to climatic inputs for both poplar and black locust.

The model output displayed high sensitivities to the tree parameters: initial number of shoots ($nShoot_0$), radiation use efficiency (ε_t), radiation extinction coefficient (k_t), and maximum leaf area for a single shoot (LA_{ss}^{max}) in descending order. Dominant soil parameters in descending order were: pF value at field capacity (*pF(FC)*), potential evaporation (η), saturated volumetric water content (θ_s), and soil depth. Regarding the climate inputs, the modelled output was highly sensitive to global radiation (*TR*) and precipitation (*TP*) but unresponsive to changes in average air temperature.

3.3.3. Model Validation

In what concerns the above-ground tree woody biomass production accumulated after four years of growth, the Yield-SAFE model rendered good correspondences with the measured tree woody biomass (Figure 12).

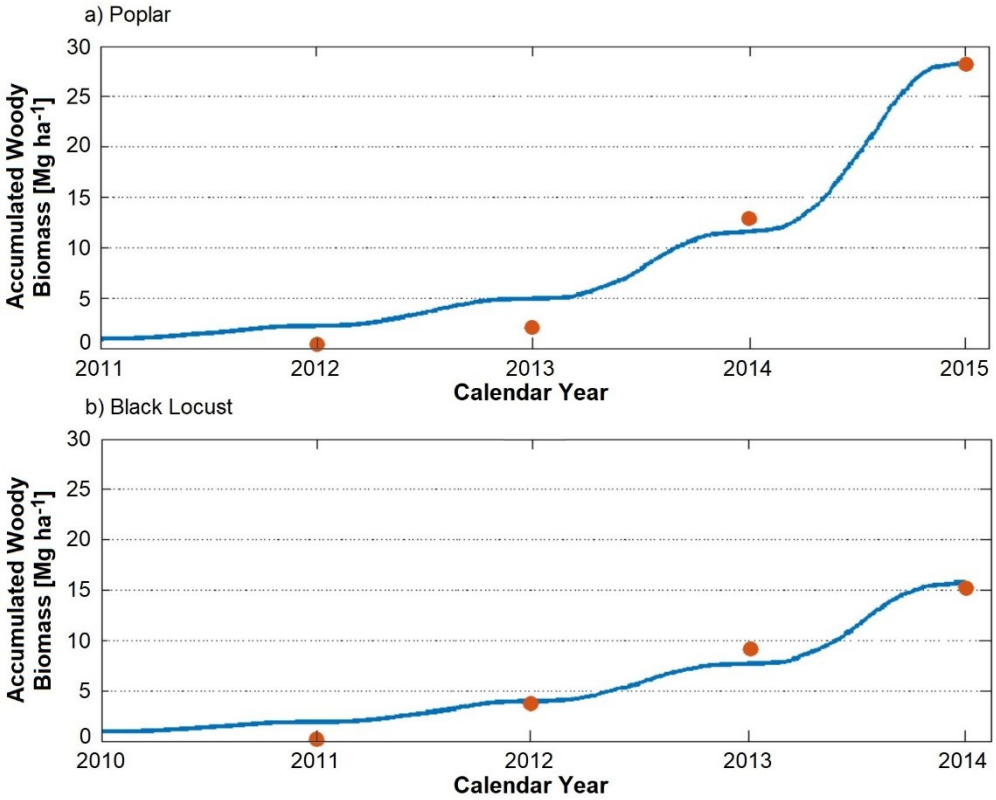

Figure 12. Measured woody biomass (dots) and modelled accumulated woody biomass (line) for: (**a**) poplar over a rotation period from 2011 to the end of 2014, and with regard to the planting density and number of samples (n=50:333) and (**b**) black locust over a rotation period from 2010 to the end of 2013, and with regard to the planting density and number of samples (n=50:360).

The modelled tree woody biomass values accumulated during the four years of growth nearly matched the measured biomass values for both tree species, except for a higher deviation in the second growing year of poplar. However, at the end of the investigation period, the deviation of measured to modelled biomass values accounted for +0.3% for poplar and +2.8% for black locust, implying very small overestimations of modelled accumulated tree woody biomass.

The relative errors of the modelled fits were low (NRMSE values of 4.6% and 5.5% for the Yield-SAFE validations of poplar and black locust, respectively, always with a P value < 0.0001) and the fit was highly significant (R^2 values of 0.99 and 0.97 for poplar and black locust, respectively).

3.3.4. Modelled Woody Biomass under STAR 2K Weather Realisations

3.3.4.1. A forty-year comparison with respect to the average precipitation sum

The main realisations with minimum, mean, and maximum average precipitation sum and air temperature for the timeframe 2015-2054 compared to the values for the timeframe 1974-2014, which served as a base period in this study, and with respect to the vegetation period of each tree species are presented in Table 9.

Table 9. Realisations (highlighted in parenthesis) that rendered minimum, mean, and maximum average precipitation sum and air temperature values with respect to the vegetation period of both tree species and under a timeframe of forty years.

Average Values for the Vegetation Period	**Poplar**				**Black Locust**			
	Base Period (1974-2014)	Min. (2015-2054)	Mean (2015-2054)	Max. (2015-2054)	Base Period (1974-2014)	Min. (2015-2054)	Mean (2015-2054)	Max. (2015-2054)
P [mm]	324	254 (**R13**)	296 (**R4,R27**)	327 (**R41**)	336	271 (**R13**)	303 (**R28,R58**)	335 (**R82**)
T [°C]	16.0	17.0 (**R35**)	17.2 (**R15,R86**)	17.5 (**R38**)	15.3	16.2 (**R84**)	16.6 (**R43**)	16.9 (**R32,R41**)

The average precipitation sum during the vegetation period of the base period corresponded to the maximum values indicated by the projected time period in the case of both poplar and black locust. This would suggest that, taking into account all 100 realisations over a forthcoming timeframe of forty years, a maximum of 2.5 mm more precipitation would be achieved in the vegetation period of poplar and only 0.8 mm less in the vegetation period of black locust. The long-term average precipitation of the realisations representing mean values is about 10% lower than the base period (28 mm in case of poplar, 33 mm in case of black locust). Also, it was noticed that the values for the average precipitation sum were revealed by different realisations for the two considered tree species, which made the usage of vegetation periods specific to each tree species relevant. The long-term average precipitation in the vegetation period for the driest realisation, R13, is approximately 20% lower than the average of the base period (poplar: 70 mm, black locust: 65 mm).

Simulations of tree growth under the aforementioned realisations with minimum, mean, and maximum average precipitation sum values were performed in terms of woody biomass for poplar (Figure 13) and black locust (Figure 14) in order to visually analyze the correspondences with the tree woody biomass accumulated after four years of growth.

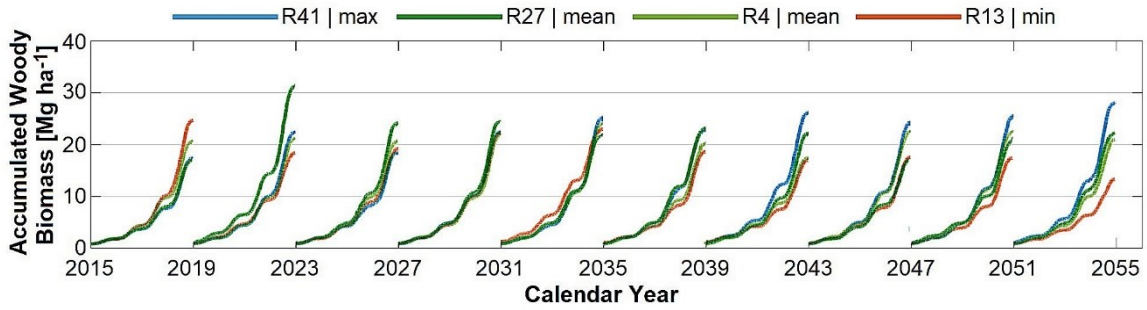

Figure 13. Projected accumulated woody biomass of poplar trees under realisations that rendered minimum (R13, orange), mean (R4, light green; R27, dark green), and maximum (R41, blue) average precipitation sum values during the vegetation period from 2015 to the end of 2054.

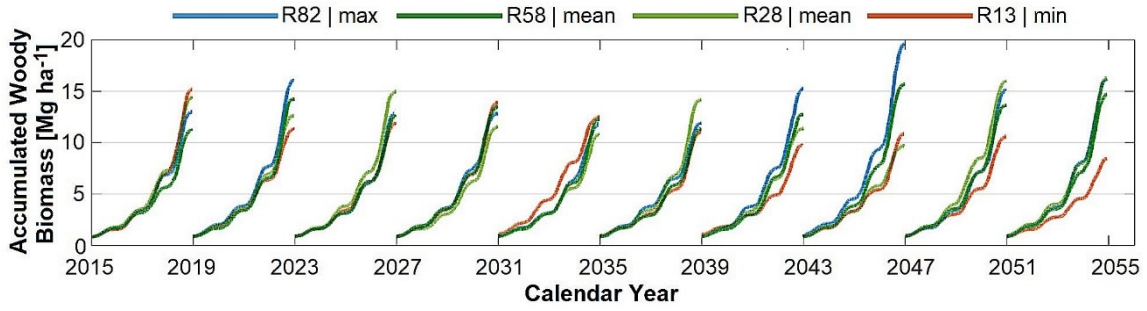

Figure 14. Projected accumulated woody biomass of black locust trees under realisations that rendered minimum (R13, orange), mean (R28, light green; R58, dark green), and maximum (R82, blue) average precipitation sum values during the vegetation period from 2015 to the end of 2054.

While it could be generally said that a lack of precipitation leads to lower woody biomass and that a higher amount of precipitation leads to a higher woody biomass accumulated in four growing years, it was not always the case. Realisation 13, for example, had the lowest average precipitation sum in the forty-year timeframe but rendered the maximum accumulated biomass in the first period (2015-2018) for both tree species as well as in the fourth (2027-2030) and fifth period (2031-2034) for black locust. This result implied that in order to find a clear correlation between a climatic input and the production of tree woody biomass, the established growing periods or even the individual vegetation periods should be evaluated.

3.3.4.2. A forty-year comparison with respect to the mean temperature

The mean temperature during the vegetation period of the base period (poplar: 16°C, black locust: 15.3°C) was 1.2 K lower than the mean values and 1.5 K lower than the maximum values indicated by the 100 realisations under the projected time period, in the case of both poplar and black locust (Table 9). Also, it was noticed that the values for the mean, minimum, and maximum temperature were revealed by different realisations each for the two considered tree species, which made the usage of vegetation periods specific to each tree species relevant.

Consequently, simulations of tree growth under aforementioned realisations with minimum, mean, and maximum mean temperature values were performed in terms of woody biomass for poplar (Figure 15) and black locust (Figure 16) in order to visually analyse the correspondences with the tree woody biomass accumulated after four years of growth.

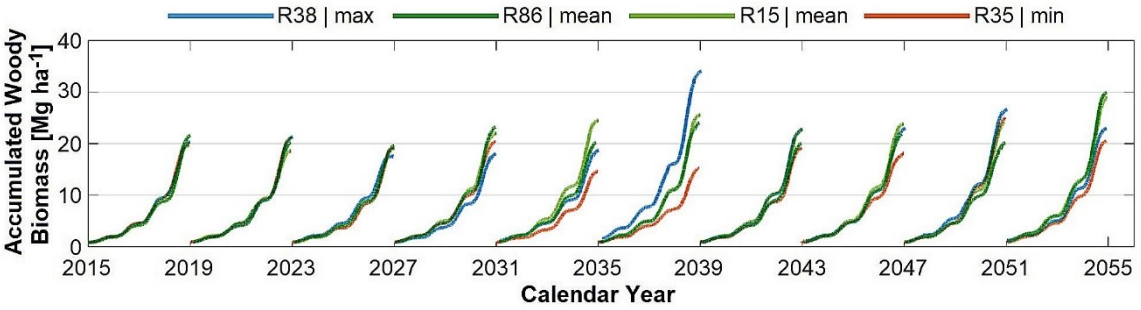

Figure 15. Projected accumulated woody biomass of poplar trees under realisations that rendered minimum (R35, orange), mean (R15, light green; R86, dark green), and maximum (R38, blue) average temperature values during the vegetation period from 2015 to the end of 2054.

For poplar, it seemed that medium average temperature values during the vegetation period rendered the highest woody biomass, with the exception of the sixth period (2035-2038), where the realisation with a maximum value for temperature also achieved a maximum accumulated woody biomass. Generally, the results showed that extremities in mean temperature rendered lower accumulated woody biomass.

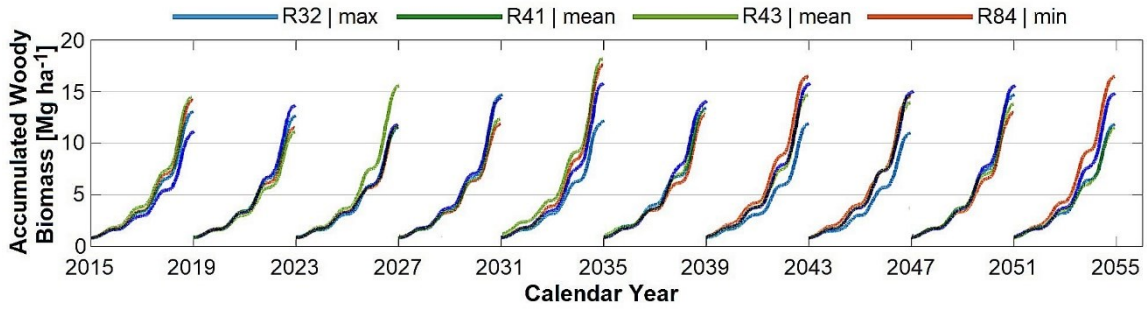

Figure 16. Projected accumulated woody biomass of black locust trees under realisations that rendered minimum (R84, orange), mean (R43, light green), and maximum (R41, dark blue; R32, light blue) average temperature values during the vegetation period from 2015 to the end of 2054.

For black locust, there seemed to be no explicit pattern correlating mean temperature with the production of tree woody biomass, as the highest woody biomass was achieved in different periods by realisations rendering both extreme and mean temperature values.

3.3.4.3. Comparison between the ten year growing periods in terms of average precipitation sum

In this step, ten hypothetical four-year growing periods from 2015 to 2054 were simulated under the assumption that shoots and seedlings were replanted at the beginning of each growing period, in the same system, and under the same management and soil conditions. Accordingly, two reference periods were created in terms of average precipitation sum, mean temperature, and global radiation accounting for the distinct vegetation period and planting year of poplar (2011) and black locust (2010) trees.

The main realisations with minimum and maximum values for the average radiation sum, precipitation sum, and temperature for the established growing periods from 2015-2054 are presented in Table 10 with respect to the vegetation period of each tree species.

Table 10. Realisations (highlighted in parenthesis) that rendered minimum and maximum average precipitation (P_{min}, P_{max}), air temperature (T_{min}, T_{max}), and global radiation (R_{min}, R_{max}) values in the established ten growing periods with respect to the vegetation period of both tree species. The reference period for poplar (2011-2014) and black locust (2010-2013) trees accounted for their distinct vegetation period.

Average Values	Reference Period	2015-2018	2019-2022	2023-2026	2027-2030	2031-2034	2035-2038	2039-2042	2043-2046	2047-2050	2051-2054
						Poplar					
$P_{max.}$	366	389	435	413	378	442	450	376	406	413	416
[mm]		**(R31)**	**(R7)**	**(R43)**	**(R41)**	**(R98)**	**(R96)**	**(R60)**	**(R10)**	**(R78)**	**(R39)**
$P_{min.}$		225	201	211	184	212	205	203	176	197	190
[mm]		**(R26)**	**(R56)**	**(R11)**	**(R2)**	**(R10)**	**(R79)**	**(R69)**	**(R2)**	**(R8)**	**(R79)**
						Black Locust					
$P_{max.}$	395	400	440	423	408	459	445	390	413	422	429
[mm]		**(R79)**	**(R7)**	**(R43)**	**(R50)**	**(R98)**	**(R96)**	**(R60)**	**(R82)**	**(R78)**	**(R39)**
$P_{min.}$		226	207	222	188	205	209	192	196	188	200
[mm]		**(R19)**	**(R56)**	**(R11)**	**(R2)**	**(R10)**	**(R79)**	**(R79)**	**(R2)**	**(R46)**	**(R13)**
						Poplar					
$T_{max.}$	16.6	17.5	17.6	18.0	17.9	18.2	18.3	18.3	18.3	18.6	18.5
[°C]		**(R16)**	**(R33,R69)**	**(R55)**	**(R98)**	**(R62)**	**(R1,R17)**	**(R97)**	**(R36,R81)**	**(R37)**	**(R47)**
$T_{min.}$		15.2	15.9	16.1	15.9	16.1	16.5	16.5	16.8 **(R10,**	16.4	17.1
[°C]		**(R71)**	**(R7,R79)**	**(R75)**	**(R1)**	**(R3)**	**(R42,R95)**	**(R26)**	**R30,R94)**	**(R66)**	**(R91)**
						Black Locust					
$T_{max.}$	15.6	16.6	17.1	17.1**(R27,**	17.4	17.3	17.4	17.6	17.7	17.8	17.8
[°C]		**(R64,R74)**	**(R41)**	**R55,R83)**	**(R4)**	**(R96)**	**(R26,R65)**	**(R22)**	**(R4)**	**(R51)**	**(R73)**
$T_{min.}$		14.6	15.3	15.6	15.4	15.2	15.9	16.0	16.1	16.0	16.5
[°C]		**(R71)**	**(R84)**	**(R67)**	**(R1)**	**(R3)**	**(R81)**	**(R26)**	**(R31)**	**(R66)**	**(R91)**
						Poplar					
$R_{max.}$	3119	2926	3002	3017	3016	3069	3133	3082	3165	3146	3158
[W m^{-2}]		**(R64)**	**(R53)**	**(R22)**	**(R4)**	**(R13)**	**(R17)**	**(R24)**	**(R100)**	**(R37)**	**(R79)**
$R_{min.}$		2497	2640	2709	2701	2593	2653	2741	2745	2789	2738
[W m^{-2}]		**(R71)**	**(R34)**	**(R60)**	**(R1)**	**(R3)**	**(R95)**	**(R26)**	**(R67)**	**(R3)**	**(R3)**
						Black Locust					
$R_{max.}$	2966	2812	2932	2887	2913	2898	2952	2958	3045	2981	3003
[W m^{-2}]		**(R11)**	**(R51)**	**(R22)**	**(R4)**	**(R6)**	**(R46)**	**(R79)**	**(R100)**	**(R13)**	**(R79)**
$R_{min.}$		2379	2560	2538	2573	2419	2517	2621	2597	2632	2559
[W m^{-2}]		**(R71)**	**(R79)**	**(R67)**	**(R41)**	**(R3)**	**(R95)**	**(R8)**	**(R67)**	**(R3)**	**(R3)**

A directly proportional relationship can be noticed between the average radiation sum and the mean temperature, as averaged over the vegetation period.

Subsequently, four compound-realisations were created by using realisations that rendered either a minimum or a maximum average precipitation sum in the given growing period. For example, the first compound-realisation, which contained the highest precipitation values for poplar, was made by putting together R31, R7, R43, R41, R98, R96, R60, R10, R78, and R39, from the first period (2015-2018) to tenth period (2051-2054), respectively. Simulations were carried under these four compound-realisations for poplar (Figure 17) and black locust (Figure 18).

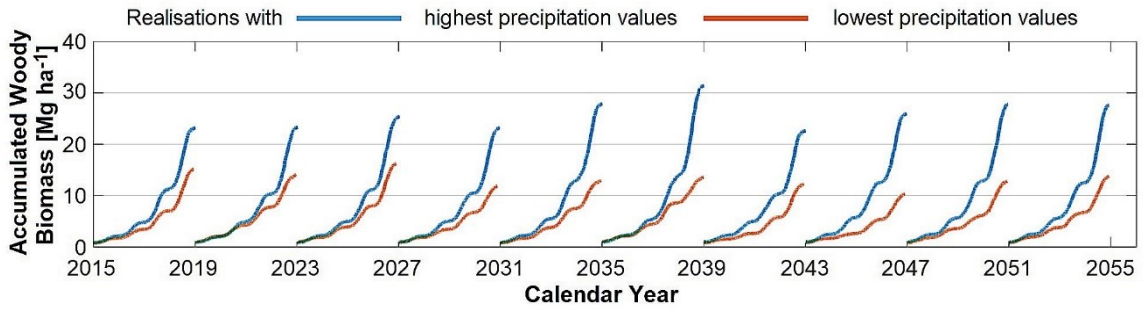

Figure 17. Projected woody biomass of poplar trees under special realisations describing either the highest precipitation values (blue) or the lowest precipitation values (orange) with respect to the ten established growing periods.

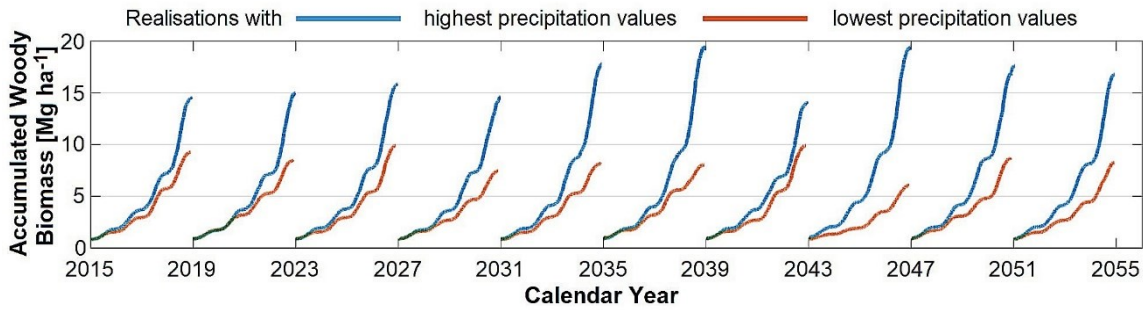

Figure 18. Projected woody biomass of black locust trees under special realisations describing either the highest precipitation values (blue) or the lowest precipitation values (orange) with respect to the ten established growing periods.

A strong, directly-proportional correlation between the average precipitation sum and the woody biomass accumulated after four years of growth was noticed for both tree species. However, even if the base period for both tree species had an average precipitation sum lower than any of the maximum values found for the projected periods, the accumulated

biomass after four years of growth was sometimes higher in the base period rather than in the projected timeframes.

Additionally, it was noticed that R79 has a strong intra-annual variability of precipitation shown by a shift between the minimum and maximum values for precipitation over the vegetation period. However, this realisation does not seem to render marginal values for accumulated tree biomass, except for black locust, in period 6 (2035-2038). Therefore, a compilation of climographs was made for realisation 79 with respect to the established growing periods and according to the vegetation period (appendixed Figure B.1.). The average radiation sum and the accumulated biomasses for both tree species were added for comparison purposes.

Regarding the mean monthly temperature, it seemed that those growing periods with a warm April (≈12°C) rendered lower biomass values than those periods that had a colder April (≈9°C). This happened perhaps due to late April frosts that can affect tree growth. Alternatively, no strong influence of mean temperature on the accumulated tree biomass could be seen over the years. In what concerns the average monthly precipitation, meaningful shifts were noticed, especially between earlier growing periods (2015-2018) and later growing periods (2047-2050). Accumulated tree biomass also seemed to have a noticeable increase in those periods where precipitation was high between May and July. The average radiation increased from period to period, but to no avail for the biomass accumulated after four growing years.

3.3.4.4. Comparison between the ten year growing periods in terms of mean temperature

Similarly to Section 3.3.4.3, four compound-realisations were created by using realisations that offered either a minimum or a maximum mean temperature in the given growing period (Table 10). The tree growth was simulated in terms of woody biomass under these four compound-realisations for poplar (Figure 19) and black locust (Figure 20).

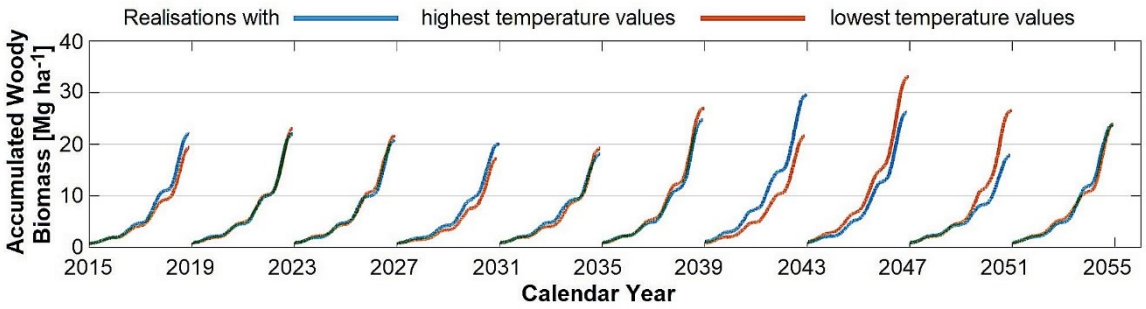

Figure 19. Projected woody biomass of poplar trees under special realisations describing either the highest temperature values (blue) or the lowest temperature values (orange) with respect to the ten established growing periods.

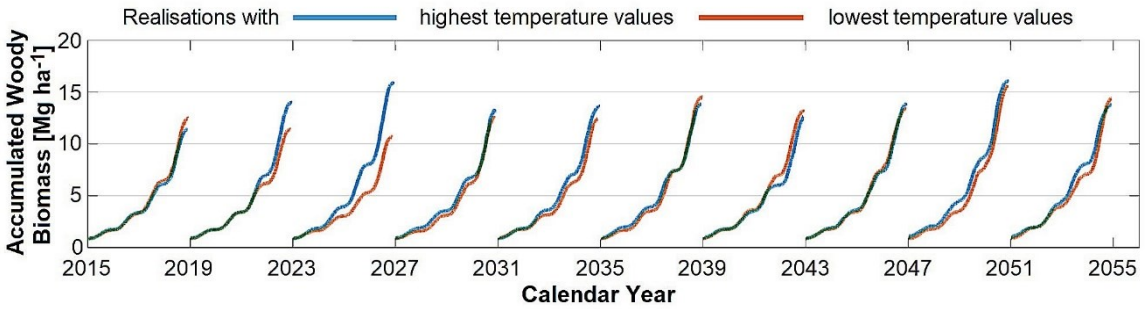

Figure 20. Projected woody biomass of black locust trees under special realisations describing either the highest temperature values (blue) or the lowest temperature values (orange) with respect to the ten established growing periods.

3.3.4.5. Comparison between the ten year growing periods in terms of accumulated woody biomass

Table 11 presents the minimum and maximum woody biomass accumulated after four growing years for both tree species, with respect to the established growing periods, and together with their corresponding realisation. Highlighted in red are those realisations that rendered low accumulated woody biomass while having a low precipitation input or on the contrary, that rendered a high accumulated woody biomass while having a high precipitation input.

Table 11. Realisations that rendered minimum and maximum accumulated woody biomass values for both tree species with respect to the ten established growing periods. Highlighted in red are those realisations that rendered low accumulated woody biomass while having a low precipitation input or on the contrary, that rendered a high accumulated woody biomass while having a high precipitation input.

Accumulated Woody Biomass [Mg ha^{-1}]	**2015-2018**	**2019-2022**	**2023-2026**	**2027-2030**	**2031-2034**	**2035-2038**	**2039-2042**	**2043-2046**	**2047-2050**	**2051-2054**
	Poplar									
Max.	24.7	31.3	34.7	33.8	39.4	34.5	30.6	33.1	33.5	38.8
Realisation	13	27	6	49	100	37	75	82	75	62
Min.	15.0	14.6	15.9	12.9	13.7	15.3	13.5	10.9	12.9	12.9
Realisation	26	56	18	2	10	35	69	2	16	90
	Black Locust									
Max.	15.3	18.3	16.8	17.9	20.6	19.1	18.0	19.61	18.2	21.8
Realisation	51	27	6	74	100	96	75	82	75	63
Min.	9.4	8.9	10.0	7.9	8.6	9.3	8.5	7.1	8.0	8.2
Realisation	19	56	18	2	10	79	87	2	16	24

According to these results, Figure 21 was created for poplar and black locust, respectively, as a bandwidth of accumulated woody biomass from all realisations from 2015 to the end of 2054.

An initial decrease in accumulated woody biomass was noticed between the reference and the first projected period for both tree species (Figure 21). However, this was expected, as the realisations that rendered maximum values for accumulated biomass (R13 and R51 for poplar and black locust, respectively) had lower average values than those of the reference period for all climatic inputs.

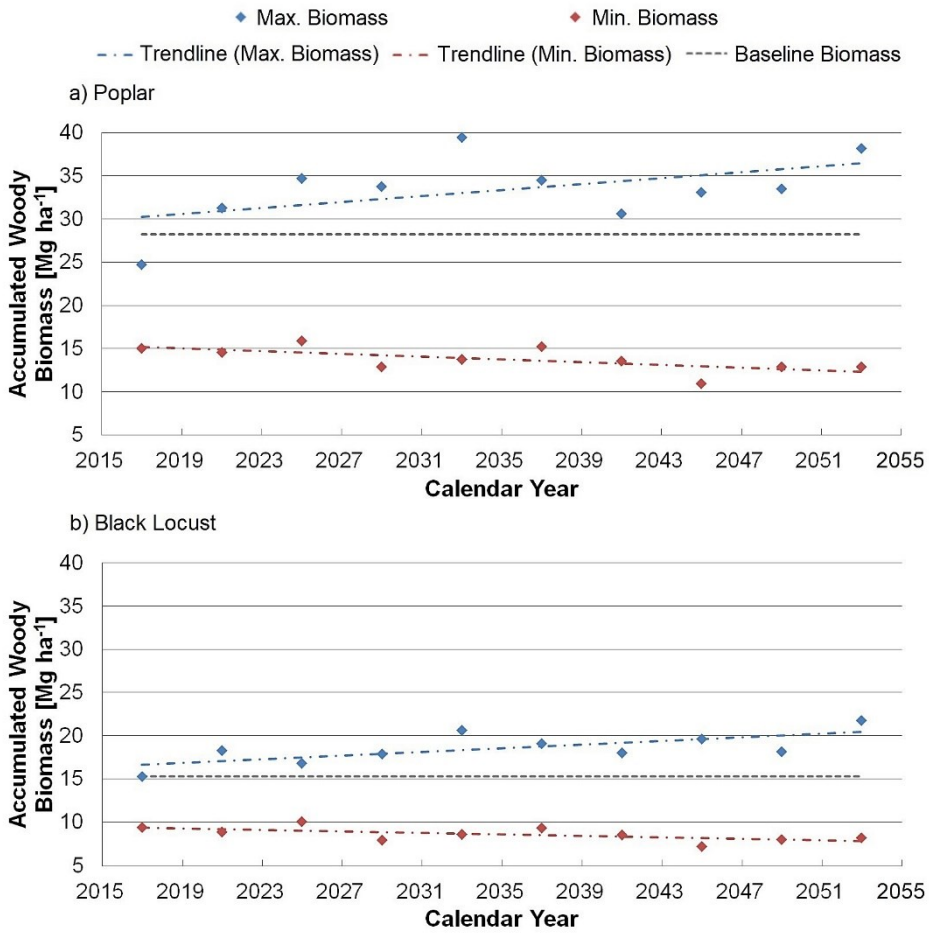

Figure 21. The range of possible accumulated woody biomass shown by maximum (blue) and minimum (red) values obtained after four years of growth with respect to the ten established growing periods for (**a**) poplar and (**b**) black locust. Trend lines for the woody biomass are described by dash-dotted lines. The dashed lines represent the woody biomass, as per reference period.

Following the trend lines of biomass increase for poplar, it could be said that in the most optimistic case, an increase of about 10 Mg ha^{-1} (35%) would be achieved in the last period (2051-2054) compared to the reference period and in the most pessimistic case a decrease of about 15 Mg ha^{-1} (54%). For black locust, the accumulated woody biomass in the last period would be subjected to either an increase of about 7 Mg ha^{-1} (43%), in the most optimistic case, or a decrease of 7 Mg ha^{-1} (47%), in the most pessimistic case. However, when accounting for the variability of observations, the simulations showed that the assumed climate change could lead to a decrease in the median woody biomass accumulated in the last period of about 5 Mg ha^{-1} (18%) for poplar and 1.7 Mg ha^{-1} (11%) for black locust trees with respect to the median observed in the reference period.

Additionally, it was noticed that in the first period (2015-2018), the maximum accumulated biomass of poplar was given by realisation R13 (i.e., a woody biomass value

of 24.7 Mg ha^{-1}; average radiation sum of 3284 W m^{-2}), whereas the maximum precipitation input for the first period is given by realisation R31 (i.e., a biomass value of 23.2 Mg ha^{-1}; average radiation sum of 3023 W m^{-2}). In order to establish what other climatic factors were involved in the tree woody biomass production, appendixed Figure B.2. was created.

As also observed in appendixed Figure B.1., the accumulated tree woody biomass seemed to have a noticeable increase in those periods where precipitation was high between May and July. Also, the average monthly radiation sum was significantly higher in realisation R13 than R31 with respect to the vegetation period, except for 2017, where values dropped slightly behind for realisation R13 than R31. Likewise, the average monthly temperature was significantly higher in realisation R13 than R31 with respect to the vegetation period, except for 2017, where values dropped slightly behind for realisation R13 than R31.

3.3.4.6. Comparison between the ten year growing periods in terms of woody biomass increment

The minimum and maximum woody biomass increments for both tree species under a timeframe of forty years are presented in Table 12, together with their corresponding realisation. Taking into consideration the average values for precipitation and temperature of all realisations under the entire projected timeframe of forty years, an overall mean temperature and precipitation sum were established and highlighted.

Table 12. Realisations that rendered minimum, mean, and maximum average woody biomass increment values for both tree species under a timeframe of forty years, together with their climatic characteristics in terms of average annual values for precipitation sum and air temperature.

Average Woody Biomass Increment [Mg ha^{-1} a^{-1}]	**Projected Period (2015-2054)**		**R2**		**R44**	**R45**	**R70**		**R62**	**R25**	
	Poplar	Black locust	Poplar	Black locust	Poplar	Black locust	Poplar	Black locust	Black locust	Poplar	Black locust
	-	-	4.5	2.8	5.4	3.3	5.4	3.3	3.3	6.5	3.8
P [mm a^{-1}]	**296**	**303**	270	279	313	316	304	301	310	306	313
T [°C a^{-1}]	**17.2**	**16.6**	17.3	16.9	17.1	16.5	17.3	16.7	16.6	17.3	16.6

Furthermore, labels were given to the realisations presented in Table 12 by comparing their average annual precipitation and temperature values with those values obtained for the entire projected timeframe from 2015 to the end of 2054. Consequently, R2 was regarded as *dry-warm* for both tree species, R44 as *wet-cold*, R45 as *wet-cold*, R70 as *wet-warm* for poplar and *dry-warm* for black locust, R62 as *wet-medium*, and R25 as *wet-warm* for poplar and *wet-medium* for black locust. The yearly woody biomass increments were projected for poplar (Figure 22) and black locust (Figure 23) trees under these realisations with respect to the ten established growing periods.

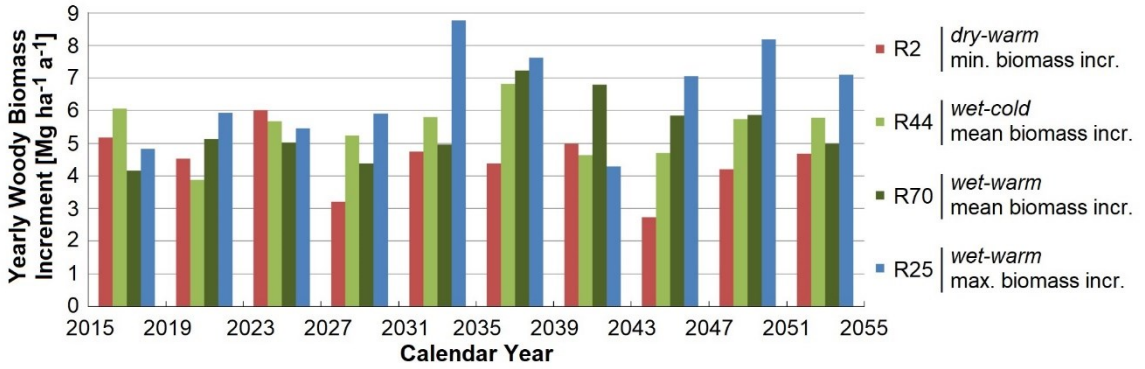

Figure 22. Projected minimum (orange), mean (green), and maximum (blue) yearly woody biomass increment of poplar trees with respect to the ten established growing periods.

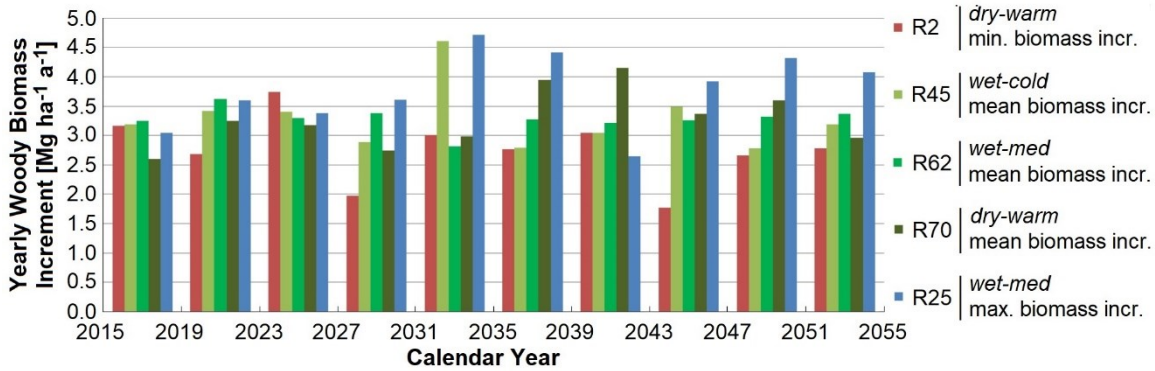

Figure 23. Projected minimum (orange), mean (green), and maximum (blue) yearly woody biomass increment of black locust trees with respect to the ten established growing periods.

The empirical data for the yearly woody biomass increment, regarded as the reference period values, were significantly higher than the maximum values achieved under the timeframe of forty years. However, given the established growing periods, an increase in biomass increment was noticed after the fifth period. For poplar, this increase exceeded the reference period value with merely 1.7 Mg ha^{-1} a^{-1} (24%), whereas for black locust it decreased with at least 0.6 Mg ha^{-1} a^{-1} (11%). Regarding the mean temperature obtained for

the given growing period, it seemed that realisations labelled as both cold and warm rendered minimum, medium, and maximum biomass increments.

3.4. Discussion

The results of this study corroborated the growth vulnerability of poplar and black locust trees in terms of woody biomass to prospective climate change and particularly to changes in water availability. Similar results were obtained by Weemstra *et al.* (2013), who found that summer drought decreased tree growth of ten deciduous tree species at an experimental forest setting in The Netherlands. Using climate-tree-growth relationships for study sites in Mecklenburg-Vorpommern, north-eastern Germany, Scharnweber *et al.* (2011) have identified a strong dependency of growth of common European beech (*Fagus sylvatica* L.) and pedunculated oak (*Quercus robur* L.) on water availability, especially during early summer. Comprehensive studies were conducted with *Populus* and *Salix* in field experiments for short-rotation forestry and for breeding of clones (Monclus *et al.*, 2005; Calfapietra *et al.*, 2010).

In contrast to the previously mentioned tree species, information about the implication of environmental and climatic factors on the growth performance of black locust is rare. As a pioneer tree, black locust is regarded as a drought-adapted tree species, showing high morphological and physiological plasticity and therefore, it is planted even in regions with annual precipitation sum values below 600 mm a^{-1} (Veste *et al.*, 2018). Subjected to water limitation, the leaf area of black locust reduces drastically in order to minimize transpiration, although affecting the growth performance (Veste & Kriebitzsch, 2013; Mantovani *et al.*, 2015a), whereas the production of nodules for biological nitrogen fixation increases in order to overcome the limitation of nitrogen uptake from the soil (Mantovani *et al.*, 2015b).

Field investigations at our study site in Neu Sacro during a summer heat period in 2015 indicated that both poplar and black locust tree species maintained a high photosynthesis and growth performance under maximum daily temperatures of 30-34°C due to the fact that water uptake from the groundwater was guaranteed (Veste & Halke, 2017). Under such well-watered conditions, black locust did not down-regulate the transpiration and was regarded as water-saving tree species (Mantovani *et al.*, 2014). However, long-term studies aiming to understand the biomass production under different climatic conditions do not exist for black locust and for management practices such as short-term forestry.

3.4.1. Parameterization and Validation of the Yield-SAFE Model

The low relative errors of the woody biomass fits and the high coefficient of determination suggested a satisfactory agreement between the modelled and observed woody biomass yields and thus, a high model performance, accounting for a great proportion of the variance.

However, some differences existed between the modelled biomass and the measured one, which could be reduced by revising those parameters which influenced the modelled output the most. One of the parameters that would need a better appraisal would be the initial biomass, which was assumed to be 0.87 Mg ha^{-1} in the Yield-SAFE model, whereas the measured biomass was of 0.4 Mg ha^{-1} for poplar and 0.001 Mg ha^{-1} for black locust after the first year of growth. Evidently the initial biomass of the cuttings (poplar) and rooted seedlings (black locust) should be adjusted in the future to a more realistic situation.

Another solution would be to improve the Yield-SAFE model by a dynamic vegetation period determination depending on weather conditions rather than the static approach using tabulated values of the day of budburst and leaf-fall of the year. The adaptation could be based on a weighting model determined by the atmospheric drivers (i.e., daily values for air temperature, precipitation, and global radiation), in order to boost or hinder the tree vegetation period to a more realistic situation. Shifts in the phenological phases have already been observed in the region (Chmielewski *et al.*, 2005; Menzel *et al.*, 2006) and further changes are expected for the future. Since this solution would use existing parameters, it would not increase the parameter range in the Yield-SAFE model and therefore, the model would remain parameter-sparse.

3.4.2. Evaluating the Woody Biomass Productivity under Prospective Climate Realisations

The above-ground woody biomass, as simulated by the Yield-SAFE model, was highly sensitive to global radiation and precipitation but to a lesser extend to changes in average air temperature. This was also supported by the results of the sensitivity analysis. However, strong correlations were detected between global radiation and air temperature and therefore, the variations noticed in the tree woody biomass production were attributed to various extents to all three climatic inputs.

In our comparison between realisations R13 and R31 under the first growing period (2015-2018) for example, a higher woody biomass production was provided by R13 than by R31. We firstly linked this difference to the monthly precipitation sum values, which

were higher in R13 than in R31. This was especially important for the months May, June, and July, where the modelled output increased with increasing precipitation values, as also observed in experimental studies by Gallardo (2014) for poplar trees and Mantovani *et al.* (2014) for black locust trees.

Additionally, the average monthly radiation was significantly higher in realisation R13 than R31 with respect to the vegetation period, except for 2017, where values dropped slightly behind for realisation R13 than R31. Likewise, the average monthly temperature was significantly higher in realisation R13 than R31 with respect to the vegetation period, except for 2017. This indicated that the tree growth depended somewhat on global radiation, but most predominantly on precipitation.

Water availability during the main vegetation period has been confirmed to be an important factor in the determination of the eco-physiological and growth performance of trees (Scharnweber *et al.*, 2011; Leuzinger *et al.*, 2015; Gessler *et al.*, 2007; Kriebitzsch & Veste, 2012; Weemstra *et al.*, 2013). Especially when subjected to extreme summer droughts, as expected for the ongoing climate change, the soil water availability can imprint a long-lasting effect on tree growth performance, forest functioning and management (Lindner *et al.*, 2010; Anderegg *et al.*, 2013; Bolte *et al.*, 2017).

Numerous studies have emphasized the complex effects of climate change on common forest trees (Anderegg *et al.*, 2013, Anderegg *et al.*, 2015). The increasing air temperature was reported to alter the plant phenology and length of the vegetation period, which in turn affects plant productivity (Chmielewski *et al.*, 2005; Menzel *et al.*, 2006). Bud phenology of many temperate trees depends on air temperature and photoperiod (Körner & Basler, 2010; Vitasse & Basler, 2013; Malyshev *et al.*, 2018). Regional warming might increase the length of the growing period, albeit increasing evaporative demand, especially in combination with decreasing precipitation, may limit growth (Ceulemans *et al.*, 1996; Lasch *et al.*, 2002).

The climate change impacts on short rotation coppices with aspen were assessed by Lasch *et al.* (Lasch *et al.*, 2010) across Eastern Germany and increasing growth rates were reported on most sites together with high ranges based on three selected realisations of STAR 2K. A European-wide simulation study showed inconsistent tendencies of changes in tree growth in Central Europe with high uncertainties of climate change impacts on tree growth arising from climate models (Reyer *et al.*, 2014).

Due to the non-linear responses of tree growth to interacting factors such as global radiation, air temperature, precipitation, and soil moisture, estimating climate change impacts on tree growth is challenging and subject to large uncertainties (Medlyn *et al.*, 2011; Asseng *et al.*, 2013; Lindner *et al.*, 2014).

As noted by Medlyn *et al.* (2011), the comparability of simulation results of tree growth under climate change can be hampered by various uncertainties, many of those related to the underlying assumptions in the tree growth model. Our results also indicated that climate changes, as assumed in STAR 2K, may result in high uncertainties of the simulated tree growth, even for the same scenario and regional climate model. This might be attributed to the fact that different realisations of one scenario may cause more pronounced differences in forest productivity than different regional climate models or emission scenarios, as found by a European-wide comparison study (Reyer *et al.*, 2014).

STAR 2K has been used in several studies to estimate the potential climate change effects on hydrology whereby the direction of change was in agreement towards increasing potential evapotranspiration and declining discharge and groundwater recharge (Gädeke *et al.*, 2014; Pohle *et al.*, 2015; Huang *et al.*, 2010), but only the magnitude of change showed high differences between individual realisations. The potential tree growth might also be subjected to hindrance by the declining groundwater recharge, as investigated by Pohle *et al.* (2015) for bio-energy crops in the wider study region under STAR and WettReg.

These results are in line with the findings of our study in what concern the uncertainties in climate variability implications on the growth performance of poplar and black locust trees, both in terms of direction and magnitude of potential future changes.

3.5. Conclusions and Outlook

By a combined experimental and simulation study, we investigated the potential growth vulnerability of two fast-growing tree species managed as short rotation coppices (SRCs) to a considerable spectrum of weather conditions and long-term climate change. We achieved this by means of field measurements in an SRC established in Brandenburg, Germany, and simulations using the Yield-SAFE model and 100 realisations of the regional climate model Statistical Analogue Resampling scheme STAR, scenario 2K.

The Yield-SAFE model simulated the daily above-ground woody biomass of hybrid-poplar clone “Max I” and black locust with satisfactory accuracy and responded sensitively to changes in the meteorological input data. The model showed a strong sensitivity to tree

parameters such as the initial number of shots, the radiation use efficiency and the radiation extinction coefficient, as well as the maximum leaf area per shot and to a lesser extent, to soil parameters. In terms of climatic inputs, the modelled output was highly sensitive to global radiation and precipitation but to a lesser extend to changes in average temperature.

Our findings showed that the tree yields in an SRC were positively impacted by air temperature increase and negatively by decreasing precipitation. Additionally, the notion that climate change impacts cannot be categorized as solely positive or negative was reinforced, as tree yield productivity has shown to react diametrically contrary to shifts in climate: higher temperature values might boost tree growth due to a prolonged vegetation period, or contrarily, it might hinder tree growth due to higher evapotranspiration and lower soil water availability.

However, as the extreme events are to be intensified in their frequency and intensity within the framework of the anticipated climate changes, the investigation of the effects of extreme weather conditions will be given more prominence in the future. Also, there may be some restrictions on production as groundwater levels might decline under climate change (Pohle *et al.*, 2015), restricting the future possibilities for the use of groundwater for irrigation, especially of agricultural land.

Based on the implications of this study, it will be possible to furthermore develop and optimize the SRC designs with respect to the specific field conditions, spatial arrangement, and planting density and to provide with a reliable estimation of achievable woody biomass yields according to tree species, management, and climate change effects.

In the future, the model of this study could be extended to situations that demand more details such as different nutrient levels, different species of trees and arable crops and interactions between plants. This is especially relevant with the current need for diversification of land-use and the generation of not only food, feed and fibre on arable land, but also fuel with respect to the water-energy-food nexus.

Author Contributions

The SIGNAL project was initiated and planed in relation to the proposal call “Soil as a Sustainable Resource for the Bioeconomy – BonaRes” (http://www.signal.uni-goettingen.de). Diana Seserman analysed the data together with Ina Pohle and Maik Veste, and wrote the manuscript. Ina Pohle, Maik Veste, and Dirk Freese contributed by revising the manuscript.

Funding

This research was carried out as part of the BonaRes-SIGNAL project funded by the BMBF - German Federal Ministry of Education and Research (FKZ 031A562E).

Acknowledgments

We thank the Potsdam Institute for Climate Impact Research (PIK) for provision of the STAR 2K realisations and the German Weather Service (Deutscher Wetterdienst, DWD) for the provision of weather data. We gratefully acknowledge the various students for their help with the field work and the Agrargenossenschaft Forst e.G. for their promotion and management of the agroforestry systems at Neu Sacro.

Conflicts of Interest

The authors declare no conflict of interest. The founding sponsors had no role in the design of the study; in the collection, analyses, or interpretation of data, in the writing of the manuscript, and in the decision to publish the results.

4. Trade-Off between Energy Wood and Grain Production in Temperate Alley-Cropping Systems: An Empirical and Simulation-Based Derivation of Land Equivalent Ratio

Diana-Maria Seserman [1,*], Dirk Freese [1], Anita Swieter [2], Maren Langhof [2], Maik Veste [3]

[1] Brandenburg University of Technology Cottbus–Senftenberg, Institute of Environmental Sciences, Soil Protection and Recultivation, Konrad-Wachsmann-Allee 8, 03046 Cottbus, Germany; seserman@b-tu.de, dirk.freese@b-tu.de

[2] Federal Research Center for Cultivated Plants, Julius Kühn-Institut (JKI), Bundesallee 58, 38116 Braunschweig, Germany; anita.swieter@julius-kuehn.de, maren.langhof@julius-kuehn.de

[3] CEBra – Centre for Energy Technology Brandenburg e.V., Friedlieb-Runge-Strasse 3, 03046 Cottbus, Germany; veste@cebra-cottbus.de

* Correspondence: seserman@b-tu.de

MDPI Publisher of Open Access Journals: Agriculture Journal

Received: 24th May 2019 / Revised: 21st June 2019 / Accepted: 4th July 2019 / Published: 8th July 2019

Abstract: The alley-cropping systems (ACSs), which integrate parallel tree strips at varying distances on an agricultural field can result, complementarity of resource use, in an increased land-use efficiency. Practitioners' concerns have directed towards the productivity of such systems given a reduced area covered by agricultural crops. The land equivalent ratio (LER) serves as a valuable productivity indicator of yield performance and land-use efficiency in ACSs, as it compares the yields achieved in monocultures to those from ACSs. Consequently, the objective of this combined experimental and simulation study was to assess the tree- and crop yields and to derive the LER and gross energy yield for two temperate ACSs in Germany under different design scenarios, i.e., tree arrangements (lee- or windward) and ratios of tree area to crop area. Both LER and gross energy yields resulted in a convex curve where the maximum values were achieved when either tree or crop component was dominant (> 75 % of the land area) and minimum when these components shared similar proportions of land area. The implications of several design scenarios have been discussed in order to improve the decision-making, optimization, and adaptation of the design of ACSs with respect to site-specific characteristics.

Keywords: Agroforestry; Land-use efficiency; Tree yield; Crop yield; Yield-SAFE

4.1. Introduction

As a consequence of the industrialisation and specialization of the agricultural production, field sizes across Europe have expanded with negative implications for the environment, particularly for landscape diversity and biodiversity (Wesche *et al.*, 2012; Meyer *et al.*, 2013; Tsiafouli *et al.*, 2015). The increased biomass demand for a bio-based economy will only heighten the pressure on arable lands, which will eventually compete with other land-uses in terms of food and feed production (Zscheischler *et al.*, 2016). In this context, a need to redesign the agricultural landscapes towards a multifunctional land-use has been identified in order to promote ecosystem services and to ensure a sustainable and resilient agricultural production in the 21st century (Landis, 2017; Birkhofer *et al.*, 2018).

Agroforestry systems, which integrate trees into agriculturally managed fields, are often regarded as a flexible multi-crop land-use strategy to provide ecological and economic benefits (Morhart *et al.*, 2014; Veste & Böhm, 2018). Agroforestry systems have been shown to preserve high levels of agricultural yields while delivering ecosystem services, hence increasing land-use efficiency (Fagerholm *et al.*, 2016; Paul *et al.*, 2017), and concurrently providing effective climate change mitigation, such as reducing the atmospheric carbon dioxide (De Stefano & Jacobson, 2018), and adaptation measures (Verchot *et al.*, 2007; Schoeneberger *et al.*, 2012).

A variation of agroforestry is represented by the so-called alley-cropping systems for the production of woody biomass (ACSs) for energy purposes, in which several hedgerows of fast-growing trees are established in parallel strips at varying distances on an agricultural field (Morhart *et al.*, 2014). The tree strips can be managed as short-rotation coppices and repeatedly harvested every 2–6 years, while the alleys between them are managed as conventional agricultural areas with annual crops (Tsonkova *et al.*, 2012).

Practitioners have expressed concern about the productivity of such systems due to the reduced area covered by agricultural crops (Tsonkova *et al.*, 2018). Through negative attributes reported by practitioners, the existence of trees has been perceived to decline the crop yield (Graves *et al.*, 2009), to impede farm machinery, and to attract diseases (Rois-Díaz *et al.*, 2018). In order to improve the design of ACS, research focused on identifying optima for the tree arrangement (scattered or lined, leeward or windward), the distance between trees, and proportion of land covered by the tree strips (Böhm, 2017).

In this context, the land equivalent ratio (LER) can serve as a valuable productivity indicator of yield performance and land-use efficiency in ACSs. LER is defined as the ratio of the area needed under monocultures compared to the area under intercropping, at the same management level and over the same period, that is required to provide an equivalent yield (Mead & Willey, 1980).

However, calculating the LER is a retrospective assessment and experiments with different ACS designs aiming at finding an optimum proportion of land covered by either trees or crops, while considering the specific site-conditions, would be time-consuming and would demand a notable large funding. Moreover, empirical data on these systems are scarce and therefore, an alternative method is crucial for achieving yield predictions under different implementation scenarios. Such a method is given by simulations capable of predicting the yield of both trees and crops in ACSs under different climatic, soil, and management conditions.

Consequently, the objective of this combined experimental and simulation study was to determine the potential energy wood and grain (winter wheat and winter barley) or seed (winter rapeseed) production, as well as to derive the LER, for two temperate ACSs in northern and north-eastern Germany, under different design scenarios. The emphasis of the design was set on tree arrangement (lee- or windward) and ratio of tree area to crop area. By evaluating these empirical and simulation-based responses, we have pursued optima in the design of ACSs comprising of most advantageous ratios of tree area to crop area with respect to tree arrangement, potential energy wood and grain or seed production, as well as LER values and gross energy yield.

4.2. Materials and Methods

4.2.1. Experimental Sites

Data used for this study was gathered in 2016 and 2017 at two short-rotation alley-cropping systems (ACSs) established near Wendhausen (Lower Saxony) and Neu Sacro (Brandenburg), Germany. The ACS at Wendhausen consists of nine tree strips having a width of 10 m (without the so-called buffer zone, a distance of about 1.5 m allocated between the tree strip and crop alleys for the agricultural machinery) and a length of 225 m, with agricultural alleys of 48 m and 96 m width between the tree strips (Swieter *et al.*, 2018). The ACS at Neu Sacro consists of seven tree strips having a width of 10 m (without the buffer zone of 1.5 m) and a length of 660 m, with agricultural alleys of 24 m, 48 m, and

96 m width between the tree strips (Kanzler & Böhm, 2016). The information for both sites is summarised in Table 13.

Table 13. Description of the experimental sites at Wendhausen and Neu Sacro.

Experimental site	**Wendhausen**	**Neu Sacro**
Latitude; Longitude	52˚19'54'' N; 10˚37'52'' E	51˚46'54'' N; 14˚37'18'' E
Altitude	85m a.s.l.	67m a.s.l.
Year of planting	Winter season 2007/2008 [a]	Winter season 2010/2011 [b]
Year of first harvest	Winter season 2013/2014 [a]	Winter season 2014/2015 [b]
Year of second harvest	Winter season 2017/2018	Winter season 2017/2018
Soil characteristics		
Soil type	Pelosol [a]	Pseudogleysol [b]
Soil texture	Silty clay [a]	Loamy sand [b]
Meteorological conditions		
Mean annual temperature [°C]	9.8 [c]	9.6 [d]
Average annual precipitation [mm]	616 [c]	568 [d]
Monoculture system		
Tree species	Poplar (*Populus nigra* L. x *P. maximowicii* Henry, clone "Max I")	
Tree rotation cycle	3-year [a]	4-year (1st rotation) [21] 3-year (2nd rotation)
Tree row orientation	North-South	North-South
Area trees [m^2]	70 x 70 [a,e]	11 x 25
Tree spacing [m]	2 x 0.5 [a]	1.3 x 0.9 [b]
Tree planting density [ha^{-1}]	10,000 [a]	8,700 [b]
Crop species (2016; 2017)	Winter rapeseed (*Brassica napus* L.); Winter wheat (*Triticum aestivum* L.)	Winter wheat (*Triticum aestivum* L.); Winter barley (*Hordeum vulgare* L.)
Area cropped [ha]	3 [f]	30 [b]
Alley-cropping system		
Tree species	Poplar (*Populus nigra* L. x *P. maximowicii* Henry, clone "Max I"),	

	with cultivated cropped alleys	
Tree rotation cycle	6-year	4-year (1st rotation) 3-year (2nd rotation)
Tree row orientation	North-South	North-South
Area tree strips [m^2] *	10 x 225 [f]	10 x 660 [b]
Tree spacing [m]	2 x 0.5 [a,f]	2.6 x 0.4
Tree planting density [ha^{-1}]	10,000 [a,f]	9,800
Crop species (2016; 2017)	Winter rapeseed (*Brassica napus* L.); Winter wheat (*Triticum aestivum* L.)	Winter wheat (*Triticum aestivum* L.); Winter barley (*Hordeum vulgare* L.)
Area cropped alleys [m^2]	48 x 225 [f]	48 x 660 [b]

[a] Lamerre *et al.* (2015); [b] Kanzler & Böhm (2016); [e] Lamerre *et al.* (2016); [f] Swieter *et al.* (2018);
[c] Weather station Braunschweig of the German Weather Service (DWD), 15 km west of the site;
[d] Weather station Cottbus of the German Weather Service (DWD), about 25 km west of the site.

Monthly values for mean air temperature and total rainfall during the two years of investigation were used for creating Walter-Lieth climate diagrams (appendixed Figure C.1.) in order to gain insight into the compound effects that influence the growth of trees and crops.

4.2.2. Plot Design and Yield Assessment

Four alley-cropping-plots (APs) and four monoculture-plots (MPs) representing an ACS and monoculture, respectively, were established at Wendhausen and Neu Sacro in winter season 2015/2016. At both sites, the APs were 24 m wide, placed on half of the 48 m agricultural alleys, and included half of the 10 m tree strips, hence accounting for a size of 29 m x 30 m. Furthermore, as the tree strips were perpendicular to the main wind direction at both sites, and in order to account for the yield variability in the tree-crop competition zone, two APs were arranged leeward and two APs windward.

Annual measurements of breast height diameter (i.e., at a height of 1.3 m above the ground) were taken from the short rotation coppices in winter season 2016/2017 and 2017/2018. In addition, 25 shoots were chosen, cut manually 10 cm above the ground, chipped and weighted. An allometric equation of the form $M = a \cdot D^{b}$ was used in order to derive the dry matter of all measured diameters, where *M* is the tree biomass [kg], *D* is the

shoot basal diameter [cm] and *a* and *b* are the intercept and slope of a least-square linear regression of ln-transformed data. The above-ground tree woody biomass production per hectare was estimated using the average number of shoots per hectare and the average dry weight of the shoots according to the mean stool method (Hytönen *et al.*, 1987).

Regarding the crop grain yield, winter rapeseed (*Brassica napus* L.) was harvested in the summer of 2016 and winter wheat (*Triticum aestivum* L.) in summer 2017 at Wendhausen, whereas at Neu Sacro, winter wheat was harvested in summer 2016 and winter barley (*Hordeum vulgare* L.) was harvested in summer 2017. Crop yields in the APs of 29 m x 30 m were harvested with a plot combine harvester with a cutting width of 2 m x 10 m, centred at 1 m, 4 m, 7 m, and 24 m distance from the tree strips (Figure 24).

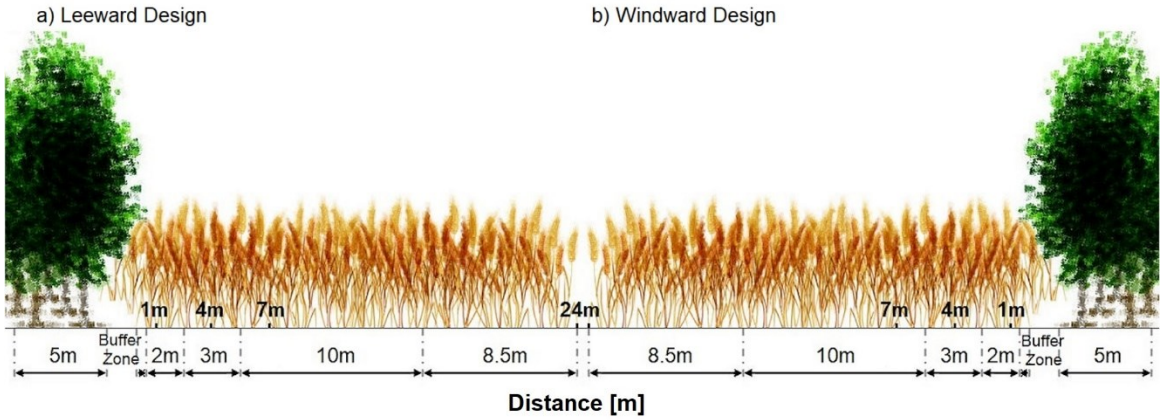

Figure 24. To-scale design of the leeward (**a**) and windward (**b**) alley-cropping-plots, together with the harvest points set at 1 m, 4 m, 7 m, and 24 m away from the tree strips. The supplemented distances (i.e., 2 m, 3 m, 10 m, and 8.5 m) sum up half of the neighboring distances of the harvest points and represent the weights used for calculating the overall crop yield. The buffer zone represents a distance of 1.5 m between the tree strip and crop alleys.

Additional information on the location, design, and harvest points of the APs is presented in appendixed Figure C.2.(**a)** for Wendhausen and Figure C.2.(**b**) for Neu Sacro.

For the overall crop yield in the APs, weighted averages were used (Equation 5), where the weights were determined assuming half of the distance between the harvest points. Thus, the weight for the harvest point located 7 m away from the tree strip, for example, considered half of the distance between the points set at 4 m and 7 m (i.e., 1.5 m), and half of the distance between points 7 m and 24 m (i.e., 8.5 m), leading to an overall distance of 10 m.

$$Grain_{Overall} = Grain_{1m} \cdot (0.5 + 1.5) + Grain_{4m} \cdot (1.5 + 1.5) + Grain_{7m} \cdot (1.5 + 8.5) + Grain_{24m} \cdot 8.5 \quad \text{Eq.(5)}$$

The crop yields in the MPs with a size of 10 m x 10 m were harvested with the same plot combine harvester with a cutting width of 2 m x 10 m centred in the middle of the plot. The measurements in the tree MPs underwent some changes due to lacking an identical planting scheme.

At Wendhausen, the available control field for trees contrasted with the APs by the age of the rotation cycle (i.e., 3-years instead of 6-years). Although this meant that the tree harvest at Wendhausen occurred in the winter season 2013/2014 (Lamerre *et al.*, 2015) for the control field and in the winter season 2017/2018 for the APs, we opted for this control field as representative for a tree MP in order to analyse poplar trees belonging to the same rotation and planted at the same density as the trees in APs. Moreover, the weather data observed in the two growing periods (i.e., from 2011 to 2013 for the MPs and from 2014 to 2016 for the APs) displayed a relatively low interannual variation of + 0.8 °C in mean annual air temperature and of -19 mm in average precipitation sum. At Neu Sacro, we assumed that the trees belonging to a double-row plot of the ACS would be comparable to those in an MP and therefore, measurements were collected from poplar trees grown at the same time as the trees from the APs, although the tree density varied somewhat, albeit insignificantly due to a different mortality rate of the two areas.

In order to avoid the border edge effect (Langton, 1990) reported at Wendhausen by Lamerre *et al.* (2015) and at Neu Sacro by Veste *et al.* (2018), we employed the dry matter woody biomass values obtained from the middle rows of the tree MPs to compare with the rows of their counterpart APs. Accordingly, the dry matter woody biomass value at Wendhausen was set at 9.4 Mg DM ha^{-1} a^{-1} (Lamerre *et al.*, 2015) and 9.0 Mg DM ha^{-1} a^{-1} at Neu Sacro (own measurements).

For gaining insight into the significance of our measurements, the coefficients of variation were calculated for the measured dry matter woody biomass values, either between APs and MPs, in order to confirm the differences in production stemming from the chosen two systems, as well as within plots belonging to the same system (i.e., separately for APs and MPs) in order to check whether meaningful differences exist between lee- and windward arranged plots. Additionally, t-tests were performed, where p values were compared to a significance level of 0.05 in order to determine whether

significant differences existed between the lee- and windward APs, as well as between APs and MPs. For this, the Analysis ToolPak from Excel (Microsoft) was employed.

Furthermore, the dry matter woody biomass values recorded over the investigated period of two years were converted to energy units in order to better compare the overall production from ACSs with monocultures. This was done by using the gross heat of combustion for each component as proposed by Kaltschmitt *et al.* (2016) and namely 18.5 GJ Mg^{-1} for the poplar woody biomass, 17.0 GJ Mg^{-1} for the grains of winter wheat, 17.5 GJ Mg^{-1} for the grains of winter barley, and 26.5 GJ Mg^{-1} for the seeds of winter rapeseed.

4.2.3. Empirically Determined Land Equivalent Ratio

The LER was determined for each system and scenario with respect to the area covered by both trees and crops in a land area and under the assumption that the yields of both trees and crops are of equal economic importance, after Mead & Wiley (1980) (Equation 6):

$$\mathrm{LER} = {Y_{Tree}^{AP}}\Big/{Y_{Tree}^{MP}} \cdot Area_{Tree} + {Y_{Crop}^{AP}}\Big/{Y_{Crop}^{MP}} \cdot Area_{Crop} \qquad \text{Eq.(6)}$$

where Y_{Tree}^{AP} [Mg DM ha^{-1} a^{-1}] and Y_{Crop}^{AP} [Mg DM ha^{-1} a^{-1}] are respective dry matter yields of wood and grains (winter wheat and winter barley) or seeds (winter rapeseed) per cropped area in APs and Y_{Tree}^{MP} [Mg DM ha^{-1} a^{-1}] and Y_{Crop}^{MP} [Mg DM ha^{-1} a^{-1}] are dry matter yields of wood and grains or seeds per cropped area in MPs.

In order to express these yields per alley-cropping system and not per cropped area, a weighted ratio was used for both tree and crop components depending on their land area proportion [%]. While LER ≤ 1 would mean that there is no productivity advantage of an ACS over a monoculture, a LER > 1 would suggest that the production in the ACS is higher than the one in a monoculture system (Mead & Willey, 1980).

4.2.4. Calibration and Validation of the Yield-SAFE Model

For the site-specific yield production of trees and crops in ACSs under competitive conditions, we employed the Yield-SAFE model (Yield Estimator for Long-term Design of Silvoarable AgroForestry in Europe), a parameter-sparse, eco-physiological, and process-based simulation model developed for predicting resource capture, growth, and production in forestry, arable, and agroforestry systems (van der Werf *et al.*, 2007). The reasoning behind choosing the Yield-SAFE model stays in its capacity to render credible yield estimates of trees and crops in relation to different weather, soil, and management

conditions from available, but scarce data (Graves *et al.*, 2010). In this version of the model, the potential tree and crop growth is simulated in terms of primarily air temperature (for the developmental and phenological processes), global solar radiation (for the derivation of photosynthesis), and water availability. Under this growth assumption, the nutrient availability is not considered to be a yield-limiting factor (van der Werf *et al.*, 2007). Improvements proposed by Palma *et al.* (2016) were integrated into the model, notably being the effect of trees on microclimate (temperature, wind speed, and evapotranspiration).

The assumptions and equations embodied in the Yield-SAFE model are extensively detailed by Burgess *et al.* (2004), van der Werf *et al.* (2007), and Keesman *et al.* (2011) regarding the states, rates and static relationships, and management of the tree growth, crop growth, and soil water dynamics. Moreover, a comprehensive description of the Yield-SAFE model, along with default parameter values for a substantial range of tree and crop species is provided by Burgess *et al.* (2005).

Heretofore, the Yield-SAFE model was calibrated and validated for poplar, walnut, cherry, holm oak, and stone pine trees, planted at low densities, alongside wheat, forage maize, grain maize, sunflower, and oilseed, leading to appraisals of both tree and crop yields and LER values in Atlantic and Mediterranean regions of Europe (Burgess *et al.*, 2004; Burgess *et al.*, 2005; van der Werf *et al.*, 2007; Palma *et al.*, 2007; Keesman *et al.*, 2011; Palma *et al.*, 2014).

In this paper, two sets of data were reserved, one for calibration of the Yield-SAFE model and one for validation of the model output. Initially, distinctions were made between the four APs, two arranged leeward and two windward. However, since the woody biomass measurements showed no significant differences between the two lee- and two windward plots, the woody biomass was analyzed considering four replicates. For the model calibrations, we retrieved information about the trees (planting density, management, yield, DOYplant, DOYharvest), crops (management, yield, DOYsow, DOYharvest), and soil physical characteristics (texture, structure, porosity, bulk density, organic matter) reported by Lamerre *et al.* (2016) and Swieter *et al.* (2018) for the site at Wendhausen and by Kanzler and Böhm (2016) at Neu Sacro. This information, together with model ecophysiological parameters based on bibliography and expert knowledge, as instructed in Graves *et al.* (2010), Keesman *et al.* (2011), Burgess *et al.* (2005), and Wösten *et al.* (1999), created the data set used for the calibration of the model. For example, the reported soil

characteristics helped achieve the Mualem-van Genuchten parameters as instructed by Wösten *et al.* (1999), used for the calibration of the Yield-SAFE model. Altogether, the tree parameters are presented in appendixed Table C.1., the crop parameters in Table C.2., and the soil parameters in Table C.3.. The daily climate input was obtained through the German Weather Service, stations Braunschweig and Cottbus, for the sites at Wendhausen and Neu Sacro, respectively. The validation data set encompasses the measured woody biomass values, as averaged between the APs. Therefore, the model output was validated against measured values in order to test the ability of the Yield-SAFE model to generate potential energy wood and grain or seed production, as well as to derive the LER, under different ratios of tree area to crop area.

The performance of the Yield-SAFE model was evaluated visually, by comparing the simulated tree and crop yields with measured ones, as well as by determining the normalized root-mean-square error (NRMSE), the coefficient of determination (R^2), the concordance correlation coefficient (CCC) (Ojeda *et al.*, 2017), which measured the agreement between the simulated and measured yields, and the bias function of the simulated yields (SB). Statistical analysis was performed using the R software (version 3.4.2, R Core Team 2017) independently for determining the NRMSE, R^2, and SB and using the package "epiR" (Stevenson *et al.*, 2019) for calculating the CCC.

4.2.5. Yield-SAFE Simulations of Tree and Crop Yields and Land Equivalent Ratio

The experimental, calibration, and validation sections of this study considered APs with a ratio of tree area to crop area of 17:83, i.e., the trees were planted on 17 % and the arable crop on 83 % of the land area. Once validated, the Yield-SAFE model was used to simulate the potential dry matter woody biomass and crop yield for the considered ACSs, as well as to derive the LER, under ratios of tree area to crop area of 20:80, 25:75, 40:60, 50:50, 60:40, 75:25, and 80:20 (appendixed Figure C.2.(**c**)). Throughout these simulations, the planting density remained constant.

By evaluating these empirical and simulation-based responses, optimum ratios of tree area to crop area in the design of the investigated ACSs were identified with respect to the potential energy woody and grain production, as well as LER values and gross energy yield. Conversely, designs not belonging to these ratio optima were considered ineffective in ACSs compared to other design options. Furthermore, key factors influencing the considered design of ACSs were discussed.

4.3. Results

4.3.1. Yield Assessment

The dry matter yields of wood and grains (winter wheat and winter barley) or seeds (winter rapeseed) per cropped area are presented in Table 14, together with the inferred gross energy yield, coefficient of variation, as well as the results of t-tests where p-values were compared to a significance level of 0.05.

Table 14. Dry matter yields of wood and grains (winter wheat and winter barley) or seeds (winter rapeseed) per cropped area obtained from alley-cropping- (AP) and monoculture-plots (MP) at Wendhausen and Neu Sacro for the investigated years and their inferred gross energy yield. APs 1 and 2 were arranged leeward and APs 3 and 4 windward. The coefficient of variation (CV) and level of significance are included.

		Location	**Wendhausen**				**Neu Sacro**			
		Species	**WR**	**WW**	**Poplar**		**WW**	**WB**	**Poplar**	
		Year	2016	2017	2016/2017	2017/2018	2016	2017	2016/2017	2017/2018
Alley-cropping-plots	Dry matter yield [Mg DM ha^{-1} a^{-1}]	AP1	3.1	6.0	10.3	12.9	6.5	4.5	13.8	12.8
		AP2	2.9	5.7	10.7	12.6	6.0	5.0	13.4	12.6
		AP3	2.7	6.8	10.9	14.0	6.3	6.0	13.9	12.5
		AP4	3.0	6.0	10.3	12.9	6.4	4.6	14.6	13.0
		Average AP	**2.9**	**6.1**	**10.5**	**13.1**	**6.3**	**5.0**	**13.9**	**12.8**
	Energy [GJ ha^{-1}]		619				689			
	CV AP [%]		7 $^{-}$	8 $^{-}$	3 $^{-}$	5 $^{-}$	3 $^{-}$	13 $^{-}$	4 $^{-}$	2 $^{-}$
Monoculture-plots	Dry matter yield [Mg DM ha^{-1} a^{-1}]	M1	3.5	7.0			4.2	3.2		
		M2	3.9	6.8			4.2	3.5		
		M3	3.9	7.6			5.5	3.7		
		M4	3.5	7.4			6.3	4.5		
		Average MP	**3.7**	**7.2**	**9.4**		**5.1**	**3.7**	**9.0**	
	Energy [GJ ha^{-1}]		221		348		151		333	
	CV MP [%]		6	5			20	16		
CV AP vs. MP [%]			14*	10*	6*	18*	17 $^{-}$	21*	23*	19*

WR: winter rapeseed, WW: winter wheat, WB: winter barley; * $p < 0.05$, $^{-}$ $p > 0.05$.

At Wendhausen, the APs were generally less productive than their counterpart MPs, especially in 2016. This, however, was only true for the dry matter yield obtained for the crops and not for the trees. At Neu Sacro, the APs were more productive than the MPs in both years and for all investigated species.

In 2016, the dry matter woody biomass increment resulted from the APs at Wendhausen was significantly lower (-25%) than that at Neu Sacro, whereas in 2017, similar values were obtained between the two sites. However, the dry matter woody biomass resulted from the MPs at Wendhausen was slightly higher (+5%) than that at Neu Sacro.

Worth mentioning would also be fact that the dry matter yields of winter wheat grains at the two locations produced similar values from the APs, while the yields from MPs were considerably higher at Wendhausen than at Neu Sacro.

Regarding the energy production over the investigated two years at Wendhausen, 221 GJ ha^{-1} would be achieved from crop MPs or 348 GJ ha^{-1} would be achieved from tree MPs, but an overall gross energy yield of 619 GJ ha^{-1} from the APs. Likewise, the crop- and tree MPs established at Neu Sacro would deliver a gross energy yield of 151 GJ ha^{-1} or 333 GJ ha^{-1}, respectively, over the two years, whereas the APs would provide with an overall gross energy yield of 689 GJ ha^{-1}.

The coefficients of variation within the APs at both locations were rather low, except for the one at Neu Sacro, in 2017, of 13%. The level of variation within the MPs was also minor at Wendhausen, contrasting to the one at Neu Sacro with 20% and 16% in 2016 and 2017, respectively. The yield variation between APs and MPs was relatively high for most of the investigated cases except for the dry matter woody biomass at Wendhausen in 2016.

Regarding the lee- and windward arranged APs, none of our investigations showed positive statistical significance, implying no effect of tree arrangement in relation to wind on the dry matter yield. Significant differences were found between the yields from APs and MPs, except for the dry matter yield of winter wheat grains at Neu Sacro (Table 14).

The measurements at Wendhausen and Neu Sacro were converted to relative yields, referring to the yield of each AP against its counterpart MP (Figure 25).

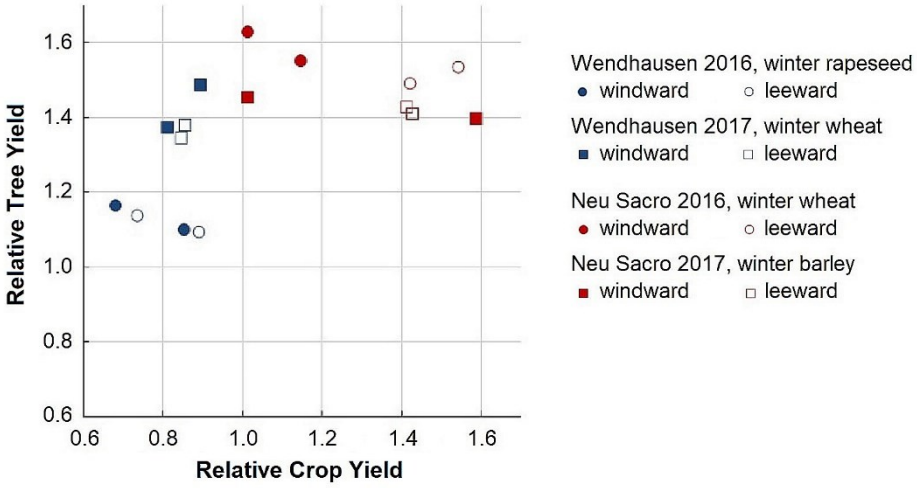

Figure 25. Relative tree and crop yields obtained from lee- and windward arranged poplar strips with cropped alleys at Wendhausen and Neu Sacro, over the investigated years.

The relative yield of the tree component was above 1.0 at both locations and in both years, suggesting that trees in APs were more productive than in MPs. Similar results were found for the relative yield of the crop component at Neu Sacro in both years, contrary to the one obtained at Wendhausen, which remained below 1.0, suggesting that both winter wheat and winter rapeseed were more productive in the MPs than in the APs.

In 2016, the relative crop yields from the leeward plots observed at Neu Sacro rendered values of 1.4 and 1.5, whereas the windward plots had values of 1.0 and 1.2. Otherwise, no concrete pattern was noticed for the lee- and windward plots at the two locations in the investigated years.

4.3.2. Empirically Determined Land Equivalent Ratio

The annual LER of each AP against its counterpart MP is presented in Figure 26, as determined for each experimental site and for both investigated years.

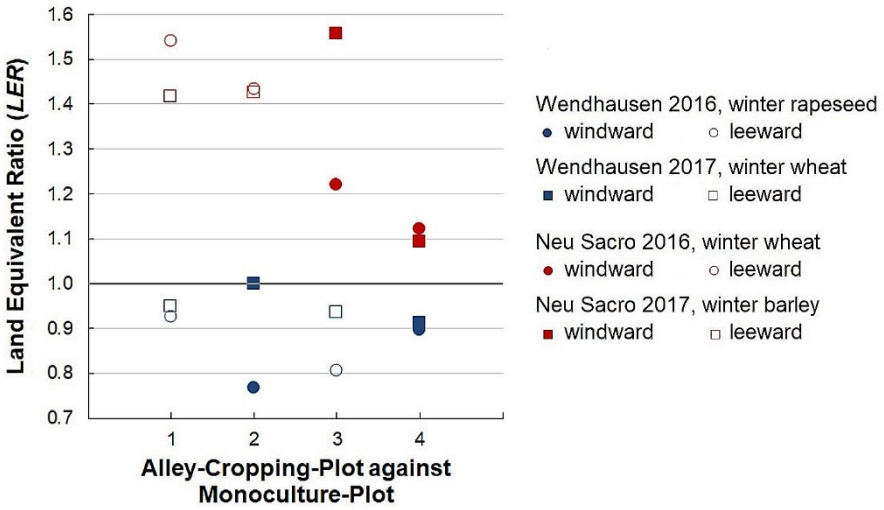

Figure 26. Annual land equivalent ratio (LER) obtained in 2016 and 2017 at Wendhausen and Neu Sacro. The grey line serves as a threshold above which the alley-cropping-plots have a greater productivity than the monoculture-plots.

The APs at Wendhausen rendered LER values from 0.8 (plots 2 and 3, in 2016) to 1.0 (plot 2, in 2017), whereas at Neu Sacro, LER values from 1.1 (plot 4, in both years) to 1.6 (plot 3, in 2017) were obtained.

4.3.3. Validation of the Yield-SAFE Model

Throughout the investigated timeframe, the Yield-SAFE model was able to simulate the tree and crop dry matter yields from the ACSs at Wendhausen (Figure 27(**a**)) and Neu Sacro (Figure 27(**b**)) with satisfactory accuracy.

At Wendhausen, the deviations of the simulated tree woody biomass accounted for 0.00%, 0.01%, and 0.05% from the tree woody biomass observed at the beginning of 2016, 2017, and 2018, respectively. Between the simulated and the observed crop yields, deviations of -0.02% and 0.08% were rendered for 2016 and 2017, respectively.

At Neu Sacro, the deviations of the simulated tree woody biomass accounted for -46%, 1%, and 1% from the tree woody biomass observed at the beginning of 2016, 2017, and 2018, respectively. Between the simulated and the observed crop yields, deviations of -3% and -8% were rendered for 2016 and 2017, respectively.

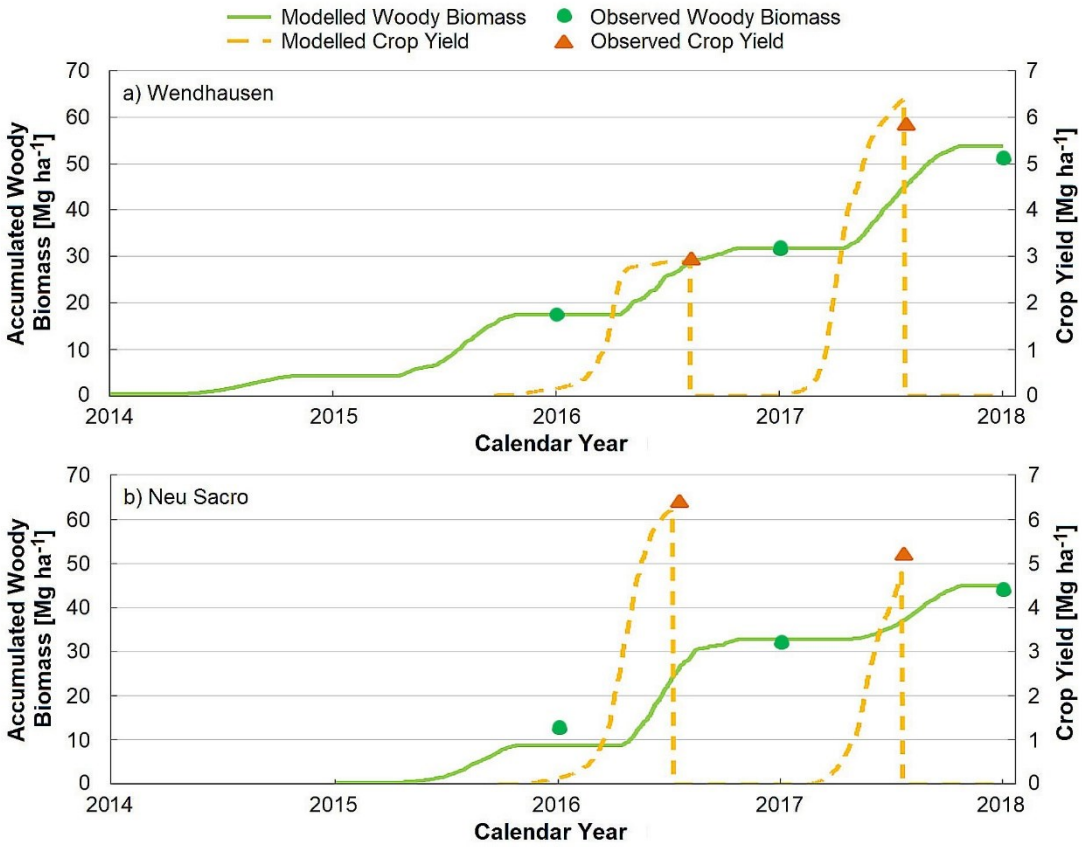

Figure 27. Above-ground tree woody biomass and crop yields accumulated at Wendhausen (**a**) and Neu Sacro (**b**) over the investigated period, as simulated with the Yield-SAFE model (lines) and as observed for the trees (circles) and crops (triangles; winter rapeseed and winter wheat in 2016 and 2017, respectively at Wendhausen; winter wheat and winter barley in 2016 and 2017, respectively at Neu Sacro).

The relative errors of the simulated fits were generally low, with normalized root-mean-square error (NRMSE) values of 5% and 8% for the Yield-SAFE tree and crop validations, respectively, at Wendhausen and NRMSE values of 8% and 6% for the Yield-SAFE tree and crop validations, respectively, at Neu Sacro. For both locations, the fit was highly significant (i.e., the R^2 values were more than 0.99 for both tree and crop validations). The concordance correlation coefficient (CCC) was 0.99 and 0.97 for the Yield-SAFE tree and crop validations, respectively, at Wendhausen and 0.99 and 0.89 for the Yield-SAFE tree and crop validations, respectively, at Neu Sacro.

4.3.4. Yield-SAFE Simulations of Tree and Crop Yields and Land Equivalent Ratio

Once satisfyingly validated for APs with a ratio of tree area to crop area of 17:83, the Yield-SAFE model was used to simulate the dry matter yields of wood and grains or seeds per

cropped area emerging from APs with ratios of tree area to crop area of 20:80, 25:75, 40:60, 50:50, 60:40, 75:25, and 80:20 at Wendhausen (Figure 28) and Neu Sacro (Figure 29).

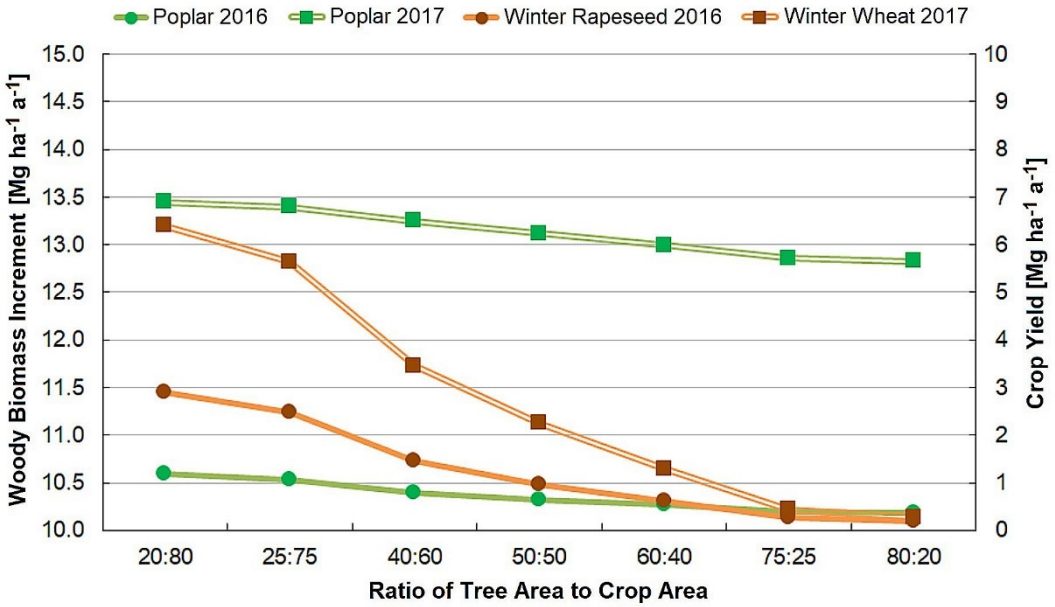

Figure 28. Above-ground tree woody biomass and crop yields, as simulated by the Yield-SAFE model at Wendhausen, under different ratios of tree area to crop area.

A clear downfall in the simulated grain (winter wheat) and seed (winter rapeseed) yield was noticed after the ratio of tree area to crop area of 25:75 at Wendhausen, whereas a rather small decline was noted for the woody biomass beyond the same point. Subjected to the ratio of tree area to crop area of 80:20, the Yield-SAFE simulations for both years rendered about 93% less crop yield and 4% less yearly tree woody biomass compared to the values obtained for a ratio of tree area to crop area of 20:80.

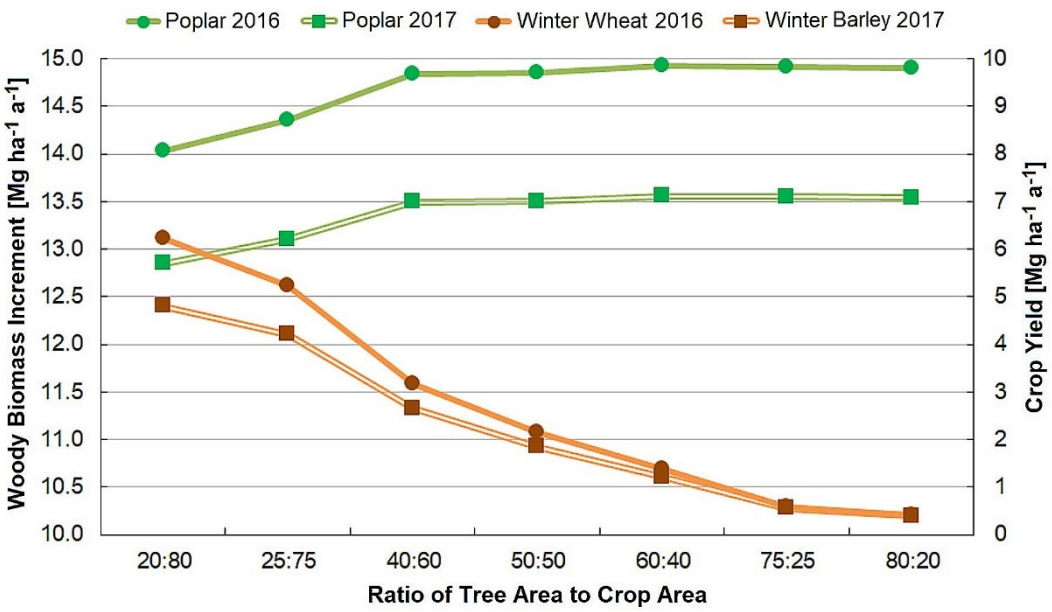

Figure 29. Above-ground tree woody biomass and crop yields, as simulated by the Yield-SAFE model at Neu Sacro, under different ratios of tree area to crop area.

The simulated grain yield at Neu Sacro was subjected to a downfall after the ratio of tree area to crop area of 25:75, although an upward surge was observed in the yearly woody biomass beyond the same point, until the ratio of tree area to crop area of 40:60, where a rather protracted yearly woody biomass was noticed. Between the first and the last design scenarios, about 93% less crop yield and 6% more yearly woody biomass were rendered by the Yield-SAFE model for both years.

These values simulated for the dry matter yields of wood and grains or seeds per cropped area and per alley-cropping system are presented in appendixed Table C.4. together with their respective relative yields and hence, the LER and gross energy yield determinations. Furthermore, Figure 30 presents the LER values as simulated by the Yield-SAFE model under ratios of tree area to crop area of 20:80, 25:75, 40:60, 50:50, 60:40, 75:25, and 80:20 for both locations and investigated years.

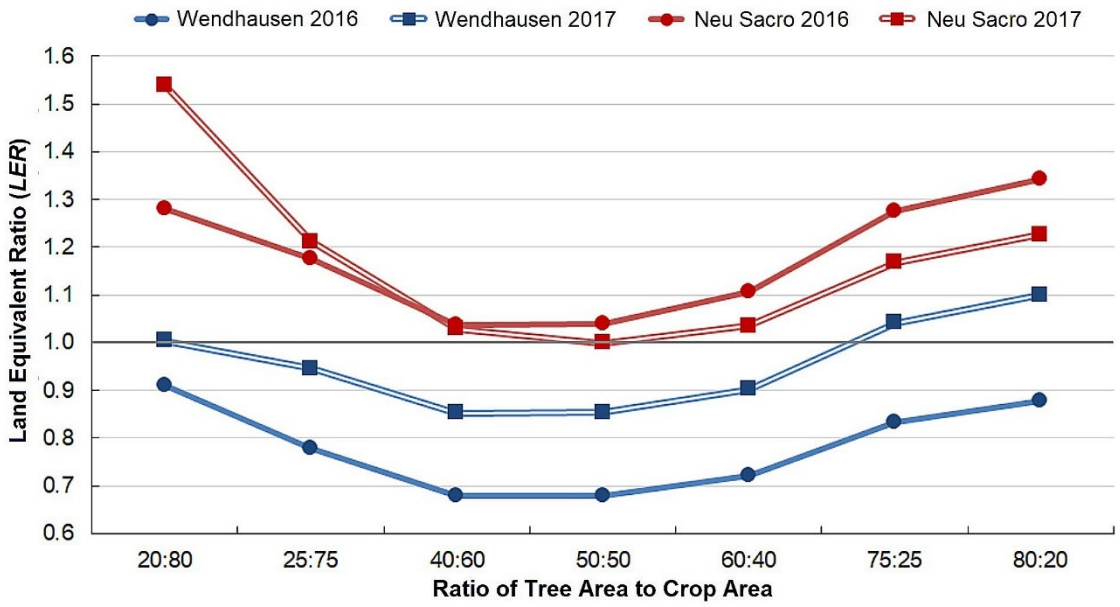

Figure 30. The effect of different ratios of tree area to crop area on the land equivalent ratio (LER), as simulated by the Yield-SAFE model for the ACSs at Wendhausen and Neu Sacro, in 2016 and 2017. The grey line serves as a threshold above above which the alley-cropping system has a greater productivity than the monoculture system.

The LER values simulated for different ratios of tree area to crop area follow a convex curve where the maximum values are achieved when either tree or crop component was dominant (i.e., when one of these components occupy at least 75% of the land area) and minimum when these components shared similar proportions of land area. At Wendhausen, aside from very few cases, the LER remained below 1.0 no matter the ratio of tree area to crop area, suggesting that the simulated alley-cropping system was less productive than the monoculture system. Conversely, at Neu Sacro integrating trees and crops under all area proportions caused the simulated LER to be above 1.0, hence the alley-cropping system to be more productive than the monoculture system.

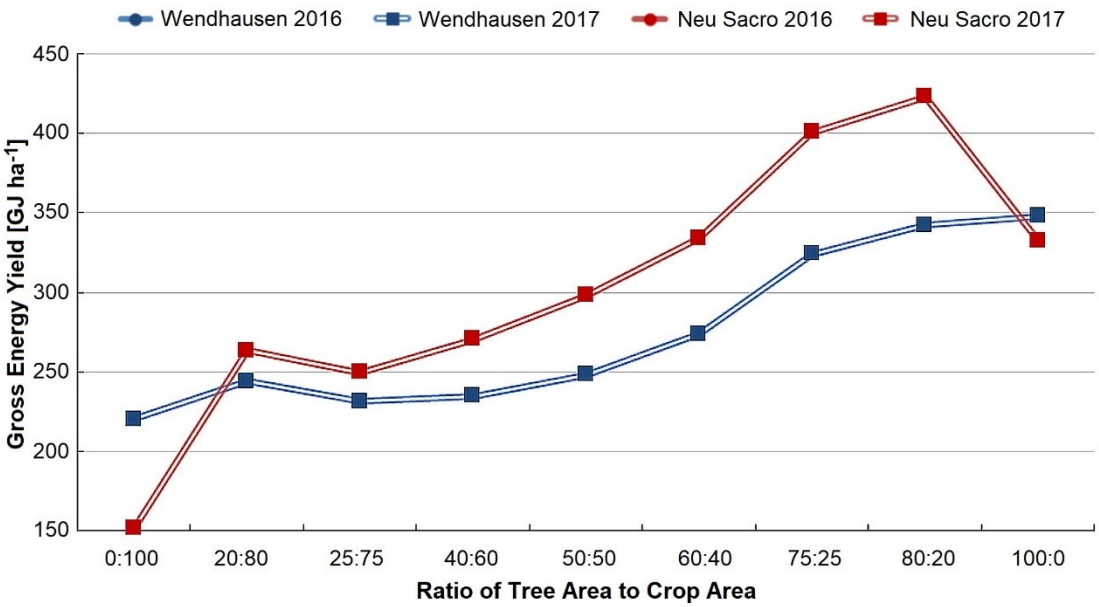

Figure 31. The effect of different ratios of tree area to crop area on the gross energy yield, calculated with simulated yields for the ACSs at Wendhausen and Neu Sacro, in 2016 and 2017.

The gross energy yields over the two investigated years (Figure 31; appendixed Table C.4.) at Wendhausen would follow a softer curve by decreasing slightly, with 5% from the ratio of tree area to crop area of 20:80, and increasing thereafter up to 40% more gross energy yield achieved in the ratio of tree area to crop area of 80:20, compared to that of 20:80. Similar results were observed for Neu Sacro, i.e., a slight decrease of 5% followed by an upward surge up to 60% more gross energy yield achieved in the ratio of tree area to crop area of 80:20, compared to that of 20:80.

At the highest simulated proportion of land area covered by the crop (i.e., 20:80), the ACS at Wendhausen and Neu Sacro rendered 11% and 74% more gross energy yield, respectively, compared to the crop monoculture (i.e., 0:100). Similarly, compared to the tree monoculture (i.e., 100:0), the highest simulated proportion of land area occupied by the trees (i.e., 80:20) rendered 27% more gross energy yield at Neu Sacro, albeit 2% less gross energy yield at Wendhausen.

4.3.5. Optimum Ratios of Tree Area to Crop Area

According to the simulated energy wood and grains (winter wheat and winter barley) or seeds (winter rapeseed) at our considered ACSs, the ratios of tree area to crop area from 20:80 to 25:75 would be the most advantageous to the design of such systems. The

accretion accounting for the highest potential tree and crop yields emerged from these ratios regardless of the tree arrangement of the APs.

The simulated LER values inferred two main ratios of tree area to crop area, i.e., from 20:80 to 25:75, but also from 75:25 to 80:20. While the implication at Wendhausen was that the productivity of the ACS was below a monoculture's regardless of the proportion of area covered by either trees or crops, these main ratios were preferable compared to other design options, and quite favourable in 2017.

The gross energy yield values suggested that all ratios of tree area to crop area above 75:25 would be advantageous at Wendhausen, but only from 75:25 to 80:20 at Neu Sacro, since the values decreased thereafter (Figure 31).

4.4. Discussion

4.4.1. Yield Assessment

Although the annual increment of tree woody biomass reported for poplar can vary with tree clone of choice, weather, and other growth-limiting factors such as mortality and seasonal variation of light, studies performed on second rotation poplar trees planted at around 10,000 cuttings ha^{-1} recorded biomass values in the range of 2.8–9.0 Mg DM ha^{-1} a^{-1} (Mitchell *et al.*, 1999), 2.0–9.6 Mg DM ha^{-1} a^{-1} (Aylott *et al.*, 2008), and sometimes above 20 Mg DM ha^{-1} a^{-1} (Calfapietra *et al.*, 2010). In a study made on 6-year, second rotation cycle poplar trees planted at 11,000 cuttings ha^{-1}, Bemmann *et al.* (2007) reported woody biomass values between 11.5 Mg DM ha^{-1} a^{-1} and 19.0 Mg DM ha^{-1} a^{-1} obtained at vigorous locations and between 4.5 Mg DM ha^{-1} a^{-1} and 9.0 Mg DM ha^{-1} a^{-1} achieved at less vigorous site types.

The poplar tree yields found in the present study were in line with findings from literature, although significant differences arose between APs compared to their corresponding MPs. A tree yield advantage from the tree strips in APs would stem from additional space and higher light availability thanks to the crop alleys. The tree yield from MPs purposefully did not consider these border edges so that a fair resemblance to a monoculture forestry was ensured (Langton, 1990), despite the reported lower yields.

According to the yield potential tables for energy crops in Germany proposed by Döhler (2005), the crop yields measured at our study sites would be classified as medium to low, which we would attribute to the weather conditions, but also to waterlogging during

the winter months (Lamerre *et al.*, 2015), extreme heterogeneity in water content (Lamerre *et al.*, 2016; Kanzler & Böhm, 2016), and soil texture reported at Wendhausen by Lamerre *et al.* (2015, 2016) and at Neu Sacro by Kanzler & Böhm (2016).

Regarding the weather conditions, the results presented in Table 14 indicate towards unfavourable growing conditions for trees and crops in 2016, compared to 2017, at Wendhausen, whereas at Neu Sacro, the tree and crop growth were similar, albeit more prosperous for trees in 2016 than in 2017. This implication was corroborated by the Walter-Lieth climate diagrams (appendixed Figure C.1.), revealing 314 mm less annual average precipitation in 2016 than in 2017 at Wendhausen and only 28 mm less in 2016 than in 2017 at Neu Sacro. Moreover, the rainfall in 2016 in both locations was subjected to a drastic decline precisely in those months essential for tree and crop growth. The mean annual temperatures were around 10.3°C in both years and for both locations. Since even minor changes in average precipitation sum, global solar radiation, and mean air temperature have been reported to significantly alter the growth of poplar trees (Seserman *et al.*, 2018), oilseed rape (Pohle *et al.*, 2015), winter wheat, and barley (Gerstengarbe *et al.*, 2003), the auspicious weather conditions from 2017 might explain why tree and crop yields at Wendhausen were lower in 2016 than in 2017.

At Wendhausen, small variation was noticed within crop yields from APs and MPs, although the absolute values would indicate a slight yield advantage stemming from the windward arranged plots, caused mainly by the leaf litter deposition (Swieter *et al.*, 2018). Significant differences at Wendhausen were observed between the APs and MPs, with crop yield advantages inclining toward the latter plots. The reduced crop yield in APs was correlated with tree height (i.e., more than 6 m), hence, higher tree shading causing crop developmental delays up to 7 m away from the tree strips (Swieter *et al.*, 2018).

At Neu Sacro, the crop yields particularly varied within MPs, but also within APs, in 2017. This might have been the result of extreme temperatures throughout the day, heterogeneity in water content and soil texture, as well as remarkable differences in relative humidity and water evaporation rates between MPs and APs reported at the site (Kanzler *et al.*, 2018). Consequently, the crop yields from the MPs were significantly lower than the ones from APs, highlighting the contribution of tree strips to crop yield production in terms of increased soil moisture and relative humidity, temperature regulation, wind protection, and hence, a reduced evapotranspiration, as also reported by Kanzler & Böhm (2016) and Kanzler *et al.* (2018) at the Neu Sacro site.

According to studies, the yield production of winter cereals benefits from the presence of tree strips in dry conditions but is hindered by them in well-watered conditions (Kanzler *et al.*, 2018; Bruckhaus & Büchner, 1995). This could explain why the winter wheat yield from MPs at Wendhausen reached 7.2 Mg DM ha^{-1} a^{-1} in 2017 and only 5.1 Mg DM ha^{-1} a^{-1} in 2016 at Neu Sacro, whilst the APs at both locations rendered similar results, around 6.0 Mg DM ha^{-1} a^{-1}. The amount of rainfall in 2017 was relatively high at Wendhausen, theoretically allowing for a considerable crop yield production in the MPs, but under the presence of trees in the APs, crops might have suffered from waterlogging, as well as from the height of the trees and a lack of litter coverage, which resulted in lower planting density and hence, lower crop yield (Swieter *et al.*, 2018). At Neu Sacro, on the other hand, the crops in the APs might have benefitted from the drier conditions of 2016, along with the above-mentioned contribution of tree strips.

Regarding the lee- and windward arranged APs, none of our investigations showed high variance or a positive statistical significance between the tree and crop DM yields. Therefore, the implication was either that no windbreaking effect of tree strips existed in relation to the crop DM yield or that, while the main wind direction pointed from South-West, it changed throughout the year at Wendhausen (Swieter *et al.*, 2018) and Neu Sacro (Kanzler *et al.*, 2018), thus affecting all APs in a similar way.

Lastly, the appropriateness of using winter crops at high latitudes (i.e., more than 50° latitude North) in ACS should be further examined, since the sun irradiance reaching the crop can be hindered by the trees leafing precisely at key phenological stages for winter crops, i.e., in December (when crop germination and early growth occurs), March (for crop flowering), and June (when grain filling is concerned) (Dupraz *et al.*, 2018). By comparison, poplar trees open their buds in April and drop their leaves in November. Given our establishment (i.e., 24 m wide crop alleys with North-South tree strip orientation), trees can capture more than 50 % of the sun irradiation that would have reached the crop, strongly affecting the crop yields (Dupraz *et al.*, 2018).

4.4.2. Empirically Determined Land Equivalent Ratio

Aside from one case in 2017, the LER values at Wendhausen were lower than 1.0, indicating that the ACS was consistently less productive than the monoculture system within the observed two years. Conversely, at Neu Sacro, all LER values were higher than 1.0, favouring the ACS by comparison to the monoculture system.

Nevertheless, since the border edge effects can influence the DM woody biomass in an MP to different extents, it can produce favouring of a certain system when determining the LER. For example, at Wendhausen the reported DM woody biomass from the middle rows was 9.4 Mg DM ha^{-1} a^{-1}, but 13.7 Mg DM ha^{-1} a^{-1} in the leeward border of the tree monoculture system (Lamerre *et al.*, 2015). Similarly, at Neu Sacro, 9.0 Mg DM ha^{-1} a^{-1} were determined from the middle rows, by comparison to 11.0 Mg DM ha^{-1} a^{-1} from the leeward border of the tree monoculture system (own measurements). However, given the proportion of the total area that these values account for and for the purpose of this study, it was paramount to ensure a fair resemblance to a monoculture forestry, despite the reported lower yields. In a comprehensive study on different types of edge effects and their disadvantages to the overall yield estimations, Langton (1990) recommended eliminating edge effects, hence improving accuracy of yield estimation.

Shortcomings of the LER approach include the lack of consideration for by-products and their revenue, the rectangularity of the planting scheme, the assumption that the production is constant, reliable, and happens in a static temporal context, and the idea that the interactions between trees and crops would automatically lead to either benefits or competition (Terreaux & Chavet, 2004).

4.4.3. Yield-SAFE Simulations of Tree and Crop Yields and Land Equivalent Ratio

The concordance correlation coefficient (CCC) and the simulation bias (SB) were also used to assess the model performance of APSIM (Agricultural Production Systems Simulator) to predict the dry matter (DM) yield of switchgrass (*Panicum virgatum* L.) and *Miscanthus* (*Miscanthus x giganteus*) and classifications were introduced pertaining to these two parameters (Ojeda *et al.*, 2017). Accordingly, the Yield-SAFE model rendered "very-good" (CCC > 0.90 and SB < 20%; Ojeda *et al.*, 2017) correspondences with the observed above-ground DM yields of woody biomass and crop yield, which implied that the Yield-SAFE model was able to capture the crucial aspects of the crop-tree interactions in our ACSs over the investigated period.

The crop yield simulations showed a steady decline in crop yield as the ratio of tree area to crop area increased, which was expected since the area occupied by the crops decreased. Additionally, our results were corroborated by measurements performed from 2008 to the end of 2014 at Wendhausen on ACSs with ratios of tree area to crop area of 20:80 and 27:73 (Lamerre et al., 2016). Comparing the compound yields of trees and crops

stemming from these two ratios of tree area to crop area, Lamerre et al. (2016) reported less crop yield in the 27:73 ratio than in 20:80 one, albeit higher tree yield.

Our tree yield simulations showed slight differences between the first and the last design scenarios, i.e., 4% less tree yield at Wendhausen and 6% more tree yield at Neu Sacro. In the Yield-SAFE model, a higher tree area on the total land area did not presume a higher planting density of the trees, but rather wider tree strips with narrower crop alleys in between, as presented in appendixed Figure C.2.(c). This increase in tree yield observed at Neu Sacro would be plausible since the poplar trees planted at a planting density of 8700 tree ha-1 would be able to intercept the major proportion of the incoming light early in the tree rotation during well-watered conditions. At higher planting densities, however, the competition for incoming light could hamper the potential yield increase even during well-watered conditions, similar to an edge effect. In the Yield-SAFE model, these soil water conditions are given by the water balance equation, but also in terms of the ground water levels (i.e., 0.9m at Wendhausen (Lamerre *et al.*, 2016) and 1.4m at Neu Sacro (Kanzler & Böhm, 2016)).

Progressively higher tree yields in the APs than in the MPs, together with the gradually increasing percentage of total land area occupied by trees, caused an initial descent followed by an upraise in the simulated LER values. Similarly, the gross energy yields increased progressively with the percentage of total land area occupied by trees, as the energy derived from the dry matter yields of wood largely matched the energy lost from grains (winter wheat and winter barley) or seeds (winter rapeseed).

Compared to their corresponding tree and crop monocultures, the investigated ACSs rendered higher simulated energy yields. This is largely because, compared to the monoculture simulations of tree and crop yields, the ACS simulations accounted for the competition for water availability and incoming light, but also considered the algorithms for tree effects on microclimate, hence conserving soil moisture (Palma *et al.*, 2016; Palma *et al.*, 2017). This was important since previous studies did not include such effects in Yield-SAFE, albeit the need was clearly stated (Crous-Duran *et al.*, 2018).

Nevertheless, simulating the energy wood and grain or seed production in ACSs with respect to the monoculture systems can be hampered by various uncertainties, many of those related to the underlying assumptions in the model, which do not account for plant

mortality, nutrients, and pests, but also because of the difficulty in discriminating between intra- and inter-specific plant competition.

4.4.4. Optimum Ratios of Tree Area to Crop Area

Considering the highest potential tree and crop yields, LER values, and gross energy yields, optimum ratios in the design of our investigated ACSs would encompass the ratios of tree area to crop area from 20:80 to 25:75, but also from 75:25 to 80:20. While this later uprise in the simulated LER values would assume that certain ACSs might favour narrower crop alleys, difficulties would appear in reality in terms of machinery use and expenses required for establishing a narrow crop alley at the outcome of a virtually insignificant production.

The empirical and simulation-based approaches of this study have not taken into account the environmental benefits brought by the presence of trees on an agricultural land, such as the reduction in plant mortality, due to disease or wind-throw (Calfapietra *et al.*, 2010), the reduction of atmospheric carbon dioxide (De Stefano & Jacobson, 2018), and reduced nutrient leaching (Mitchell *et al.*, 1999). These factors should be calculated in the future and summed to the whole nexus of advantages and disadvantages of integrating trees on an agricultural land.

4.5. Conclusions

Based on the measurements and simulations of dry matter yields of energy wood and grains (winter wheat and winter barley) or seeds (winter rapeseed) in ACSs, we derived the land equivalent ratio (LER) and the gross energy yield for two years, locations, and several ratios of tree area to crop area.

Optima in the design of ACSs comprising of most advantageous tree arrangement and ratio of tree area to crop area were identified with respect to tree arrangement, potential energy wood and grain or seed production, as well as LER values and gross energy yield. Furthermore, the implications of several ratios of tree area to crop area have been discussed in order to improve the decision-making, optimization, and adaptation of the design of ACSs with respect to site-specific characteristics.

The notion that the trade-off between wood and grain production does not solely implicate the production of ACSs was reinforced, as the presence of trees can also bring many environmental benefits to the agricultural land that should be calculated and summed

to the whole nexus of advantages and disadvantages of ACSs before establishing such systems or choosing against it.

Last but not least, this study emphasized the considerable potential of modelling approaches in ACSs, as they can simulate tree and crop yields for specific site-conditions in a non-intrusive, inexpensive, and prompt way while supporting an early site-setup planning.

Author Contributions

The SIGNAL project was initiated and planed in relation to the proposal call "Soil as a Sustainable Resource for the Bioeconomy – BonaRes" (http://www.signal.uni-goettingen.de). Diana Seserman analysed the data and wrote the manuscript. Anita Swieter, Maren Langhof, Maik Veste, and Dirk Freese contributed by revising the manuscript.

Funding

This research was carried out under the BonaRes - SIGNAL project (FKZ 031A562E, 2015-2018) and funded by BMBF - German Federal Ministry of Education and Research (Bundesministerium für Bildung und Forschung).

Acknowledgments

We are grateful to our colleagues at the Julius Kühn-Institut in Braunschweig for their support and scientific collaboration. Additionally, we thank the Agrargenossenschaft Forst/L. e.G. for their promotion and management of the agroforestry system at Neu Sacro and the German Weather Service (Deutscher Wetterdienst, DWD) for the provision of weather data. We gratefully acknowledge the various students for their help with the field work. Last but not least, we would also like to thank the editor and reviewers for their assistance and helpful comments on the manuscript.

Conflicts of Interest

The authors declare no conflict of interest. The founding sponsors had no role in the design of the study; in the collection, analyses, or interpretation of data, in the writing of the manuscript, and in the decision to publish the results.

5. General Conclusions and Outlook

The central resolution of the present dissertation was to evaluate the prospective implications of different site-specific conditions and scenarios on tree growth in ACSs. By several experimental and simulation-based studies, the ability of a process-oriented, eco-physiological tree and crop growth model was investigated, concluding the following:

a) The role of several modelling approaches in imputing missing empirical data from existent but scarce availability of data was confirmed. While some of the investigated modelling approaches imputed the missing data with satisfactory accuracy, simulating tree growth required a holistic approach, equivalently incorporating the components of the soil-plant-atmosphere nexus. Accordingly, a process-oriented, eco-physiological model, capable of simulating the growth of hybrid-poplar trees from scarce availability of data and with respect to the specific tree phenology and light and water availability, was identified in the Yield-SAFE model.
b) Based on the growth characteristics of poplar and black locust trees measured over a growing period of four and five years, respectively, together with climatic inputs and soil and tree parameters adapted from literature, the Yield-SAFE model has been calibrated and validated with satisfactory accuracy.
c) Once calibrated and validated, the Yield-SAFE model has projected the growth sensitivity of poplar and black locust trees to a variety of weather conditions and prospective long-term climate change, from 2015 to 2054.
d) By enabling the crop module in the Yield-SAFE model, the growth of poplar trees was simulated in strong relation to the interactions with different adjacent crops and their respective resource capture.
e) Based on climatic inputs and tree, crop, and soil measurements, reports, and adaptations from literature, the Yield-SAFE model has simulated the yield of both trees and crops in ACSs under different climatic and edaphic conditions, as well as projected the tree and crop yields under several implementation design scenarios.
f) Consequently, the LER and gross energy yield were derived for two existing ACSs schemes and under several implementation design scenarios, thus assessing the implications of integrating trees on an arable land, as compared to forestry and conventional monocultures with annual arable crops.

5.1. Synthesis of Main Results

Understanding whether and to which degree is tree growth affected by external factors demands for systematic monitoring and inventorying of tree growth characteristics. However, in cases where missingness is unavoidable and simply disposing of the data points is not an option, modelling approaches can be effective. By applying several models belonging to (**i**) regression analysis, (**ii**) statistical imputation, (**iii**) forest growth functions, and (**iv**) a process-oriented tree growth model, insight has been provided into finding a handy tool for both researchers and practitioners dealing with incomplete data sets.

From the curve-fitting models, the Gaussian model performed the best, being tightly followed by the Power model with two terms, Sum of Sine, and the Polynomial of 1st Degree, then the Polynomial of 2nd Degree. Nearing this performance, the interpolation models Linear, Cubic, and PCHIP have also shown good correspondences with the measurements, both under 72% and 43% data gap representations. The forest growth functions rendered good results, following the sequence: Korsun (1935) > Michailoff (1943) and Petterson (1955) > Prodan (1951) > Assmann (1943). Unsurprisingly, most of these models performed better under higher data availability, i.e., under 72% of existing data, as compared to 43% of existing data.

The Yield-SAFE model, a process-oriented, eco-physiological model, was identified as able to simulate the growth of poplar trees from limited availability of data and with respect to the specific tree phenology and light and water availability. The Yield-SAFE model imputed the data gaps with satisfactory accuracy by simulating the daily growth of poplar trees over the entire investigated timeframe. Additionally, the performance of the model was sustained by other parameters, such as the tree woody biomass and soil water content, which matched reported values. While tree growth models are widely used for prediction purposes, either for future risk assessments, or under different climatic, edaphic, and management scenarios, the findings of this dissertation have emphasized another role of such models and namely for filling the gaps in field measurements.

Furthermore, the Yield-SAFE model simulated the daily above-ground woody biomass of hybrid-poplar and black locust with satisfactory accuracy and responded sensitively to changes in the climatic and edaphic conditions. The model output displayed high sensitivities to the tree parameters: initial number of shoots, radiation use efficiency, radiation extinction coefficient, and maximum leaf area for a single shoot in descending

order. Dominant soil parameters in descending order were: pF value at field capacity, potential evaporation, saturated volumetric water content, and soil depth.

Regarding the climate inputs, the modelled output was highly sensitive to changes in global radiation and precipitation, but the responses to changes in air temperature were mostly attributed to the directly proportional relationship between global radiation and air temperature. Accordingly, the findings of this dissertation showed that the tree yields in an SRC were positively impacted by increasing air temperature and negatively by decreasing precipitation. Additionally, the notion that climate change impacts cannot be categorized as solely positive or negative was reinforced, as tree yield productivity has shown to react diametrically contrary to shifts in climate. This was evidenced, for example, by the fact that higher average annual temperatures could either increase the tree growth due to a prolonged vegetation period or, on the contrary, decrease the tree growth due to higher potential evapotranspiration.

Once the appropriateness of the Yield-SAFE model to simulate and predict tree growth under different site-specific conditions and scenarios was conclusive, the crop module was also enabled. Accordingly, the Yield-SAFE model was calibrated and validated to simulate the growth of poplar trees in strong relation to the interactions with different adjacent crops and their respective resource capture. The yield of both trees and crops stemming from two existing ACSs were simulated under different climatic and edaphic conditions, as well as projected under several implementation design scenarios.

Optima in the design of two existing ACSs comprising of most advantageous tree arrangement and ratio of tree area to crop area were identified. The LER and gross energy yields were derived for two ACSs schemes and under several implementation design scenarios, thus assessing the implications of integrating trees on an arable land, as compared to forestry and conventional monocultures with annual arable crops.

The notion that the trade-off between wood and grain production does not solely implicate the production of ACSs was reinforced, as the presence of trees can also bring many environmental benefits to the agricultural land that should be calculated and summed to the whole nexus of advantages and disadvantages of ACSs before establishing such systems or choosing against it.

Collectively, the considerable potential of process-oriented tree and crop growth models, such as Yield-SAFE, was highlighted. At all times, the simulations were performed

under scarce availability of data, for a gradient of site-specific conditions, and in a non-intrusive, inexpensive, and prompt way. This, together with the appropriateness of the Yield-SAFE model to project tree and crop yields on different temporal scales, can progressively support early and sustainable site-setup plannings of ACSs, as well as upcoming risk assessments, and adaptation scenarios in the near and distant future.

5.2. Research Limitations

Throughout the studies encompassed in this dissertation, the ability to provide with robust projections of tree and crop yields under scarce availability of data was a very desirable modelling feature, heavily weighting in the final decision towards the Yield-SAFE model. However, this same feature can hold disadvantages when higher accuracy in projecting the overall tree and crop yield is required (e.g., accounting for leaves and below-ground biomass) or when additional ecosystem services need to be considered (e.g., nutrient cycle and carbon sequestration).

As a negative consequence of this feature, for example, the simulation assumed a one-dimensional soil layer, homogeneous in its physical characteristics, above which lay the horizontal extents of trees and arable crops (van der Werf *et al.,* 2007). On a daily temporal scale, the model projected the above-ground woody biomass (i.e., from the tree stems and crop grains) accounting for the plant and atmospheric factors, as well as for the water limitations stemming from the water balance model, microclimate, and soil water dynamics. Therefore, in terms of potential, limited, and actual production of plant yield, the Yield-SAFE model accounted for half the processes succinctly describedby Figure 32.

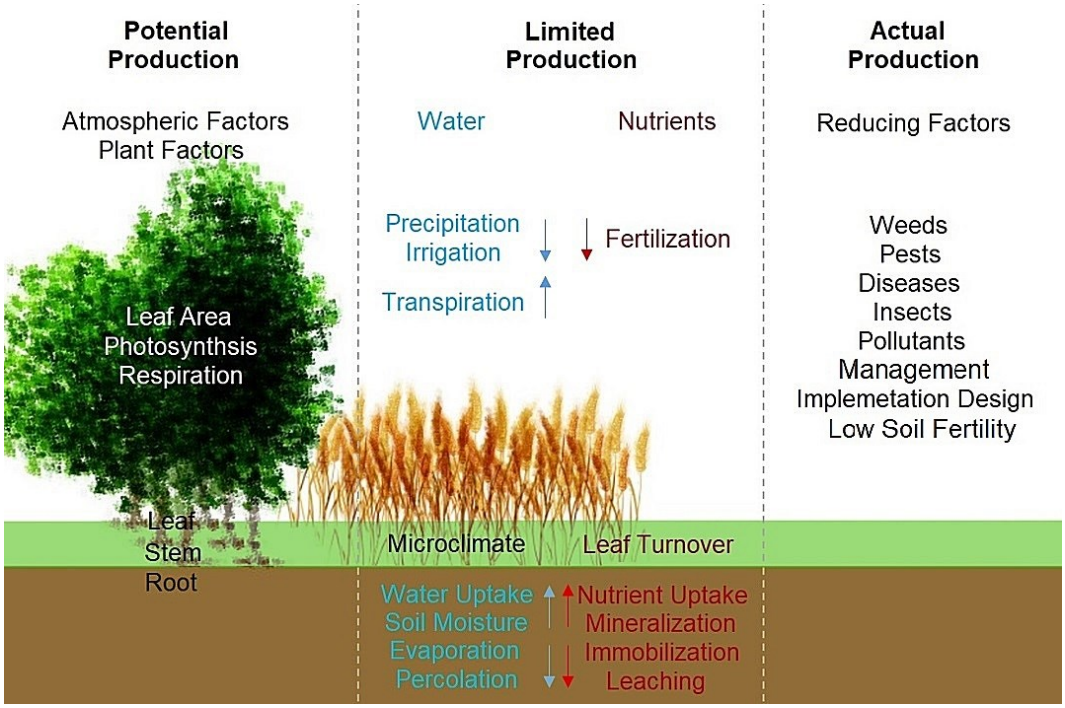

Figure 32. Potential, limited, and actual production in ACSs, adapted after Young (1989) and van Ittersum *et al.*, (2013)

Except for the below-ground woody biomass, which accounts for the root development, the simulations performed in the current dissertation took into consideration all processes and rates presented in Figure 32, under the potential production section. Regarding the limited production section, the present studies accounted for the water-limited production, together with the effect of trees on microclimate (i.e., temperature, wind speed, and evapotranspiration). From the actual production, the Yield-SAFE model considered management factors (e.g., early / late planting, sowing, bud-burst, leaf-fall), together with several implementation designs in ACSs.

Withing the AGFORWARD project, improvements were added to the Yield-SAFE model in order to better account for the ecosystem services delivered by agroforestry systems (Palma *et al.*, 2016). While increasing the number of required parameters, the model was, hence, enhanced with new state variables and equations pertaining to (**i**) trees (leaf-fall, leaf biomass, fine root mortality and biomass, water assimilation by roots, tree effects on microclimate and livestock, cork production, fruit production and its energy content), (**ii**) crops (straw and roots as residues, water uptake, carbon inputs to soil), (**iii**) grass (maintenance respiration), (**iv**) livestock (utilisable metabolisable energy requirement, manure), and (**v**) soil (carbon dynamics, nitrogen leaching).

However, the Yield-SAFE version employed by the present dissertation did not account for the nutrient states, rates, and processes, nor for the majority of other reducing factors existent in the soil-plant-atmosphere nexus presented in Figure 32.

5.3. Scientific and Practical Recommendations and Outlook

Predictive accuracy could be added to the Yield-SAFE model by integrating a dynamic vegetation period determination depending on weather conditions rather than the static approach using tabulated values of the day of budburst and leaf-fall of the year. The adaptation could be based on a weighting model determined by the atmospheric drivers (i.e., air temperature, precipitation, and global radiation), in order to boost or hinder the vegetation period to a more realistic situation.

Monitoring and systematically updating an ACS repository with a focus on the second, third, and following rotations of the SRC would be paramount for validating the performance of multi-rotation growth models. In future works, the model of this study could also be extended to situations that demand more details such as the different processes and rates pertaining to the nutrient-limited production and actual production, as shown in Figure 32.

With the advent of artificial neural network models, imputing incomplete or inaccurate parts of the data could largely be automated in the future. However, vast repositories of tree and crop growth characteristics would be needed for this, in strong relation to the age of plants, the latitude, and longitude of the site, implementation design, and site-specific conditions.

For future investigations into the existing soil-plant-atmosphere interrelations, as well as for prospective impacts assessments of such nexus, there is a paramount demand for far-sighted, long-term research projects. Repositories of tree and crop growth characteristics covering a gradient of climatic and edaphic conditions should systematically be maintained, expanded, and, if possible, made available.

For practical purposes and based on experimental findings, the Yield-SAFE model could henceforth allow for the upscaling of the simulated outputs from plot- to farm- to landscape-scale by employing soil maps and local meteorological stations. Accordingly, the soil layer, currently integrated into the Yield-SAFE model as a one-dimensional, homogeneous soil layer, could be adapted to more realistic situations by means of multiple, two-dimensional cells. The soil maps could be integrated into the model in the shape of

meshed grids and triangulation, or kriging methods could be used for gridding climatic inputs from meteorological stations. Considerations of distances between trees and crops, as well as intra- and inter-specific plant resource allocation would also require a two-dimensional soil layer.

Upscaling the tree and crop yield production in ACSs from a plot-scale to landscape would be indispensable for an early site-specific planning considering most advantageous locations for an ACSs establishment. Additionally, landscape simulations would allow for investigating whether and under which conditions could ACSs furtherly expand, magnify, or hinder their effects on agricultural production, soil erosion, or carbon storage.

In turn, upscaling the simulated outputs of the Yield-SAFE model would allow for furtherly optimizing the implementation design of ACSs, identifying new management strategies that promote landscape multifunctionality, and predicting the landscape-level impacts of prospective climatic and edaphic changes. This would be especially relevant with the ongoing need for diversification of land-use and the generation of not only food, feed and fibre on arable land, but also fuel, with respect to the water-energy-food nexus.

List of Publications and Conference Papers

Seserman, D.M.; Quinkenstein, A.; Freese, D. Modelling of the tree yield in an alley cropping system. In: Proceedings International Crop Modelling Symposium (15-17th of March **2016**, Berlin, Germany), 382 – 383.

Seserman, D.M. & Freese, D. Modellierung der Baumbiomasse unter unterschiedlichen Standortbedingungen. In: Proceedings 5. Forum Agroforstsysteme (31st of November - 1st of December **2016**, Senftenberg, Germany).

Seserman, D.M.; Veste, M.; Freese, D. Optimisation of Biomass Productivity of Black Locust (*Robinia pseudoacacia* L.) on Marginal Lands – a Case Study in Lower Lusatia, NE Germany. In: Proceedings European Geosciences Union (EGU), General Assembly (23-28th of April **2017**, Vienna, Austria).

Seserman, D.M.; Pohle, I.; Freese, D.; Veste, M. Variabilität der holzigen Biomasseproduktion von Pappel und Robinie als Folge des Klimawandels in einem Alley-Cropping System in der Lausitz. In: Konferenzveröffentlichung Erfurter Tagung: "Schnellwachsende Baumarten - Etablierung, Management und Verwertung„ (16-17th Nov. **2017**, Erfurt, Germany), ISSN 2567-8922, 88–89.

Seserman, D.M.; Veste, M.; Freese, D. Modelling Tree Growth in Relation to Soil Water Dynamics in Alley-Cropping Systems in Brandenburg, Lower Saxony, and Thuringia, Germany. In: Proceedings BonaRes Conference (26-28th of Feb. **2018**, Berlin, Germany).

Seserman, D.M.; Pohle, I.; Freese, D.; Veste, M. Climate Change Impacts on the Growth of Hybrid Poplar Trees in an Agroforestry System in Brandenburg, NE Germany. In: Proceedings European Geosciences Union (EGU), General Assembly (8-13th of April **2018**, Vienna, Austria), Geophysical Research Abstracts, 20, EGU2018-13178.

Seserman, D.M.; Veste, M.; Freese, D.; Swieter, A.; Langhof, M. Benefits of Agroforestry Systems For Land Equivalent Ratio – Case Studies In Brandenburg And Lower Saxony, Germany. In: Proceedings The 4th European Agroforestry Conference: Agroforestry as sustainable land use, EURAF (28-31st of May **2018**, Nijmegen, The Netherlands), 26–29.

Seserman, D.M.; Pohle, I.; Veste, M.; Freese, D. Simulating Climate Change Impacts on Hybrid-Poplar and Black Locust Short Rotation Coppices. *Forests* **2018**, *9(7)*, 419.

Seserman, D.M.; Freese, D.; Swieter, A.; Langhof, M.; Veste, M. Trade-Off between Energy Wood and Grain Production in Temperate Alley-Cropping Systems: An Empirical and Simulation-Based Derivation of Land Equivalent Ratio. *Agriculture* **2019**, *9(7)*, 147.

Seserman, D.M.; Pohle, I.; Veste, M.; Freese, D. Growth vulnerability of hybrid-poplar and black locust to prospective climatic changes. In: Proceedings World Congress on Agroforestry (20-22th of May **2019**, Montpellier, France).

Seserman, D.M.; Freese, D. Handling Data Gaps in Reported Field Measurements of Short Rotation Forestry. *Data* **2019**, *4(4)*, 132.

References

Abbasi, T.; and Abbasi, S.A. Biomass energy and the environmental impacts associated with its production and utilization. *Renew. Sust. Energ. Rev.* **2010**, *14*, 919–937.

Anderegg, W.R.L.; Kane, J.M.; Anderegg, L.D.L. Consequences of widespread tree mortality triggered by drought and temperature stress. *Nat. Clim. Change* **2013**, *3*, 30–36.

Anderegg, W.R.L.; Hicke, J.A.; Fisher, R.A.; Allen, C.D.; Aukema, J.; Bentz, B.; Hood, S.; Lichstein, J.W.; Macalady, A.K.; McDowell, N.; Pan, Y.; Raffa, K.; Sala, A.; Shaw, J.D.; Stephenson, N.L.; Tague, C.; Zeppel, M. Tree mortality from drought, insects, and their interactions in a changing climate. *New Phytol.* **2015**, *208*, 674–683.

Aravanopoulos, F.A.; Kimb, K.H.; Zsuffa, L. Genetic diversity of superior *Salix*clones selected for intensive forestry plantations. *Biomass Bioenerg.* **1999**, *16*, 249–255.

Asseng, S.; Ewert, F.; Rosenzweig, C.; Jones, J.W.; Hatfield, J.L.; Duane, A.C.; Boote, K.J.; Thorburn, P.J.; Rötter, R.P.; Cammarano, D.; Brisson, N.; Basso, B.; Martre, P.; Aggarwal, P.K.; Angulo, C.; Bertuzzi, P.; Biernath, C.; Challinor, A.J.; Doltra, J.; Gayler, S.; Goldberg, R.; Grant, R.; Heng, L.; Hooker, J.; Hunt, L.; Ingwersen, J.; Izaurralde, R.K.; Kersebaum, K.C.; Müller, C.; Naresh Kumar, S.; Nendel, C.; O'Leary, G.; Olesen, J.E.; Osborne, T.M.; Palosuo, T.; Priesack, E.; Ripoche, D.; Semenov, M.A.; Shcherbak, I.; Steduto, P.; Stöckle, C.; Stratonovitch, P.; Streck, T.; Supit, I.; Tao, F.; Travasso, M.; Waha, K.; Wallach, D.; White, J.W.; Williams, J.R.; Wolf J. Uncertainty in simulating wheat yields under climate change. *Nat. Clim. Change* **2013**, *3*, 827–832.

Assmann, E. Untersuchungen über die Höhenkurven von Fichtenbeständen. *Allgemeine Forst- und Jagdzeitung*, **1943**, *119*, 77–88, 105–123, 133–151.

Aylott, M.J.; Casella, E.; Tubby, I.; Street, N.R.; Smith, P.; Taylor, G. Yield and spatial supply of bioenergy poplar and willow short-rotation coppice in the UK. *New Phytol.* **2008**, *178*, 358–370.

Bärwolf, M.; Jung, L.; Harzendorg, D.; *et al. Schlussbericht zum Verbundvorhaben AgroForstEnergie II; Teilvorhaben 1: Ertragseffekte und Ökonomie*, Abschlußbericht, Fachagentur für Nachwachsende Rohstoffe, Gülzow, **2016**, 263 p.

Bemmann, A.; Feger, K.H.; Gerold, D.; Große, W.; Hartmann, K.U.; Petzold, R.; Röhle, H.; Schweinle, J.; Steinke, C. Kurzumtriebsplantagen auf landwirtschaftlichen Flächen in der Region Großenhain im Freistaat Sachsen. *Forstarchiv* **2007**, *78*, 95–101.

Beuschel, R.; Piepho, H.P.; Joergensen R.G.; Wachendorf, C. Similar spatial patterns of soil quality indicators in three poplar-based silvo-arable alley cropping systems in Germany. *Biol. Fert. Soils* **2018**, *55 (1)*, 1–14.

Bielefeldt, J.; Bolte, A.; Busch, G.; Dohrenbusch, A.; Kroiher, F.; Lamersdorf, N.; Schulz, U.; Stoll, B. Energieholzproduktion in der Landwirtschaft. Chancen und Risiken aus Sicht der Natur-und Umweltschutzes. *NABU Bundesverb.* **2008**, *1*, 17–19.

Birkhofer, K.; Andersson, G.K.S.; Bengtsson, J.; Bommarco, R.; Dänhardt, J.; Ekbom, B.; Ekroos, J.; Hahn, T.; Hedlund, K.; Jönsson, A.M.; Lindborg, R.; Olsson, O.; Rader, R.; Rusch, A.; Stjernman, M.; Williams, A.; Smith, H.G. Relationships between multiple biodiversity components and ecosystem services along a landscape complexity gradient. *Biol. Conserv.* **2018**; *218*; 247–253.

Böhm, C.; Quinkenstein, A.; Freese, D. Yield prediction of young black locust (*Robinia pseudoacacia L.*) plantations for woody biomass production using allometric relations. *Ann. For. Res.* **2011**, *54*, 215–227.

Böhm, C. *Erarbeitung einer kontrollfähigen Definition für Agroforstschläge. Eine Initiative der Innovationsgruppe AUFWERTEN in Zusammenarbeit mit der Arbeitsgemeinschaft Agroforst Deutschland.* **2017** http://agroforst-info.de/rechtliche-und-politische-rahmenbedingungen (accessed on 3rd August 2018).

Bolte, A.; Madsen, P.; Derkyi, M.A.A.; Stanturf, J.A. Forest adaptation and restoration under global change - concept and status of an IUFRO Task Force. *Flora Mediterranea* **2017**, *27*, pp. 6.

Bruckhaus, A.; Buchner, W. Hecken in der Agrarlandschaft: Auswirkungen auf Feldfruchtertrag und ökologische Kenngrößen. *Berichte über Landwirtschaft* **1995**, *73*, 435–465.

Burgess, P.J.; Graves, A.; Metselaar, K.; Stappers, R.; Keesman, K.; Palma, J.; Mayus, M.; van der Werf, W. *Description of Plot-SAFE Version 0.3*. Unpublished Document, 15 September **2004**. Cranfield University, Silsoe, Bedfordshire, 52 pp.

Burgess, P.; Graves, A.; Palma, J.; Herzog, F.; Keesman, K.; van der Werf, W. EU SAFE Project Deliverable 6.4: Parametrization of the Yield-SAFE model and its use to determine yields at the landscape test sites, *Cranfield University - Institute of Water and Environment*, Silsoe, **2005**, 53 pp.

BWE. Bekanntmachung über die Förderung von Forschung und Entwicklung zur kosten- und energieeffizienten Nutzung von Biomasse im Strom- und Wärmemarkt „Energetische Biomassenutzung“. *BAnz AT* 21.07.**2015** *B1*, 1–7.

Calfapietra, C.; Gielen, B.; Karnosky, D.; Ceulemans, R.; Mugnozza, G.S. Response and potential of agroforestry crops under global change. *Environ. Pollut.* **2010**, *158*, 1095–1104.

Carl, C.; Biber, P.; Landgraf, D.; Buras, A.; Pretzsch, H. Allometric Models to Predict Aboveground Woody Biomass of Black Locust (Robinia pseudoacacia L.) in Short Rotation Coppice in Previous Mining and Agricultural Areas in Germany. *Forests* **2017**, *8(9)*, 328.

Ceulemans, R.; McDonald, A.J.S.; Pereira, J.S.A. A comparison among eucalypt, poplar and willow characteristics with particular reference to a coppice, growth-modelling approach. *Biomass Bioenerg.* **1996**, *11*, 215–231.

Ceulemans, R.; and Deraedt, W. Production physiology and growth potential of poplars under short-rotation forestry culture. *Forest Ecol. Manag.* **1999**, *121*, 9–23.

Chmielewski, F.M.; Müller, A.; Küchler, W. Possible impacts of climate change on natural vegetation in Saxony (Germany). *Int. J. Biometeorol.* **2005**, *50*, 96–104.

Christensen, J.; Hewitson, B.; Busuioc, A.; Chen, A.; Gao, X.; Held, I.; Jones, R.; Kolli, R.; Kwon, W.T.; Laprise, R.; Magaña Rueda, V.; Mearns, L.; Menéndez, C.; Räisänen, J.; Rinke, A.; Sarr, A.; Whetton, P. Regional climate projections. In *Climate Change* **2007**: The Physical Science Basis. Contribution of Working Group I to the Fourth Assessment Report of the Intergovernmental Panel on Climate Change. Solomon, S.; Qin, D.; Manning, M.; Chen, Z.; Marquis, M.; Averyt, K.; Tignor, M.; Miller, H. (eds.). *Cambridge University Press* **2007**, Cambridge, UK and New York, NY.

Christersson, L.; Verma, K. Short-rotation forestry – a complement to "conventional" forestry. *Unasylva*, **2006**, *223 (57)*.

Crous-Duran, J.; Graves, A.R.; Paulo, J.A.; Mirck, J.; Oliveira, T.S.; Kay, S.; García de Jalón, S.; Palma, J.H.N. Modelling tree density effects on provisioning ecosystem services in Europe. *Agroforest. Syst.* **2018**, 1–23.

De Stefano, A.; Jacobson, M.G. Soil carbon sequestration in agroforestry systems: a meta-analysis. *Agroforest. Syst.* **2018**, *92(2)*, 285–299.

De Vries, W.; Posch, M.; Simpson, D.; Reinds, G.J. Modelling long-term impacts of changes in climate, nitrogen deposition and ozone exposure on carbon sequestration of European forest ecosystems. *Sci. Total Environ.* **2017**, *605–606*,1097–1116.

Diamantopolou, M.J. Filling gaps in diameter measurements on standing tree boles in the urban forest of Thessaloniki, Greece. *Environmental Modelling & Software*, **2016**, *25*, 1857–1865.

Döhler, H. *Faustzahlen für die Landwirtschaft, 13th ed. Kuratorium für Technik und Bauwesen in der Landwirtschaft e.V.* KTBL: Darmstadt, Germany, **2005**.

Dupraz, C.; Blitz-Frayret, C.; Lecomte, I.; Molto, Q.; Reyes, F.; Gosme, M. Influence of latitude on the light availability for intercrops in an agroforestry alley-cropping system. *Agroforest. Syst.* **2018**, *92(4)*, 1019–1033.

European Commission. Communication from The Commission to The European Parliament, The Council, The European Economic And Social Committee And The Committee Of The Regions Energy Roadmap 2050 /* COM/2011/0885 final */.

Evans, A.; Strezov, V.; and Evans, T.J. Sustainability considerations for electricity generation from biomass. *Renew. Sust. Energ. Rev.* **2010**, *14*, 1419–1427.

Fagerholm, N.; Torralba, M.; Burgess, P.J.; Plieninger, T. A systematic map of ecosystem services assessments around European agroforestry. *Ecol. Indic.* **2016**, *62*, 47–65.

Gädeke, A.; Hölzel, H.; Koch, H.; Pohle, I.; Grünewald, U. Analysis of uncertainties in the hydrological response of a model-based climate change impact assessment in a subcatchment of the Spree River, Germany. *Hydrol. Process.* **2014**, *28(12)*, 3978–3998.

Gädeke, A.; Pohle, I.; Koch, H.; Grünewald, U. Trend analysis for integrated regional climate change impact assessments in the Lusatian river catchments (North-Eastern Germany). *Reg. Environ. Chang.* **2017**, *17(6)*, 1751–1762.

Gallardo, D.A. Standortbasierte Ertragsmodellierung von Pappel- und Weidenklonen in Kurzumtriebsplantagen. Dissertation. Fakultät Umweltwissenschaften, Fachrichtung Forstwissenschaften. *Technische Universität Dresden, Qucosa, Saechsische Landesbibliothek-Staats-und Universitaetsbibliothek* Dresden, Germany. Permanent URN: http://nbn-resolving.de/urn:nbn:de:bsz:14-qucosa-144670, **2014**, p 201.

Gerstengarbe, F.W.; Badeck, F.; Hattermann, F.; Krysanova, V.; Lahmer, W.; Lasch, P.; Stock, M.; Suckow, F.; Wechsung, F.; Werner, P.C. Studie zur klimatischen Entwicklung im Land Brandenburg bis 2055 und deren Auswirkungen auf den Wasserhaushalt, die Forst- und Landwirtschaft sowie die Ableitung erster Perspektiven. *Potsdam Institute for Climate Impact Research* **2003**.

Gessler, A.; Keitel, C.; Kreuzwieser, J.; Matyssek, R.; Seiler, W.; Rennenberg, H. Potential risks for European beech (*Fagus sylvatica* L.) in a changing climate. *Trees* **2007**, *21*, 1–11.

Graves, A.R.; Burgess, P.J.; Liagre, F.; Pisanelli, A.; Paris, P.; Moreno, G.; Bellido, M.; Mayus, M.; Postma, M.; Schindler, B.; Mantzanas, K.; Papanastasis, V.P.; Dupraz, C. Farmer Perceptions of Silvoarable Systems in Seven European Countries. In: Rigueiro-Rodróguez, A., McAdam, J., Mosquera-Losada, M.R. (eds.) Agroforestry in Europe. *Adv. Agrofor.* **2009**, *6*.

Graves, A.R.; Burgess, P.J.; Palma, J.; Keesman, K.J.; van der Werf, W.; Dupraz, C.; van Keulen, H.; Herzog, F.; Mayus, M. Implementation and calibration of the parameter-sparse Yield-SAFE model to predict production and land equivalent ratio in mixed tree and crop systems under two contrasting production situations in Europe. *Ecol. Model.* **2010**, *221*, 1744–1756.

Hauck, S.; Knocke, T.; and Wittkopf, S. Economic evaluation of short rotation coppice systems for energy from biomass – a review. *Renew. Sust. Energ. Rev.* **2014**, *29*, 435–448.

Horemans, J.A.; van Gaelen, H.; Raes, D.; Zenone, T.; Ceulemans, R. Can the agricultural AquaCrop model simulate water use and yield of a poplar short-rotation coppice? *GCB Bioenergy* **2017**, *9*, 1151–1164.

Honaker, J.; King, G.; Blackwell, M. Amelia II: A Program for Missing Data. *Journal of Statistical Software*, **2011**, *45 (7)*, p.47.

Huang, S.; Krysanova, V.; Österle, H.; Hattermann, F.F. Simulation of spatiotemporal dynamics of water fluxes in Germany under climate change. *Hydrol. Process* **2010**, *24*, 3289–3306.

Hytönen, J.; Lumme, I.; Törmälä, T. Comparison of Methods for Estimating Willow Biomass. *Biomass* **1987**, *14*, 39–49.

Jacob, D.; Petersen, J.; Eggert, B.; Alias, A.; Bøssing Christensen, O.; Bouwer, L.M.; Braun, A.; Colette, A.; Déqué, M.; Georgievski, G.; Georgopoulou, E.; Gobiet, A.; Menut, L.; Nikulin, G.; Haensler, A.; Hempelmann, N.; Jones, C.; Keuler, K.; Kovats, S.; Kröner, N.; Kotlarski, S.; Kriegsmann, A.; Martin, E.; van Meijgaard, E.; Moseley, C.; Pfeifer, S.; Preuschmann, S.; Radermacher, C.; Radtke, K.; Rechid, D.; Rounsevell, M.; Samuelsson, P.; Somot, S.; Soussana, J.F.; Teichmann, C.; Valentini, R.; Vautard, R.; Weber, B.; Pascal, Y. EURO-CORDEX: New high-resolution climate change projections for European impact research. *Reg. Environ. Change* **2014**, *14*, 563–578.

Kaltschmitt, M.; Hartmann, H.; Hofbauer, H. Energie aus Biomasse: Grundlagen, Techniken und Verfahren. *Springer Vieweg*: Berlin, Germany, **2016**.

Kanzler, M. & Böhm, C. *Nachhaltige Erzeugung von Energieholz in Agroforstsystemen (AgroForstEnergie II): Teilvorhaben 2: Bodenschutz, Bodenfruchtbarkeit, Wasserhaushalt und Mikroklima.* Schlußbericht, Brandenburgische Technische Universität Cottbus-Senftenberg: Fachgebiet für Bodenschutz und Rekultivierung, Cottbus, Germany, **2016**, 161 p.

Kanzler, M.; Böhm, C.; Mirck, J.; Schmitt, D.; Veste, M. Microclimate effects on evaporation and winter wheat (*Triticum aestivum* L.) yield within a temperate agroforestry system. *Agroforest. Syst.* **2018**, 1–21.

Keesman, K.J.; Graves, A.; van der Werf, W.; Burgess, P.; Palma, J.; Dupraz, C.; van Keulen, H. A system identification approach for developing and parameterising an agroforestry system model under constrained availability of data. *Environ. Modell. Softw.* **2011**, *26*, 1540–1553.

Körner, C. and Basler, D. Phenology under global warming. *Science* **2010**, *327*, 1461–1462.

Korsun, H. Zivot normalniho porostu ve vzoroich (Das Leben des normalen Waldes in Formeln). *Lesnicka prace*, **1935**, *14*, 289–300.

Kriebitzsch, W.U. and Veste, M. Bedeutung trockener Sommer für die Photosynthese und Transpiration von verschiedenen Herkünften der Rotbuche (*Fagus sylvatica* L.). *Landbauforschung* **2012**, *62(4)*, 193–209.

Küppers, M.; Schmitt, D.; Liner, S.; Böhm, C.; Kanzler, M.; Veste, M. Photosynthetic characteristics and simulation of annual leaf carbon gains of hybrid poplar (*Populus nigra* L. x *P. maximowiczii* Henry) and black locust (*Robinia pseudoacacia* L.) in a temperate agroforestry system. *Agroforest. Syst.* **2017**, 1–20.

Lamerre, J.; Schwarz, K.U.; Langhof, M.; von Wühlisch, G.; Greef, J.M. Productivity of poplar short rotation coppice in an alley-cropping agroforestry system. *Agroforest. Syst.* **2015**, *89(5)*, 933–942.

Lamerre, J.; Langhof, M.; Sevke-Masur, K.; Schwarz, K.U.; von Wühlisch, G.; Swieter, A.; Greef, J.M.; Dauber, J.; Hirschberg, F.; Joormann, I.; Krestel, N.; Masur, D.; Reith, C. *Nachhaltige Erzeugung von Energieholz in Agroforstsystemen: Teilprojekt 3: Standort Niedersachsen, Strukturvielfalt und Biodiversität.* Schlußbericht, Julius Kühn-Institut Bundesforschungsinstitut für Kulturpflanzen (JKI) - Institut für Pflanzenbau und Bodenkunde, Braunschweig, Germany, **2016**.

Landis, D.A. Designing agricultural landscapes for biodiversity-based ecosystem services. *Basic Appl. Ecol.* **2017**, *18*, 1–12.

Langton, S. Avoiding edge effects in agroforestry experiments; the use of neighborbalanced designs and guard areas. *Agroforest. Syst.* **1990**, *12*, 173–185.

Lasch, P.; Lindner, M.; Erhard, M.; Suckow, F.; Wenzel, A. Regional impact assessment on forest structure and functions under climate change–the Brandenburg case study. *Forest Ecol. Manag.* **2002**, *162*, 73–86.

Lasch, P.; Kollas, C.; Rock, J.; Suckow, F. Potentials and impacts of short-rotation coppice plantation with aspen in Eastern Germany under conditions of climate change. *Reg. Environ. Change* **2010**, *10(2)*, 83–94.

Lasch-Born, P.; Suckow, F.; Gutsch, M.; Reyer, C.; Hauf, I.; Murawski, A.; Pilz, T. Forests under climate change: Potential risks and opportunities. *Meteorol. Zeitschrift* **2015**, *24*, 157–172.

Leuzinger, S.; Zotz, G.; Asshoff, R.; Körner, C. Responses of deciduous forest trees to severe drought in Central Europe. *Tree Physiol.* **2015**, *25*, 641–650.

Linder, A. Statistische Methoden f˙ur Naturwissenschaftler, Mediziner und Ingenieure, 2nd edn. Verlag Birkhäuser, Basel, **1951**, 238 pp.

Lindner, M.; Maroschek, M.; Netherer, S.; Kremer, A.; Barbati, A.; Garcia-Gonzalo, J.; Seidl, R.; Delzon, S.; Corona, P.; Kolström, M.; Lexer, M.J.; Marchetti, M. Climate change impacts, adaptive capacity, and vulnerability of European forest ecosystems. *Forest Ecol. Manag.* **2010**, *259*, 698–709.

Lindner, M.; Fitzgerald, J.B.; Zimmermann, N.E.; Reyer, C.; Delzon, S.; van der Maaten, E.; Schehaas, M.J.; Lasch, P.; Eggers, J.; van der Maaten-Theunissen, M.; Suckow, F.; Psomas, A., Poulter, B.; Hanewinkel, M. Climate change and European forests: What do we know, what are the uncertainties, and what are the implications for forest management? *J. Environ. Manage.* **2014**, *146*, 69–83.

Malyshev, A.V.; Henry, H.A.; Bolte, A.; Arfin Khan, M.A.; Kreyling, J. Temporal photoperiodic sensitivity and forcing requirements for budburst in temperate tree seedlings. *Agr. Forest. Meteorol.* **2018**, *248*, 82–90.

Mantovani, D.; Veste, M.; Freese, D. Black locust (*Robinia pseudoacacia* L.) ecophysiological and morphological adaptations to drought and their consequence on biomass production and water use efficiency. *New Zeal. J. For. Sci.* **2014**, *44*, 29.

Mantovani, D.; Veste, M.; Böhm, C.; Vignudelli, M.; Freese, D. Drought impact on the spatial and temporal variation of growth performance and plant water status of black locust (Robinia pseudoacacia L.) in agroforestry systems in Lower Lusatia (Germany). *iForest* **2015a**, *8*, 743–747.

Mantovani, D.; Veste, M.; Boldt-Burisch, K.; Fritsch, S.; Koning, L.; Freese, D. Carbon allocation, nodulation, and biological nitrogen fixation of black locust (*Robinia pseudoacacia* L.) under soil water limitation. *Ann. For. Res.* **2015b**, *58 (2)*, 259–274.

Mead, R.; Willey, R.W. The concept of a "Land Equivalent Ratio" and advantages in yields from intercropping. *Exp. Agr.* **1980**, *16(3)*, 217–228.

Medlyn, B.E.; Duursma, R.A.; Zeppel, M.J.B. Forest productivity under climate change: a checklist for evaluating model studies. *Wiley Interdiscip. Rev. Clim. Change* **2011**, *2*, 332–355.

Menzel, A.; Sparks, T.H.; Estrella, N.; Koch, E.; Aasa, A.; Ahas, R.; Alm-Kübler, K.; Bissolli, P.; Braslavska, O.; Briede, A.; Chmielewski, F.M.; Crepinsek, Z.; Curnel, Y.; Dahl, A.; Defila, C.; Donnelly, A.; Filella, Y.; Jatczak, K.; Mage, F.; Mestre, A.; Nordli, O.; Penuelas, J.; Pirinen, P.; Remisova, V.; Scheifinger, H.; Striz, M.; Susnik, A.; van Vliet, A.J.H.; Wielgolaski, F.E.; Zach, A.; Zust, A. European phenological response to climate change matches the warming pattern. *Glob. Change Biol.* **2006**, *12(10)*, 1969–1976.

Meyer, S.; Wesche, K.; Krause, B.; Leuschner, C. Dramatic impoverishment of arable plant communities since the 1950s/60s – a large scale analysis across geological substrate groups. *Divers. Distrib.* **2013**, *19*, 1175-1187.

Michailoff, I. Zahlenmäßiges Verfahren für die Ausf¨uhrung der Bestandeshöhenkurven. *Forstw. Cbl.* , **1943**, *6*, 273–279.

Mitchell, C.P.; Stevens, E.A.; Watters, M.P. Short rotation forestry – operations, productivity and costs based on experience gained in the UK. *Forest Ecol. Manag.* **1999**, *121*, 123–136.

Monclus, R.; Dreyer, E.; Delmotte, F.M.; Villar, M.; Delay, D.; Boudouresque, E.; Petit, J.M.; Marron, N.; Bréchet, C.; Brignolas, F. Productivity, leaf traits and carbon isotope discrimination in 29 *Populus deltoids × P. nigraclones*. *New Phytol.* **2005**, *167*, 53–62.

Morhart, C.D.; Douglas, G.C.; Dupraz, C.; Graves, A.R.; Nahm, M.; Paris, P.; Sauter, U.H.; Sheppard, J.; Spiecker, H. Alley coppice – a new system with ancient roots. *Ann. Forest Sci.* **2014**, *71(5)*, 527–542.

Mudra, A. StatistischeMethoden f¨ur landwirtschaftliche Versuche. Verlag Paul Parey, Berlin, Hamburg, **1958**, 336 pp.

Ojeda, J.J.; Volenec, J.J.; Brouder, S.M.; Caviglia, O.P.; Agnusdei, M.G. Evaluation of Agricultural Production Systems Simulator (APSIM) as yield predictor of *Panicum virgatum* and *Miscanthus x giganteus* in several US environments. *GCB Bioenergy* **2017**, *9*, 796–816.

Orlowsky, B.; Gerstengarbe, F.W.; Werner, P.C. A resampling scheme for regional climate simulations and its performance compared to a dynamical RCM. *Theor. Appl. Climatol.* **2008**, *92(3–4)*, 209–223.

Page, J.K. The estimation of monthly mean values of daily total short-wave radiation of vertical and inclined surface from sunshine records for latitudes 40°N-40°S. *Proc. UN Conf. New sources of energy* **1964**, 4–378.

Palma, J.H.N.; Graves, A.R.; Bunce, R.G.H.; Burgess, P.J.; de Filippi, R.; Keesman, K.J.; van Keulen, H.; Liagre, F.; Mayus, M.; Reisner, Y.; Herzog, F. Modeling environmental benefits of silvoarable agroforestry in Europe. *Agr. Ecosyst. & Environ.* **2007**, *119*, 320–334.

Palma, J.H.N.; Paulo, J.A.; Tome, M. Carbon sequestration of modern *Quercus suber* L. silvoarable agroforestry systems in Portugal: a YieldSAFE-based estimation. *Agroforest. Syst.* **2014**, *88*, 791–801.

Palma, J.H.N.; Graves, A.R.; Crous-Duran J.; Upson, M.; Paulo, J.A.; Oliveira, T.S.; Silvestre Garcia de Jalón, S.; Burgess, P.J. *Yield-SAFE Model Improvements*. Milestone Report 29 (6.4) for EU FP7 Research Project: AGFORWARD 613520, **2016**, 30 pp.

Palma, J.H.N.; Oliveira, T.; Crous-Duran, J.; Graves, A.R.; Garcia de Jalon, S.; Upson, M.; Giannitsopoulos, M.; Burgess, P.J.; Paulo, J.A.; Tomé, M.; Ferreiro-Dominguéz, N.; Mosquera-Losada, M.R.; Gonzalez-Hernández, P.; Kay, S.; Mirk, J.; Kanzler, M.; Smith, J.; Moreno, G.; Pantera, A.; Mantovani, D.; Rosati, A.; Luske, B.; Hermansen, J. *Modelled agroforestry outputs at field and farm scale to support biophysical and environmental assessments.* Deliverable 6.17 (6.2) for EU FP7 Research Project: AGFORWARD project 613520, **2017**, 162 pp.

Paul, C.; Weber, M.; Knoke, T. Agroforestry versus farm mosaic systems - comparing land-use efficiency, economic returns and risks under climate change effects. *Sci. Total Environ.* **2017**, *587-588*, 22–35.

Petterson, H. Die Massenproduktion des Nadelwaldes. Mitt. Schwed. Forstl. Forschungsanstalten, Stockholm, **1955**, vol. 45 (IB), 391 pp.

Pohle, I.; Koch, H.; Conradt, T.; Gädeke, A.; Grünewald, U. Potential impacts of climate change and regional anthropogenic activities in Central European mesoscale catchments. *Hydrolog. Sci. J.* **2015**, *60(5)*, 912–928.

Pretzsch, H. Forest Dynamics, Growth and Yield. From Measurement to Model. Springer, Freising, Germany **2009**, 671 p.

Pretzsch, H.; Forrester, D.I.; Rötzer, T. Representation of species mixing in forest growth models. A review and perspective. *Ecological Modelling*, **2015**, *313*, 276–292.

Prodan, M. Messung der Waldbestände. JD Sauerländer's Verlag, Frankfurt am Main, **1951**, 260 pp.

Rasch, D. Einf¨uhrung in die Biostatistik, 2nd edn. Verlag Harri Deutsch, Frankfurt am Main, **1987**, 276 pp.

Rauthe, M.; Steiner, H.; Riediger, U.; Mazurkiewicz, A.; Gratzki, A. A Central European precipitation climatology - Part I: Generation and validation of a high-resolution gridded daily data set (HYRAS). *Meteorol. Zeitschrift* **2013**, *22*, 235–256.

Reyer, C.; Lasch-Born, P.; Suckow, F.; Gutsch, M.; Murawski, A.; Pilz, T. Projections of regional changes in forest net primary productivity for different tree species in Europe driven by climate change and carbon dioxide. *Ann. Forest Sci.* **2014**, *71(2)*, 211–225.

Rois-Díaz, M.; Lovric, N.; Ferreiro-Domínguez, M.N.; Mosquera-Losada, M.R.; den Herder, M.; Graves, A.; Palma, J.H.N.; Paulo, J.A.; Pisanelli, A.; Smith, J.; Moreno, G.; García, S.; Varga, A.; Pantera, A.; Mirck, J.; Burgess P. Farmers' reasoning behind the uptake of agroforestry practices: evidence from multiple case-studies across Europe. *Agroforest. Syst.* **2018**, *92(4)*, 811–828.

Ruane, A.C.; Hudson, N.I.; Asseng, S. et al. Multi-wheat-model ensemble responses to interannual climate variability. *Environ. Modell. & Softw.* **2016**, *81*, 86–101.

Scharnweber, T.; Manthey, M.; Criegee, C.; Bauwe, A.; Schröder, C.; Wilmking, M. Drought matters - Declining precipitation influences growth of *Fagus sylvatica* L. and *Quercus robur* L. in north-eastern Germany. *Forest Ecol. and Manag.* **2011**, *262(6)*, 947–961.

Schoeneberger, M.; Bentrup, G.; de Gooijer, H.; Soolanayakanahally, R.; Sauer, T.; Brandle, J.; Zhou, X.; Current, D. Branching out: Agroforestry as a climate change mitigation and adaptation tool for agriculture. *J. Soil Water Conserv.* **2012**, *67*, 128A–136A.

Seserman, D.M.; Pohle, I.; Veste, M.; Freese, D. Simulating Climate Change Impacts on Hybrid-Poplar and Black Locust Short Rotation Coppices. *Forests* **2018**, *9(7)*, 419.

Sims, R.E.H.; Maiava, T.G.; Bullock, B.T. Short rotation coppice tree species selection for woody biomass production in New Zealand. *Biomass Bioenerg.* **2001**, *20*, 329–335.

Sochacki, S.J.; Harper, R.J.; Smettem, K.R.J. Estimation of woody biomass production from a short-rotation bio-energy system in semi-arid Australia. *Biomass Bioenerg.* **2007**, *31*, 608–616.

Spitters, C.J.T. & Schapendonk, A.H.C.M. Evaluation of breeding strategies for drought tolerance in potato by means of crop growth simulation. *Plant and Soil*, **1990**, *123*, 193–203.

Stevenson, M. with contributions from Nunes, T.; Heuer, C.; Marshall, J.; Sanchez, J.; Thornton, R.; Reiczigel, J.; Robison-Cox, J.; Sebastiani, P.; Solymos, P.; Yoshida, K.; Jones, G.; Pirikahu, S.; Firestone, S.; Kyle, R.; Popp, J.; Jay M. *epiR: Tools for the Analysis of Epidemiological Data.* R package version 1.0-2. https://CRAN.R-project.org/package=epiR (accessed on 20th June 2019).

Strelher, A. Technologies of wood combustion. *Ecol. Eng.* **2000**, *16,* 25–40.

Stappers, R.; Keesman, K.J.; van der Werf, W. The SAFE-RESULT Equations: an Agro-Forestry Model. Technical Report, *Wageningen University*, The Netherlands **2003**, 20 pp.

Swieter, A.; Langhof, M.; Lamerre, J.; Greef, J.M. Long-term yields of oilseed rape and winter wheat in a short rotation alley cropping agroforestry system. *Agroforest. Syst.* **2018**, 1–12.

Takanashi, M. Statistical Inference in Missing Data by MCMC and Non-MCMC Multiple Imputation Algorithms: Assessing the Effects of Between-Imputation Iterations. *Data Science Journal*, **2017**, *16(37)*, 1–17.

Terreaux, J.P.; Chavet, M. An intertemporal approach of Land Equivalent Ratio for agroforestry plots. *Lameta*: DT 15, **2004**.

Tsiafouli, M. A.; Thébault, E.; Sgardelis, S.P.; Ruiter, P.C.; van der Putten, W.H.; Birkhofer, K.; Hemerik, L.; de Vries, F.T.; Bardgett, R.D.; Brady, M.V.; Bjornlund, L.; Bracht Jørgensen, H.; Christensen, S.; D'Hertefeldt, T.; Hotes, S.; Gera Hol, W.H.; Frouz, J.; Liiri, M.; Mortimer, S.R.; Setälä, H.; Tzanopoulous, J.; Uteseny, K.; Pižl, V.; Stary, J.; Wolters, V.; Hedlund, K. Intensive agriculture reduces soil biodiversity across Europe. *Glob. Change Biol.* **2015**, *21(2)*, 973–985.

Tsonkova, P.; Böhm, C.; Quinkenstein, A.; Freese, D. Ecological benefits provided by alley cropping systems for production of woody biomass in the temperate region: A review. *Agroforest. Syst.* **2012**, *85(1)*, 133–152.

Tsonkova, P.; Mirck, J.; Böhm, C.; Fütz, B. Addressing farmer-perceptions and legal constraints to promote agroforestry in Germany. *Agroforest. Syst.* **2018**, *92(4)*, 1091–1103.

Van der Werf, W.; Keesman, K.; Burgess, P.J.; Graves, A.R.; Pilbeam, D.; Incoll, L.D.; Metselaar, K.; Mayus, M.; Stappers, R.; van Keulen, H.; Palma, J.; Dupraz, C. Yield-SAFE: A parameter-sparse, process-based dynamic model for predicting resource capture, growth, and production in agroforestry systems. *Ecol. Eng.* **2007**, *29(4)*, 419–433.

Van Ittersum, M.K.; Cassman, K.G.; Grassini, P.; Wolf, J.; Tittonell, P.; Hochman, Z. Yield gap analysis with local to global relevance—A review. *Field Crops Research*, **2013**, *143*, 4–17.

Van Vooren, L.; Reubens, B.; Broekx, S.; Pardon, P.; Reheul, D.; van Winsen, F.; Verheyen, K.; Wauters, E.; Lauwers, L. Greening and producing: an economic assessment framework for integrating trees in cropping systems. *Agric. Syst.* **2016**, *148,* 44–57.

Verchot, L.V.; Van Noordwijk, M.; Kandji, S.; Tomich, T.; Ong, C.; Albrecht, A.; Mackensen, J.; Bantilan, C., Anupama, K.V.; Palm, C. Climate change: Linking adaptation and mitigation through agroforestry. *Mitig. Adapt. Strat. Gl.* **2007**, *12(5)*, 901–918.

Verwijst, T. and Telenius, B. Biomass estimation procedures in short rotation forestry. *Forest Ecol. Manag.* **1999**, *121*, 137–146.

Veste, M. and Kriebitzsch, W.U. Einfluss von Trockenstress auf Photosynthese, Transpiration und Wachstum junger Robinien (*Robinia pseudoacacia* L.). *Forstarchiv* **2013**, *84*, 35–42.

Veste, M. and Halke, C. Ökophysiologische Plastizität der Photosynthese von Robinien (*Robinia pseudoacacia* L.) und Hybrid-Pappeln (*Populus nigra* L. × *P. maximowiczii* Henry) bei Hitzestress und Sommertrockenheit in der Niederlausitz. *In: Proceedings 5. Agroforstforum*, Senftenberg, **2017**, 1–12.

Veste, M.; Schillem, S.; Böhm, C. Baumarten für die Agrarholzproduktion. In: Veste M, Böhm C (eds.) Agrarholz - Schnellwachsende Bäume in der Landwirtschaft. *Springer, Heidelberg*, **2018**.

Veste, M.; Böhm, C. *Agrarholz - Schnellwachsende Bäume in der Landwirtschaft*. Springer: Heidelberg, Germany, **2018**.

Veste, M.; Malaga Linares, R.A.; Seserman, D.M.; Schmitt, D.; Wachendorf, M.; Küppers, M. Annual leaf carbon fluxes, light interception, and stand structure of poplars and black locusts in an alley-cropping system, Lower Lusatia, Germany. In: Proceedings 4th European Agroforestry Conference: Agroforestry as sustainable land use, Nijmegen, The Netherlands, **2018**, 488–492.

Vitasse, Y. and Basler, D. What role for photoperiod in the bud burst phenology of European beech. *Eur. J. Forest Res.* **2013**, *132(1)*, 1–8.

Walle, I.V.; Camp, N.V.; Van de Casteele, L.; Verheyen, K.; Lemeur, R. Short-rotation forestry of birch, maple, poplar and willow in Flanders (Belgium) II. Energy production and CO_2 emission reduction potential. *Biomass Bioenerg.* **2007**, *31*, 276–283.

Wang, G.; Garcia, D.; Liu, Y.; de Jeu, R.; Dolman, A.J. A three-dimensional gap filling method for large geophysical datasets: Application to global satellite soil moisture observations. *Environmental Modelling & Software*, **2012**, *30*, 139–142.

Wang, W.J.; He, H.S.; Thompson, F.R.; Fraser, J.S.; Dijak, W.D. Changes in forest biomass and tree species distribution under climate change in the northeastern United States. *Landscape Ecol.* **2017**, *32(7)*, 1399–1413.

Weemstra, M.; Eilmann, B.; Sass-Klaassen, U.G.W.; Sterck, F.J. Summer droughts limit tree growth across 10 temperate species on a productive forest site. *Forest Ecol. Manag.* **2013**, *306*,142–149.

Werner, P.C. and Gerstengarbe, F.W. Proposal for the development of climate scenarios. *Clim. Res.* **1997**, *8*, 171–182.

Wesche, K.; Krause, B.; Culmsee, H.; Leuschner, C. Fifty years of change in Central European grassland vegetation: large losses in species richness and animal-pollinated plants. *Biol. Conser.* **2012**, *150*, 76-85.

Wösten, J.H.M.; Lilly, A.; Nemes, A.; Le Bas, C. Development and use of a database of hydraulic properties of European soils. *Geoderma* **1999**, *90*, 169–185.

Zscheischler, J.; Gaasch, N.; Butler Manning, D.; Weith, T. *Land use competition related to woody biomass production on arable land in Germany.* In: Niewohner, J., Bruns, A., Hostert, P., Krueger, T., Nielsen, J.Ø., Haberl, H.; Lauk, C.; Lutz, J.; Müller, D. (eds.) Land use competition. Human-environment interactions. Springer: Heidelberg, Germany, **2016**, 193–213.

Zewdie, M.; Olsson, M.; Verwijst, T. Above-ground biomass production and allometric relations of *Eucalyptus globulus* Labill coppice plantations along a chronosequence in the central highlands of Ethiopia. *Biomass Bioenerg.* **2009**, *33*, 421–428.

Zianis, D. & Mencuccini, M. On simplifying allometric analyses of forest biomass. *Forest Ecol. Manag.* **2003**, *187*, 311–332.

Young, T. *Agroforestry for Soil Conservation*. Wallingford, Oxford: CAB International, **1989**, 276 pp.

Appendix A

Table A.1. Tree and soil parameter values used for the parametrization of the Yield-SAFE model for the SRF in Dornburg (Thuringia, Germany).

Symbol	Description	Unit	Value	Source
$n_{Shoots0}$	Initial number of shoots per tree	$tree^{-1}$	1	Own data
B_{t0}	Initial tree biomass	g $tree^{-1}$	40	[1]
LA_{t0}	Initial tree leaf area	m^2 $tree^{-1}$	0	[2, 3]
ε_t	Radiation use efficiency	g MJ^{-1}	1.04	Own data
k_t	Light extinction coefficient	–	0.5	Own data
t_t	The number of days after bud-burst at which the leaf area has reached 63.2% of its maximum leaf area LA_{ss}^{max}	d	10	[2, 3]
LA_{ss}^{max}	Maximum leaf area for a single shoot	m^2	0.05	[2, 3]
n_{Shoots}^{max}	Maximum number of shoots per tree	$tree^{-1}$	10000	[2, 3]
K_{main}	Relative attrition rate of tree biomass	d^{-1}	10^{-4}	[2, 3]
γ_t	Transpiration coefficient of the trees	m^3 g^{-1}	0.0002	[1]
$(pF_{crit})_t$	Critical pF value for trees	log (cm)	4.0	[2]
$(pF_{pwp})_t$	pF value at permanent wilting point	log (cm)	4.2	[2]
$DOY_{budburst}$, $DOY_{leaf\text{-}fall}$	Day of year for bud-burst and leaf-fall	DOY	105, 300	[1]
ρ_t	Planting density	trees ha^{-1}	2200	[4]
θ_0	Initial volumetric water content	m^3 m^{-3}	0.35	[5]
δ_{eva}	Potential evaporation per unit energy	mm MJ^{-1}	0.15	[2]
D	Depth of the soil compartment	mm	1000	[5]
α	Van Genuchten parameter	–	0.0083	[5]
n_{soil}	Van Genuchten parameter	–	1.2539	[5]
δ	Parameter affecting the drainage rate below root zone	–	0.07	[5]
PWP	Permanent wilting point	log (cm)	4.2	[2, 3]
$(pF_{crit})_E$	Critical pF value for evaporation	log (cm)	2.3	[2, 3]
pF_{FC}	Water tension at field capacity	log (cm)	2.3	[2, 3]
K_s	Soil hydraulic conductivity at saturation	mm d^{-1}	2.272	[5]
θ_s	Saturated volumetric water content	m^3 m^{-3}	0.43	[5]
θ_r	Residual volumetric water content	m^3 m^{-3}	0.01	[5]

[1] Crous-Duran *et al.* (2018); [2] Graves *et al.* (2010); [3] Keesman *et al.* (2011); [4] Bärwolf *et al.* (2016); [5] Wösten *et al.* (1990)

Table A.2. Goodness of validation of all applied regression models in terms of the coefficient of determination (R^2), sum of squared errors (SSE), root-mean-square error (RMSE), mean absolute error (MAE), as well as the concordance correlation coefficient (CCC) and the simulation bias (SB) from the observations.

Model	Variable	Data Gap Representation	R^2	SSE	RMSE	MAE	SB [%]	CCC	Label
Exponential	RHD	72	0.90	10.3	1.2	1.1	1.0	0.93	Acceptable
		43	-3.31 *	534.3	8.7	7.9	na	na	na
	BHD	72	-3.32 *	287.1	6.4	5.6	na	na	na
		43	-2.19 *	287.1	6.4	5.6	na	na	na
	Height	72	0.90	51868	86	78	0.7	0.94	Satisfactory
		43	-3.58 *	3013195	656	602	na	na	na
	BHD & RHD	72	0.97	2.4	0.6	0.5	1.3	0.99	Very good
		43	0.97	2.8	0.6	0.5	2.7	0.98	Satisfactory
	Height & BHD	72	0.93	4.0	0.8	0.6	1.9	0.97	Poor
		43	0.92	4.1	0.8	0.6	1.0	0.95	Satisfactory
	Height & RHD	72	0.96	3.0	0.7	0.5	0.3	0.99	Very good
		43	0.96	3.0	0.7	0.5	1.4	0.99	Satisfactory
Fourier	RHD	72	1.00	0.3	0.2	0.2	0.3	0.99	Very good
		43	na	na	na	na	na	na	na
	BHD	72	1.00	0.2	0.2	0.1	1.5	0.99	Satisfactory
		43	na	na	na	na	na	na	na
	Height	72	1.00	185	5.0	5.0	0.0	1.00	Very good
		43	na	na	na	na	na	na	na
	BHD & RHD	72	1.00	0.1	0.1	0.1	1.4	1.00	Very good
		43	na	na	na	na	na	na	na
	Height & BHD	72	1.00	0.2	0.1	0.1	1.4	0.99	Satisfactory
		43	na	na	na	na	na	na	na
	Height & RHD	72	1.00	0.1	0.1	0.1	0.2	1.00	Very good
		43	na	na	na	na	na	na	na
Gauss	RHD	72	0.99	0.4	0.2	0.2	0.1	0.99	Very good
		43	1.00	1.4	0.4	0.3	2.3	1.00	Very good
	BHD	72	0.98	1.2	0.4	0.4	2.9	0.99	Very good
		43	1.00	7.1	1.0	0.7	5.5	0.96	Acceptable
	Height	72	1.00	1627	15	15	0.3	1.00	Very good
		43	1.00	4578	26	18	1.1	1.00	Very good

	BHD &	72	1.00	0.4	0.2	0.2	1.4	1.00	Very good
	RHD	43	1.00	0.6	0.3	0.2	1.7	0.99	Satisfactory
	Height &	72	0.99	0.8	0.3	0.3	2.0	0.99	Very good
	BHD	43	1.00	1.9	0.5	0.4	0.6	0.98	Acceptable
	Height &	72	1.00	0.3	0.2	0.2	0.2	1.00	Very good
	RHD	43	1.00	0.4	0.3	0.2	0.1	1.00	Very good
Power: 1 term	RHD	72	na	na	na	na	na	na	na
		43	na	na	na	na	na	na	na
	BHD	72	na	na	na	na	na	na	na
		43	na	na	na	na	na	na	na
	Height	72	na	na	na	na	na	na	na
		43	na	na	na	na	na	na	na
	BHD &	72	0.98	1.2	0.4	0.3	1.8	0.99	Very good
	RHD	43	0.99	1.6	0.5	0.4	1.8	1.00	Satisfactory
	Height &	72	0.99	0.7	0.3	0.3	2.1	0.99	Acceptable
	BHD	43	0.99	0.7	0.3	0.3	1.2	0.99	Satisfactory
	Height &	72	1.00	0.1	0.1	0.1	0.2	1.00	Very good
	RHD	43	1.00	0.1	0.1	0.1	1.0	1.00	Very good
Power: 2 terms	RHD	72	0.98	2.5	0.6	0.6	1.3	0.99	Satisfactory
		43	0.97	2.6	0.6	0.6	2.2	0.98	Very good
	BHD	72	0.96	2.4	0.6	0.5	0.0	0.98	Acceptable
		43	0.96	2.6	0.6	0.6	2.7	0.96	Satisfactory
	Height	72	0.97	12883	43	38	1.0	0.99	Very good
		43	0.97	15558	47	41	3.1	0.98	Very good
	BHD &	72	1.00	0.2	0.1	0.1	1.4	1.00	Very good
	RHD	43	1.00	0.2	0.2	0.1	1.0	1.00	Very good
	Height &	72	1.00	0.2	0.2	0.1	1.5	0.99	Satisfactory
	BHD	43	1.00	0.4	0.2	0.1	2.5	0.98	Acceptable
	Height &	72	1.00	0.1	0.1	0.1	0.2	1.00	Very good
	RHD	43	1.00	0.1	0.1	0.1	1.1	1.00	Very good
Rational	RHD	72	1.00	0.8	0.3	0.3	0.3	0.99	Satisfactory
		43	1.00	1.5	0.5	0.3	2.3	0.99	Acceptable
	BHD	72	0.99	0.8	0.3	0.3	1.5	0.98	Poor
		43	1.00	1.7	0.5	0.3	4.0	0.98	Poor
	Height	72	0.00	479485	262	231	3.1	0.00	Poor
		43	0.00	480081	262	236	3.2	0.00	Poor

	BHD &	72	1.00	0.2	0.2	0.1	1.2	1.00	Very good
	RHD	43	1.00	0.1	0.1	0.1	0.0	1.00	Very good
	Height &	72	1.00	0.2	0.2	0.1	1.5	0.99	Satisfactory
	BHD	43	1.00	0.3	0.2	0.1	2.4	0.99	Acceptable
	Height &	72	1.00	0.1	0.1	0.1	0.2	1.00	Very good
	RHD	43	1.00	0.1	0.1	0.1	1.2	1.00	Very good
Sum of Sine	RHD	72	1.00	0.4	0.2	0.2	0.3	0.99	Very good
		43	1.00	0.6	0.3	0.2	2.1	0.99	Satisfactory
	BHD	72	1.00	0.3	0.2	0.2	1.5	0.98	Acceptable
		43	1.00	0.6	0.3	0.2	3.5	0.98	Acceptable
	Height	72	1.00	921	11	11	0.0	1.00	Very good
		43	1.00	1421	14	9	0.9	1.00	Very good
	BHD &	72	1.00	0.2	0.2	0.1	1.3	1.00	Very good
	RHD	43	1.00	0.1	0.1	0.1	0.0	1.00	Very good
	Height &	72	1.00	0.2	0.2	0.1	1.5	0.99	Satisfactory
	BHD	43	1.00	0.3	0.2	0.1	2.2	0.99	Satisfactory
	Height &	72	1.00	0.1	0.1	0.1	0.2	1.00	Very good
	RHD	43	1.00	0.1	0.1	0.1	1.2	1.00	Very good
Linear Fit	RHD	72	0.98	1.0	0.4	0.3	1.0	0.99	Very good
		43	1.00	6.0	0.9	0.7	0.0	0.97	Poor
	BHD	72	0.98	1.2	0.4	0.4	0.6	0.99	Very good
		43	1.00	7.1	1.0	0.8	3.5	0.98	Poor
	Height	72	0.99	6198	30	27	0.6	0.99	Satisfactory
		43	1.00	33105	69	51	1.1	0.97	Poor
	BHD &	72	0.95	6.4	1.0	0.8	3.9	0.97	Poor
	RHD	43	1.00	6552	30	21	45	-0.03	Poor
	Height &	72	0.97	1.8	0.5	0.4	2.0	0.98	Acceptable
	BHD	43	1.00	65.9	3.1	2.2	17.6	0.55	Poor
	Height &	72	0.98	1.7	0.5	0.4	0.4	0.99	Satisfactory
	RHD	43	1.00	60.3	2.9	2.1	11.6	0.68	Poor
Polynomial: 1st degree	RHD	72	0.98	2.6	0.6	0.6	1.3	0.99	Satisfactory
		43	0.97	2.7	0.6	0.6	2.2	0.98	Very good
	BHD	72	0.96	2.4	0.6	0.5	0.0	0.98	Acceptable
		43	0.96	2.7	0.6	0.6	2.7	0.96	Satisfactory
	Height	72	0.97	13187	43	39	1.0	0.99	Very good
		43	0.97	15939	48	42	3.2	0.98	Very good

	BHD &	72	1.00	0.2	0.2	0.1	1.3	1.00	Very good
	RHD	43	1.00	0.1	0.1	0.1	0.0	1.00	Very good
	Height &	72	1.00	0.2	0.2	0.1	1.3	0.99	Satisfactory
	BHD	43	1.00	0.2	0.2	0.1	1.4	0.99	Acceptable
	Height &	72	1.00	0.1	0.1	0.1	0.3	1.00	Very good
	RHD	43	1.00	0.1	0.1	0.1	1.1	1.00	Very good
Polynomial: 2nd degree	RHD	72	1.00	0.6	0.3	0.2	0.3	0.99	Satisfactory
		43	1.00	0.9	0.4	0.2	2.1	0.99	Satisfactory
	BHD	72	1.00	0.5	0.3	0.2	1.5	0.98	Acceptable
		43	1.00	0.9	0.4	0.2	3.6	0.98	Poor
	Height	72	1.00	1774	16	15	0.0	1.00	Very good
		43	1.00	2636	19	13	0.9	1.00	Very good
	BHD &	72	1.00	0.1	0.1	0.1	1.4	1.00	Very good
	RHD	43	1.00	0.1	0.1	0.1	0.8	1.00	Very good
	Height &	72	1.00	0.2	0.2	0.1	1.5	0.99	Satisfactory
	BHD	43	1.00	0.3	0.2	0.1	2.3	0.99	Acceptable
	Height &	72	1.00	0.1	0.1	0.1	0.2	1.00	Very good
	RHD	43	1.00	0.1	0.1	0.1	1.1	1.00	Very good

* A negative R-square is possible if the model does not contain a constant term and the fit is poor (worse than just fitting the mean); na: not available; RHD: root height diameter; BHD: breast height diameter

Table A.3. Goodness of validation of all applied regression models in terms of the coefficient of determination (R^2), sum of squared errors (SSE), root-mean-square error (RMSE), mean absolute error (MAE), as well as the concordance correlation coefficient (CCC) and the simulation bias (SB) from the observations.

Model	Variable	Data Gap Representation	R^2	SSE	RMSE	MAE	SB [%]	CCC	Label
Interpolant: Nearest Neighbor	RHD	72	1.00	4.8	0.8	0.5	2.3	0.97	Poor
		43	1.00	12.6	1.3	0.9	0.4	0.93	Poor
	BHD	72	1.00	4.0	0.8	0.4	1.0	0.97	Poor
		43	1.00	8.9	1.1	0.8	0.0	0.92	Poor
	Height	72	1.00	32985	69	36	1.5	0.97	Poor
		43	1.00	71174	101	71	1.4	0.93	Poor
	BHD &	72	1.00	6.0	0.9	0.5	6.8	0.97	Poor
	RHD	43	1.00	12.6	1.3	0.9	0.4	0.93	Poor
	Height &	72	1.00	6.3	0.9	0.5	8.7	0.95	Poor
	BHD	43	1.00	8.9	1.1	0.8	0.0	0.92	Poor
	Height &	72	1.00	6.5	1.0	0.5	5.2	0.97	Poor
	RHD	43	1.00	12.6	1.3	0.9	0.4	0.93	Poor
Interpolant: Linear	RHD	72	1.00	0.3	0.2	0.1	0.8	1.00	Very good
		43	1.00	0.5	0.3	0.2	0.4	0.99	Very good
	BHD	72	1.00	0.1	0.1	0.1	0.9	0.99	Satisfactory
		43	1.00	0.4	0.2	0.2	0.0	0.98	Satisfactory
	Height	72	1.00	211	5.0	2.0	0.4	1.00	Very good
		43	1.00	3154	21	13	1.4	1.00	Very good
	BHD &	72	1.00	0.3	0.2	0.1	1.5	1.00	Very good
	RHD	43	1.00	0.0	0.1	0.0	0.2	1.00	Very good
	Height &	72	1.00	0.1	0.1	0.1	1.3	0.99	Satisfactory
	BHD	43	1.00	0.2	0.2	0.1	1.6	0.99	Satisfactory
	Height &	72	1.00	0.2	0.2	0.1	0.5	1.00	Very good
	RHD	43	1.00	0.1	0.1	0.1	1.1	1.00	Very good
Interpolant: Cubic	RHD	72	1.00	0.3	0.2	0.1	1.2	1.00	Very good
		43	1.00	0.9	0.4	0.2	2.1	0.99	Satisfactory

	BHD	72	1.00	0.1	0.1	0.1	0.7	0.99	Very good
		43	1.00	0.9	0.4	0.2	3.6	0.98	Poor
	Height	72	1.00	594	9.0	4.0	0.3	1.00	Very good
		43	1.00	2636	19	13	0.9	1.00	Very good
	BHD &	72	1.00	0.7	0.3	0.2	2.6	1.00	Satisfactory
	RHD	43	1.00	0.1	0.1	0.1	0.8	1.00	Very good
	Height &	72	1.00	0.1	0.1	0.1	1.0	0.99	Very good
	BHD	43	1.00	0.3	0.2	0.1	2.3	0.99	Acceptable
	Height &	72	1.00	0.4	0.2	0.1	1.8	1.00	Very good
	RHD	43	1.00	0.1	0.1	0.1	1.1	1.00	Very good
Interpolant: PCHIP	RHD	72	1.00	0.2	0.2	0.1	0.8	1.00	Very good
		43	1.00	1.0	0.4	0.2	2.1	0.99	Satisfactory
	BHD	72	1.00	0.1	0.1	0.1	1.2	0.99	Satisfactory
		43	1.00	1.1	0.4	0.2	3.6	0.98	Poor
	Height	72	1.00	60	3.0	2.0	0.0	1.00	Very good
		43	1.00	3398	22	16	0.9	1.00	Very good
	BHD &	72	1.00	0.4	0.2	0.1	1.8	1.00	Very good
	RHD	43	1.00	0.1	0.1	0.1	0.8	1.00	Very good
	Height &	72	1.00	0.1	0.1	0.1	1.3	0.99	Satisfactory
	BHD	43	1.00	0.3	0.2	0.1	2.3	0.99	Acceptable
	Height &	72	1.00	0.2	0.2	0.1	0.8	1.00	Very good
	RHD	43	1.00	0.1	0.1	0.1	1.1	1.00	Very good

RHD: root height diameter; BHD: breast height diameter

Appendix B

Table B.1. Tree and soil parameter values used for the parametrization of the Yield-SAFE model for the SRC in Forst (north-eastern Germany).

Symbol	Description	Unit	Tree Species	Value	Source
Tree Parameters					
Initial Conditions					
$n_{Shoots0}$	Initial number of shoots per tree	$tree^{-1}$	Poplar Black Locust	0.3362 0.2520	Own data
B_{t0}	Initial tree biomass	g $tree^{-1}$	Poplar Black Locust	100	1, 2
LA_{t0}	Initial tree leaf area	m^2 $tree^{-1}$	Poplar Black Locust	0	1, 2
Parameters					
ε_t	Radiation use efficiency	g MJ^{-1}	Poplar Black Locust	0.2137 0.4820	Own data
k_t	Light extinction coefficient	–	Poplar Black Locust	0.8	1, 2
t_t	The number of days after bud-burst at which the leaf area has reached 63.2% of its maximum leaf area LA_{ss}^{max}	d	Poplar Black Locust	10	1, 2
LA_{ss}^{max}	Maximum leaf area for a single shoot	m^2	Poplar Black Locust	0.05 0.025	1, 2 3
n_{Shoots}^{max}	Maximum number of shoots per tree	$tree^{-1}$	Poplar Black Locust	10000	1, 2
K_{main}	Relative attrition rate of tree biomass	d^{-1}	Poplar Black Locust	10^{-4}	1, 2
γ_t	Transpiration coefficient of the trees	m^3 kg^{-1}	Poplar Black Locust	0.35 0.42	2 3
$(pF_{crit})_t$	Critical pF value for trees	log (cm)	Poplar Black Locust	4.0	1 3
$(pF_{pwp})_t$	pF value at permanent wilting point	log (cm)	Poplar Black Locust	4.2	1
Tree Leaf Phenology					
$DOY_{budburst}$, $DOY_{leaf\text{-}fall}$	Day of year for bud-burst and leaf-fall	DOY	Poplar Black Locust	105, 280 125, 310	4

Management Tree Density					
ρ_t	Planting density	trees ha^{-1}	Poplar Black Locust	8700	[5]
Soil Parameters					
Initial Conditions					
θ_0	Initial volumetric water content	$m^3\ m^{-3}$	Poplar Black Locust	0.552	[1, 2]
Parameters					
δ_{eva}	Potential evaporation per unit energy	mm MJ^{-1}	Poplar Black Locust	0.15	[2]
D	Depth of the soil compartment	mm	Poplar Black Locust	1500	[6]
α	Van Genuchten parameter	–	Poplar Black Locust	0.0383	[6]
n_{soil}	Van Genuchten parameter	–	Poplar Black Locust	1.3774	[6]
δ	Parameter affecting the drainage rate below root zone	–	Poplar Black Locust	0.07	[6]
PWP	Permanent wilting point	log (cm)	Poplar Black Locust	4.2	[1, 2]
$(pF_{crit})_E$	Critical pF value for evaporation	log (cm)	Poplar Black Locust	2.3	[1, 2]
pF_{FC}	Water tension at field capacity	log (cm)	Poplar Black Locust	2.3	[1, 2]
K_s	Soil hydraulic conductivity at saturation	mm d^{-1}	Poplar Black Locust	60	[6]
θ_s	Saturated volumetric water content	$m^3\ m^{-3}$	Poplar Black Locust	0.403	[6]
θ_r	Residual volumetric water content	$m^3\ m^{-3}$	Poplar Black Locust	0.025	[6]

[1] Keesman *et al.* (2011); [2] Graves *et al.* (2010); [3] Mantovani *et al.* (2015a); [4] Küppers *et al.* (2017); [5] Kanzler & Böhm (2016); [6] Wösten *et al.* (1990)

Figure B.1. Walter-Lieth climate diagrams for realisation 79 in terms of average annual air temperature, precipitation and global radiation, according to the established periods and with respect to the vegetation period and accumulated woody biomass for both tree species.

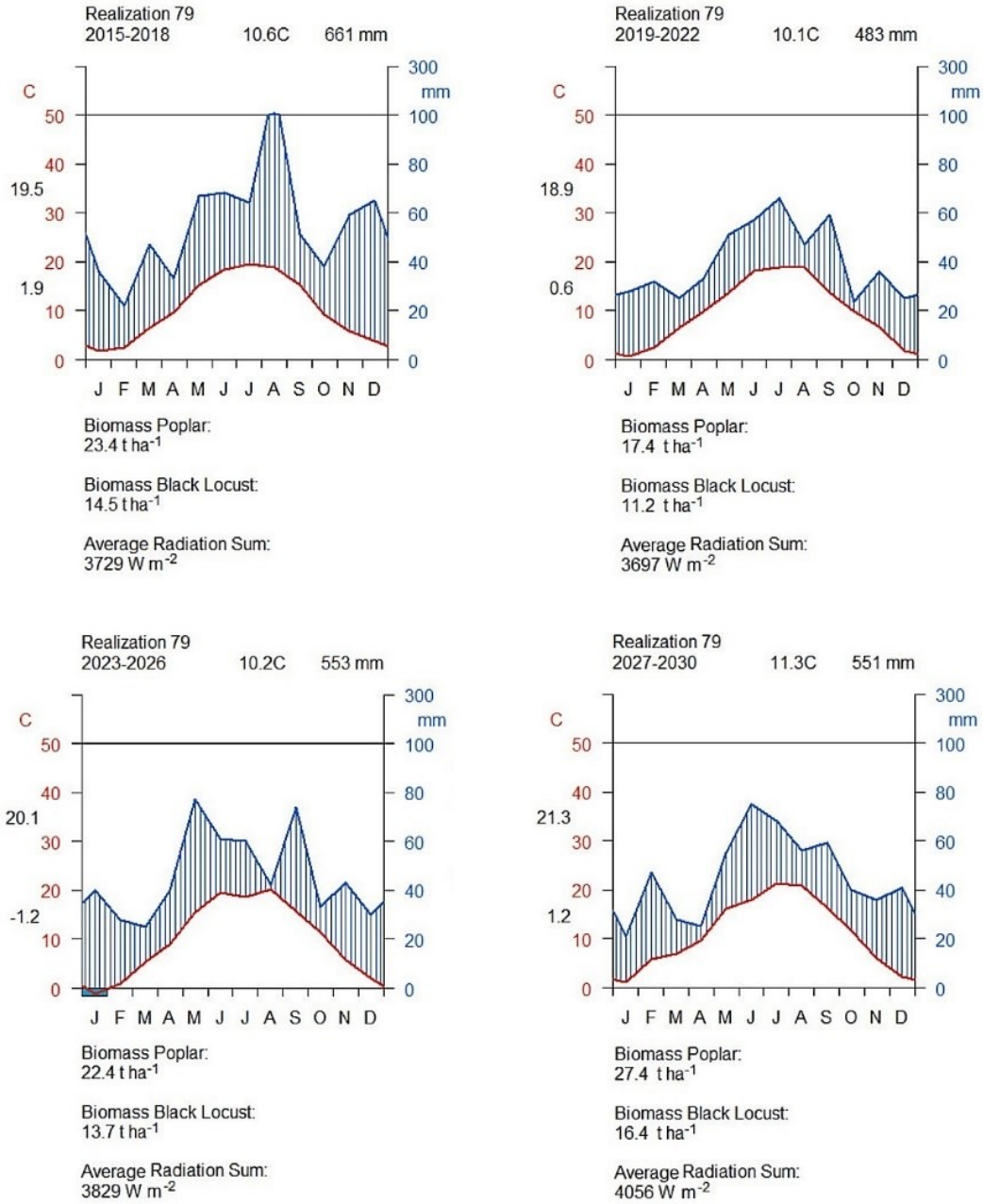

Realization 79
2031-2034 10.6C 548 mm

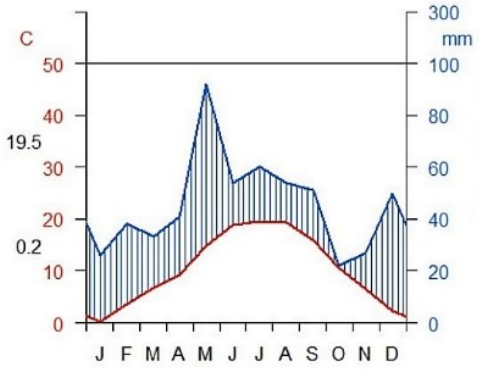

Biomass Poplar:
24.4 t ha^{-1}

Biomass Black Locust:
14.8 t ha^{-1}

Average Radiation Sum:
3850 W m^{-2}

Realization 79
2035-2038 11C 373 mm

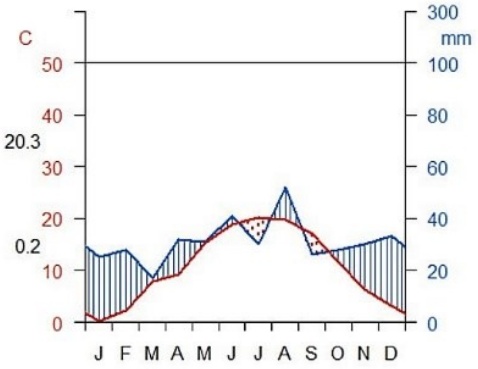

Biomass Poplar:
17.1 t ha^{-1}

Biomass Black Locust:
9.3 t ha^{-1}

Average Radiation Sum:
3978 W m^{-2}

Realization 79
2039-2042 11.8C 414 mm

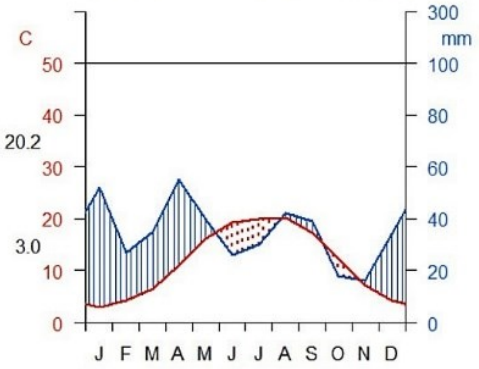

Biomass Poplar:
17.5 t ha^{-1}

Biomass Black Locust:
10.1 t ha^{-1}

Average Radiation Sum:
4180 W m^{-2}

Realization 79
2043-2046 11.5C 500 mm

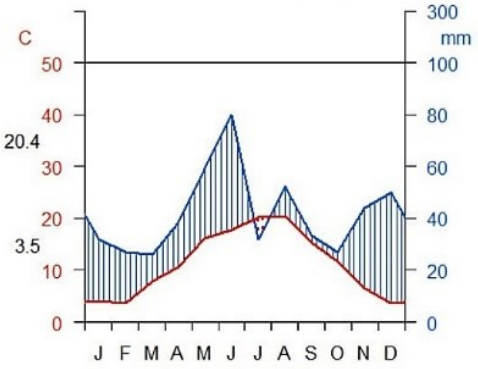

Biomass Poplar:
21.1 t ha^{-1}

Biomass Black Locust:
12.3 t ha^{-1}

Average Radiation Sum:
4040 W m^{-2}

Realization 79
2047-2050 11.5C 411 mm

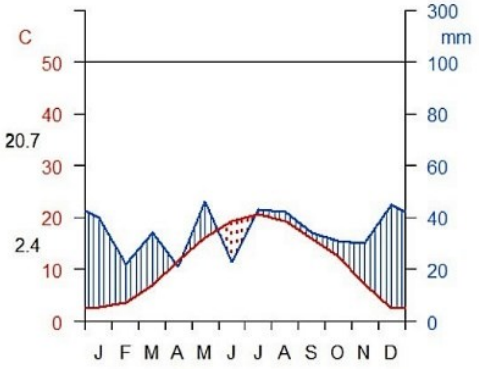

Biomass Poplar:
15.9 t ha^{-1}

Biomass Black Locust:
9.4 t ha^{-1}

Average Radiation Sum:
4092 W m^{-2}

Realization 79
2051-2054 11.9C 425 mm

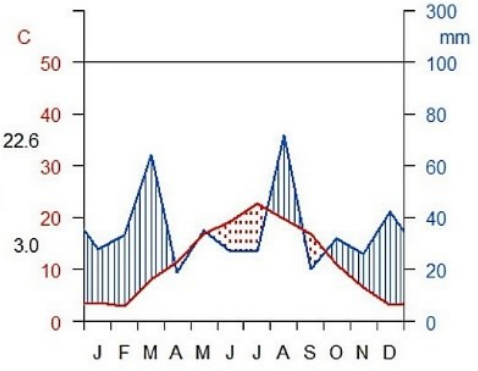

Biomass Poplar:
14.6 t ha^{-1}

Biomass Black Locust:
9.1 t ha^{-1}

Average Radiation Sum:
4216 W m^{-2}

Figure B.2. Comparison between realisation 31 and realisation 13 in terms of average monthly air temperature, precipitation and global radiation according to growing period 1 (2015-2018) and with respect to the accumulated biomass obtained by poplar.

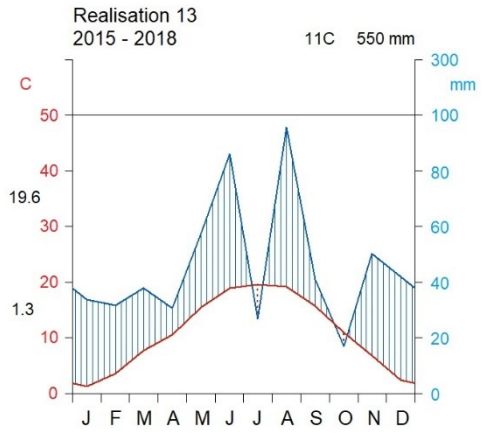

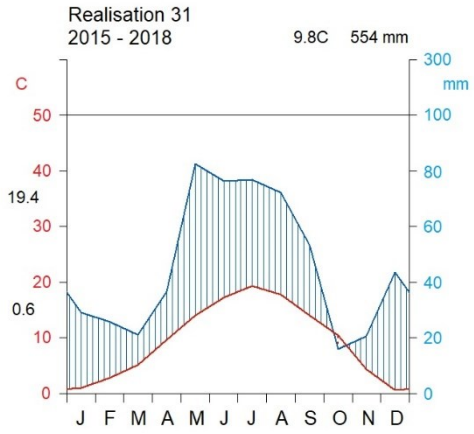

Month	2015			2016			2017			2018		
	T	P	R	T	P	R	T	P	R	T	P	R
J	-2.5	33	77	4.7	46	57	3.9	28	82	-0.7	28	98
F	-0.6	27	126	-0.6	48	111	7.4	27	184	8.1	25	325
M	6.0	37	301	8.5	42	277	9.0	17	274	7.1	56	335
A	8.0	31	339	11.2	32	468	9.9	22	476	13.2	38	485
M	15.4	2	645	15.3	110	554	17.0	97	501	14.2	22	520
J	20.0	76	585	19.4	62	633	17.8	120	478	18.9	86	601
J	19.2	4	619	23.2	23	686	18.9	20	572	17.0	61	482
A	18.1	30	518	19.8	112	439	20.6	119	509	18.1	121	480
S	16.7	35	372	14.7	58	362	14.0	64	273	17.5	6	422
O	10.4	20	256	7.7	10	245	12.0	15	288	13.8	24	328
N	5.7	44	74	9.4	36	126	5.3	78	78	7.2	43	82
D	4.1	63	55	4.6	25	70	1.3	57	50	-0.1	23	58

Month	2015			2016			2017			2018		
	T	P	R	T	P	R	T	P	R	T	P	R
J	2.1	16	78	-2.7	21	71	1.6	34	83	3.3	45	101
F	-0.3	6	137	3.1	31	141	6.4	29	142	2.2	38	116
M	6.8	19	341	5.5	21	296	5.8	11	329	2.6	34	251
A	8.7	31	490	9.7	50	350	10.0	46	379	10.3	20	393
M	14.8	137	568	14.7	55	518	15.2	70	566	11.6	69	462
J	16.9	111	548	18.3	76	528	18.2	71	565	15.9	48	528
J	18.4	84	529	20.5	121	528	21.7	77	658	17.0	26	517
A	16.1	175	416	18.0	22	487	19.7	20	561	17.1	73	414
S	14.5	29	337	12.0	45	306	14.9	103	348	15.1	37	384
O	10.8	3	220	9.0	34	149	11.8	6	200	9.9	21	143
N	5.2	30	76	5.2	17	96	3.2	33	117	4.0	2	80
D	1.3	50	44	3.6	52	53	-1.4	37	29	-1.0	36	50

Appendix C

Table C.1. Tree parameter values used for the parametrization of the Yield-SAFE model.

Symbol	Description	Unit	Location	Value	Source
Tree Parameters					
Initial Conditions					
$n_{Shoots0}$	Initial number of shoots per tree	tree^{-1}	Wendhausen Neu Sacro	1.256 1.086	Own data
B_{t0}	Initial tree biomass	g tree^{-1}	Wendhausen Neu Sacro	40	[1]
LA_{t0}	Initial tree leaf area	m^2 tree^{-1}	Wendhausen Neu Sacro	0	[1, 2, 3]
Parameters					
ε_t	Radiation use efficiency	g MJ^{-1}	Wendhausen Neu Sacro	1.1100 0.9912	Own data
k_t	Light extinction coefficient	–	Wendhausen Neu Sacro	0.8	[2, 3]
t_t	The number of days after bud-burst at which the leaf area has reached 63.2 % of its maximum leaf area LA_{ss}^{max}	d	Wendhausen Neu Sacro	10	[2, 3]
LA_{ss}^{max}	Maximum leaf area for a single shoot	m^2	Wendhausen Neu Sacro	0.04	[1]
n_{Shoots}^{max}	Maximum number of shoots per tree	tree^{-1}	Wendhausen Neu Sacro	10000	[2, 3]
K_{main}	Relative attrition rate of tree biomass	d^{-1}	Wendhausen Neu Sacro	10^{-4}	[2, 3]
γ_t	Transpiration coefficient of the trees	m^3 kg^{-1}	Wendhausen Neu Sacro	0.2	[1]
$(pF_{crit})_t$	Critical pF value	log (cm)	Wendhausen Neu Sacro	4.0	[2]
$(pF_{pwp})_t$	pF value at permanent wilting point	log (cm)	Wendhausen Neu Sacro	4.2	[2]
Tree Phenology					
$DOY_{budburst}$, $DOY_{leaf\text{-}fall}$	Day of year for bud-burst and leaf-fall	DOY	Wendhausen Neu Sacro	105, 300	[1]
Management Parameters					
ρ_t	Planting density	trees ha^{-1}	Wendhausen Neu Sacro	10,000 8,700	[4] [5]

[1] Crous-Duran *et al.* (2018); [2] Keesman *et al.* (2011); [3] Graves *et al.* (2010); [4] Lamerre *et al.* (2016); [5] Kanzler & Böhm (2016)

Table C.2. Crop parameter values used for the parametrization of the Yield-SAFE model.

Symbol	Description	Unit	Crop	Location	Value	Source
Crop Parameters						
Initial Conditions						
B_{c0}	Initial crop biomass	g m^{-2}	All	All	10	[1]
LA_{c0}	Initial crop leaf area	m^2 m^{-2}	All	All	0.1	[1]
P_{leaves}	Partitioning factor to leaves	–	All	All	0.8	[1]
Parameters						
ε_c	Radiation use efficiency	g MJ^{-1}	ww	NS	1.690	Own data
			wb	NS	1.033	
			wr	WH	1.017	
			ww	WH	0.907	
k_c	Light extinction coefficient	–	All	All	0.7	[1]
$(pF_{crit})_c$	Critical pF value	log (cm)	wb	All	2.9	[1, 2]
			ww, wr		3.2	
$(pF_{pwp})_c$	pF value at permanent wilting point	log (cm)	All	All	4.2	[1]
SLA	Specific leaf area	m^2 g^{-1}	ww, wb	NS	0.005	[2]
			wr	WH	0.020	
			ww	WH	0.005	
T_0	Base temperature	°C	All	All	5	[1]
T_{sum} *emerge*	Heat sum at emergence	°Cd	All	All	57	[1]
					79	
T_{sum} *RB*	Heat sum when partitioning to leaves starts to decrease	°Cd	All	All	456	[1]
					500	
T_{sum} *RE*	Heat sum when partitioning to leaves ceases	°Cd	All	All	464	[1]
					1300	
T_{sum} *harvest*	Heat sum at harvest	°Cd	All	All	1312	[1]
					2000	
Management Parameters						
DOY_{sow}	Day of sowing	DOY	ww	NS	-65	[4]
			wb	NS	-60	[1]
			wr	WH	-116	[1]
			ww	WH	-95	[5]
$DOY_{harvest}$	Day of harvest	DOY	ww, wb	NS	245	[5]
			wr	WH	225	[1]
			ww	WH	300	[1]

[1] Graves *et al.* (2010); [2] Crous-Duran *et al.* (2018); [3] Kanzler *et al.* (2018); [4] Swieter *et al.* (2018)

Table C.3. Soil parameter values used for the parametrization of the Yield-SAFE model.

Symbol	Description	Unit	Crop	Location	Value	
Soil Parameters						
Initial Conditions						
θ_0	Initial volumetric water content	$m^3\ m^{-3}$		Wendhausen Neu Sacro	0.552	[1, 2]
Parameters						
δ_{eva}	Potential evaporation per unit energy	mm MJ^{-1}		Wendhausen Neu Sacro	0.15	[1, 2]
D	Depth of the soil compartment	mm		Wendhausen Neu Sacro	900 1400	[3] [4]
α	Van Genuchten parameter	–		Wendhausen Neu Sacro	0.0083 0.0383	[5]
n_{soil}	Van Genuchten parameter	–		Wendhausen Neu Sacro	1.2539 1.3774	[5]
δ	Parameter affecting the drainage rate below root zone	–		Wendhausen Neu Sacro	0.07	[5]
PWP	Permanent wilting point	log (cm)		Wendhausen Neu Sacro	4.2	[1, 2]
$(pF_{crit})_E$	Critical pF value for evaporation	log (cm)		Wendhausen Neu Sacro	2.3	[1, 2]
pF_{FC}	Water tension at field capacity	log (cm)		Wendhausen Neu Sacro	2.3	[1, 2]
K_s	Soil hydraulic conductivity at saturation	mm d^{-1}		Wendhausen Neu Sacro	24.8 60.0	[5]
θ_s	Saturated volumetric water content	$m^3\ m^{-3}$		Wendhausen Neu Sacro	0.520 0.403	[5]
θ_r	Residual volumetric water content	$m^3\ m^{-3}$		Wendhausen Neu Sacro	0.010 0.025	[5]

[1] Keesman *et al.* (2011); [2] Graves *et al.* (2010); [3] Lamerre *et al.* (2016); [4] Kanzler & Böhm (2016);

[5] Wösten *et al.* (1990)

Table C.4. Tree and crop yields per cropped area and per alley-cropping system, their corresponding relative yields, the inferred LER and gross energy yield values, as projected by the Yield-SAFE model at Wendhausen and Neu Sacro in 2016 and 2017 and under different ratios of tree area to crop area.

		Wendhausen									**Neu Sacro**								
		Yield per cropped area [Mg DM ha^{-1} yr^{-1}]		**Yield per ACS (Y_i)** [Mg DM ha^{-1} yr^{-1}]		**Relative yields (Y_i/Y_{100})**		**LER** (Eq. 2)		**Gross energy yield** [GJ ha^{-1}]	**Yield per cropped area** [Mg DM ha^{-1} yr^{-1}]		**Yield per ACS (Y_i)** [Mg DM ha^{-1} yr^{-1}]		**Relative yields (Y_i/Y_{100})**		**LER** (Eq. 2)		**Gross energy yield** [GJ ha^{-1}]
Plant	**Area [%]**	2016	2017	2016	2017	2016	2017	2016	2017		2016	2017	2016	2017	2016	2017	2016	2017	
Tree	0	-	-	-	-	-	-	1	1	220	-	-	-	-	-	-	1	1	151
Crop	100	3.7	7.2	3.7	7.2	1.0	1.0				5.1	3.7	5.1	3.7	1.00	1.00			
Tree	20	10.6	13.5	2.1	2.7	0.2	0.3	0.9	1.0	244	14.0	12.9	2.8	2.6	0.3	0.3	1.3	1.5	264
Crop	80	3.2	6.4	2.6	5.1	0.7	0.7				6.1	5.8	4.9	4.6	1.0	1.3			
Tree	25	10.5	13.4	2.6	3.4	0.3	0.4	0.8	0.9	232	14.4	13.1	3.6	3.3	0.4	0.4	1.2	1.2	250
Crop	75	2.5	5.6	1.9	4.2	0.5	0.6				5.3	4.2	4.0	3.2	0.8	0.9			
Tree	40	10.4	13.3	4.2	5.3	0.4	0.6	0.7	0.9	235	14.8	13.5	5.9	5.4	0.7	0.6	1.0	1.0	270
Crop	60	1.5	3.5	0.9	2.1	0.2	0.3				3.2	2.7	1.9	1.6	0.4	0.4			
Tree	50	10.3	13.1	5.2	6.6	0.5	0.7	0.7	0.8	248	14.9	13.5	7.5	6.8	0.8	0.8	1.0	1.0	298
Crop	50	1.0	2.2	0.5	1.1	0.1	0.2				2.2	1.9	1.1	1.0	0.2	0.3			
Tree	60	10.3	13.0	6.2	7.8	0.7	0.8	0.7	0.9	274	14.9	13.6	8.9	8.2	1.0	0.9	1.1	1.0	334
Crop	40	0.6	1.3	0.2	0.5	0.1	0.1				1.4	1.2	0.6	0.5	0.1	0.1			
Tree	75	10.2	12.9	7.7	9.7	0.8	1.0	0.8	1.0	324	14.9	13.6	11.2	10.2	1.2	1.1	1.3	1.2	401
Crop	25	0.3	0.4	0.1	0.1	0.0	0.0				0.6	0.6	0.2	0.2	0.0	0.0			
Tree	80	10.2	12.8	8.2	10.2	0.9	1.1	0.9	1.1	342	14.9	13.5	11.9	10.8	1.3	1.2	1.3	1.2	423
Crop	20	0.2	0.3	0.0	0.1	0.0	0.0				0.4	0.4	0.1	0.1	0.0	0.0			
Tree	100	9.4	9.4	9.4	9.4	1.0	1.0	1	1	348	9.0	9.0	9.0	9.0	1.00	1.00	1	1	333
Crop	0	-	-	-	-	-	-				-	-	-	-	-	-			

Figure C.1. Walter-Lieth climate diagrams for the weather stations at Braunschweig (Wendhausen; **a**,**c**) and Cottbus (Neu Sacro; **b**,**d**). Monthly values from 2016 (**a**,**b**) and 2017 (**c**,**d**) were used to represent the mean air temperature (red) and average precipitation sum (blue). If the average monthly precipitation sum lies under the mean monthly air temperature, the period is considered arid (filled in dotted red vertical lines), otherwise it is considered wet (filled in blue lines). Minimum and maximum annual temperatures are located on the far-left side and annual mean temperatures are located atop, together with the annual precipitation sum. Frost months (when the absolute monthly temperature minimums are equal or lower than 0°C) are shown in solid blue boxes along the x-axis.

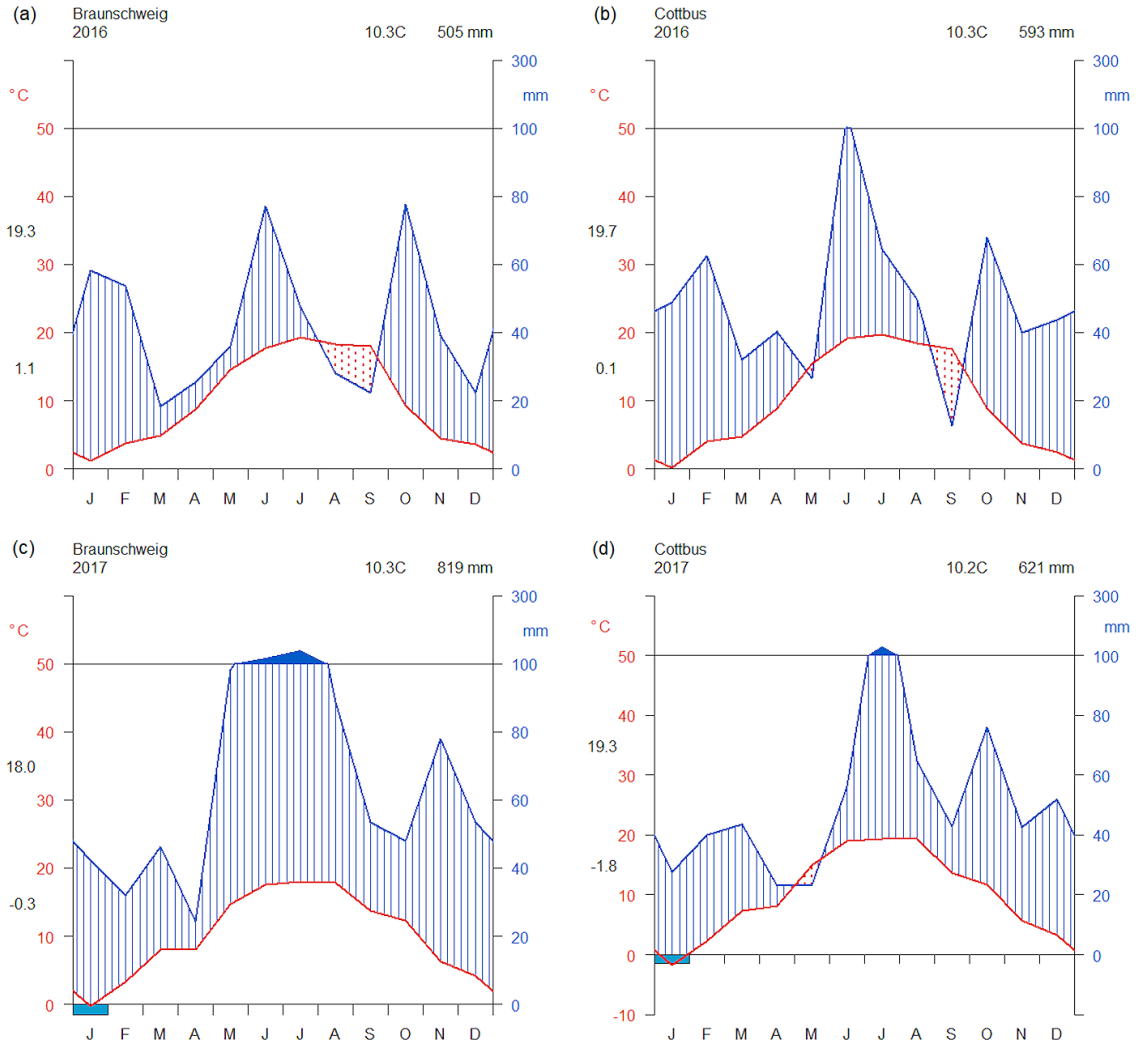

Figure C.2. To-scale sketch of the 29 m x 30 m alley-cropping-plots (APs) design at Wendhausen (**a**) and Neu Sacro (**b**). At both sites, AP1 and AP2 are arranged leeward and AP3 and AP4 windward. The solid-coloured areas correspond to the tree strips and the shaded areas to the cropped surfaces. The orange bars represent the 2 m x 10 harvest transects located 1 m, 4 m, 7 m, and 24 m away from the tree strips. As the experimental part of this study focused on a ratio of tree area to crop area of 17:82, the simulations considered design scenarios with ratios of tree area to crop area of 20:80, 25:75, 40:60, 50:50, 60:40, 75:26, and 80:20 (**c**).